

Exxon Valdez Oil Spill
Restoration Project Annual Report

Information Systems and Model Development

Restoration Project 97320-J (SEADATA)
Annual Report

This annual report has been prepared for peer review as part of the *Exxon Valdez* Oil Spill Trustee Council restoration program for the purpose of assessing project progress. Peer review comments have not been addressed in this annual report.

Principal Investigator:	Vincent Patrick	Prince William Sound Science Center
	Jennifer R. Allen	Prince William Sound Science Center
	Stephen Bodnar	Prince William Sound Science Center
	Charles S. Falkenberg	Adv. Visualization Lab., U. of Maryland
	Ravi Kulkarni	Prince William Sound Science Center & Adv. Visualiz. Lab., U. of Maryland
	Doran M. Mason	Prince William Sound Science Center & Purdue University
Pr. Investigator, Circulation Model	Christopher N. K. Mooers	Dir., Ocean Pollution Research Center, Rosenstiel Schl. Marine & Atmos. Sci., U. of Miami
	Roy Murray	Prince William Sound Science Center & Utah State University
	Ricardo H. Nochetto	Prince William Sound Science Center & Mathematics Dept., U. of Maryland
	Jia Wang	OPRC, Rosenstiel School, U. of Miami

Prince William Sound Science Center
PO Box 705
300 Breakwater Avenue
Cordova, AK 99574

April 1997

Information Systems and Model Development

Restoration Project 97320-J Annual Report

Study History: The Sound Ecosystem Assessment (SEA) Program is based upon the *Sound Ecosystem Assessment Initial Science Plan and Monitoring Program*, Rpt No. 1, Nov. 24, 1993. It began April 1994 (Restoration Project 94320) and has continued through FY97 (Projects 95-, 96- and 97320). The Information Systems and Model Development Project (SEADATA) is Restoration Project 9x320-J within the SEA Program. Prior progress is described in the SEA Annual Reports to EVOS for FY94 (Ch6), FY95 (Ch7), and FY96 (Ch7). During this reporting period the journal *Continental Shelf Research* accepted for publication in the JONSMOD '96 Special Issue the manuscript "A two-compartment model for understanding the simulated three-dimensional circulation in Prince William Sound, Alaska" by E. Dellersnijder, C. N. K. Mooers and Jia Wang. Also, the paper "A three-dimensional tidal model for Prince William Sound, Alaska" by J. Wang, C. N. K. Mooers, and V. Patrick was accepted for presentation and will appear in the forthcoming volume *Computer Modelling of Seas and Coastal Regions III*.

Abstract: There were seven task areas. **Pink salmon fry survival.** In the previous year all features of the model had been implemented, the design "frozen," and the design tested regarding prey switching. During 1997 the priority was the processes prior to, during, and after the macrozooplankton event that induces switching. The effort produced new extensions that significantly increase the model end-use value. **Overwinter survival of juvenile herring.** Model objectives presented at the February 1997 herring review were completed; models were documented and distributed for testing. **Princeton ocean model for PWS.** Fresh-water input, albeit in coarse form, was added, and the consequences for model realism are extremely promising. Validation testing continues. **Observing system specifications and operations.** Increased effort was allocated to formalizing the inputs and output of the SEA models. This task involves all of SEA. This project collects near realtime meteorological data from all sources. It maintains the met station at Applegate Rock, now at 18 months continuous, once daily transmission by repeater network. Products are published on the World Wide Web. This project is co-developer of the "subjective analysis" for surface winds **Database.** The catalog of datasets with full schemas is such that maintaining currency is a significant task. New additions are all acoustic survey data performed for ADFG and the first year of the comprehensive fishery field and laboratory database developed by Willette and Saddler. **Intranet.** The SEA project intranet continued to provide inter-project information and coordination. Emphasis turned to final year synthesis. **Applications.** Significant progress resulted from initiatives begun in reponse to review criteria of the EVOS Chief Scientist and review panel to demonstrate rapid transition of model development into applications.

Key Words: bioenergetics, circulation model, collaborative software, database, diffusion-taxis, dispersion, *Exxon Valdez*, Mellor-Blumberg, Pacific herring, packet-radio, pink salmon, Prince William Sound, Princeton Model, SEA, Sound Ecosystem Assessment, visualization, World Wide Web

Citation: Patrick, E. V., J. R. Allen, S. Bodnar, C. S. Falkenberg, D. M. Mason, C. N. K. Mooers, R. Murray, R. H. Nochetto, and J. Wang. 1998. Information Systems and Model Development Project (SEADATA) of the Sound Ecosystem Assessment Program, *Exxon Valdez Oil Spill Restoration Project Annual Report* (Restoration Project 97320-J), Prince William Sound Science Center, Cordova, Alaska.

Table of Contents

Study History	i
Abstract	i
Key Words	i
Citation	i
Table of Contents	ii
List of Figures	iv
EXECUTIVE SUMMARY	1
INTRODUCTION	2
OBJECTIVES	5
METHODS	5
RESULTS and DISCUSSION: In-depth Reports	6
RESULTS: Summary Reports	11
FIGURES	15
APPENDIX 1	16
Part I-A	
Technical note to SEA	
1997 findings from the EVOS-ADFG-PWSAC fry marking programs and	
from models for survival of pink salmon fry during migration thorough PWS	
.....	22
Part I-B	
Technical note to SEA	
Lower bounds for survival of juvenile pink salmon	
during migration as fry through PWS	33
Part I-C	
Summary of 1997 progress	
The pink salmon fry survival model with 1997 extensions:	
ecosystem production processes and their record in code-group survival ...	80

Part II	
Report on 1997 progress	
Database	
C. S. Falkenberg	83
Part III-A	
Report on 1997 progress	
Web-based Communications	
J. R. Allen	86
Part III-B	
Scientific Visualization Methods for Marine Ecosystem Research:	
Case Studies Using AVS for Display of Hydroacoustic Data	
J. R. Allen, E. V. Patrick, R. Kulkarni, G. L. Thomas, and J. Kirsch	89
Part IV	
Report on 1997 progress	
Weather Data Systems	
S. Bodnar	92
APPENDIX 2	93
A three-dimensional tidal model for Prince William Sound, Alaska	
J. Wang, C. N. K. Mooers, V. Patrick	
to appear in <i>Computer Modelling of Seas and Coastal Regions III</i>	96
A two-compartment model for understanding	
the simulated three-dimensional circulation	
in Prince William Sound, Alaska	
E. Deleersnijder, Université catholique de Louvain, Belgium	
J. Wang and C. N. K. Mooers, RSMAS, University of Miami	
to appear in <i>Continental Shelf Research JONSMOD '96 Special Issue</i>	99

List of Figures

- Figure 1.
- Figure 2.
- Figure 3.
- Figure 4.
- Figure 6.
- Figure 7.
- Figure 8.
- Figure 9.
- Figure 11.
- Figure 12.
- Figure 13.
- Figure 14.
- Figure 15.

EXECUTIVE SUMMARY

There were seven task areas. **Pink salmon fry survival.** In the previous year all features of the model had been implemented, the design "frozen," and the design tested regarding prey switching. During 1997 the priority was the processes prior to, during, and after the macrozooplankton event that induces switching. The effort produced new extensions that significantly increase the model end-use value. **Overwinter survival of juvenile herring.** Model objectives presented at the February 1997 herring review were completed; models were documented and distributed for testing. **Princeton ocean model for PWS.** Fresh-water input, albeit in coarse form, was added, and the consequences for model realism are extremely promising. Validation testing continues. **Observing system specifications and operations.** Increased effort was allocated to formalizing the inputs and output of the SEA models. This task involves all of SEA. This project collects near realtime meteorological data from all sources. It maintains the met station at Applegate Rock, now at 18 months continuous, once daily transmission by repeater network. Products are published on the World Wide Web. This project is co-developer of the "subjective analysis" for surface winds **Database.** The catalog of datasets with full schemas is such that maintaining currency is a significant task. New additions are all acoustic survey data performed for ADFG and the first year of the comprehensive fishery field and laboratory database developed by Willette and Saddler. **Intranet.** The SEA project intranet continued to provide inter-project information and coordination. Emphasis turned to final year synthesis. **Applications.** Significant progress resulted from new initiatives begun in response to review criteria of the EVOS Chief Scientist and review panel to demonstrate rapid transition of model development into applications. As many end-user public meetings as possible have been attended to understand fully pressing problems, needs, and conditions imposed on possible solutions. In addition numerous presentations and application development sessions have been held with as many end-user groups as possible, and intranets were set up with ADFG and RCAC.

INTRODUCTION

The *1998 Status Report* of the *Exxon Valdez* Oil Spill Trustee Council (EVOS) notes

The Sound Ecosystem Assessment (SEA) project ... was initiated by commercial fishers and scientists in Cordova concerned about the longterm health of Prince William Sound fisheries. SEA focuses on the factors that influence the production of adult pink salmon and Pacific herring, both of which were injured by the 1989 oil spill...

The spill had brought into strong relief the problem of major missing pieces in the understanding of the marine production processes of Prince William Sound (PWS). These production processes were the basis of principle economies of the region, yet were understood largely descriptively and not in the quantitative manner typically associated with production systems. To whatever degree that understanding had been adequate, it was not following the spill. The ecosystem was now widely and carefully watched, and each observation highlighted the limited abilities to answer questions about an observed event such as "Why did this happen? How did it happen? What would happen next?"

The objective of the SEA program is the ability to answer those questions for that part of the PWS ecosystem that determines the production processes for pink salmon fry and juvenile Pacific herring. The approach is the development of numerical models, observing systems and procedures whereby the production processes can be "tracked" as well as projected ahead for some short time interval. This tracking and short term projection is the result of "continuously running" observations and numerical model simulations. In meteorology and oceanography this operation has a careful definition and is referred to as *nowcasting* and *forecasting*. Our biological models are but early and primitive in terms of nowcast/forecast, but with apologies we borrow the terminology, for it precisely conveys the goals and the methods.

Toward this objective the Information Systems and Model Development Project (SEADATA) was organized to provide the numerical models, a database, and information resources required by SEA, and also to provide the computing, communications, and certain observation system resources maintained at the PWS regional center for SEA. That center, the Prince William Sound Science Center, is the organizational home for four of the projects, the site for the primary SEA data and information servers, and the means by which SEA has continuous access to and is continuously accessible by the community served by the project.

The project history and highlights are available at the SEA Web site at URL
<http://www.pwssc.gen.ak.us/sea/sea.html>

SEADATA is responsible for the following items. The progress and status of each is described in this report.

1. Numerical model for survival of pink salmon fry during outmigration in PWS.
2. Numerical model for survival of juvenile Pacific herring during winter fasting in PWS.
3. SEA circulation model (C. N. K. Mooers, RSMAS).
4. Information system supporting collection, analysis, and distribution of near realtime data required for nowcast/forecast. This includes independently sited and maintained meteorological stations and repeater network providing near realtime data.
5. SEA scientific database.
6. SEA project intranet.
7. Initiatives for rapid transition of model development to applications; this includes intranets supporting model application development conducted jointly with region resource managers and community organizations such as ADFG and RCAC.

For the year prior to this reporting period (i.e., FY96) the principle concern was the completion of the development and implementations needed to address the project objectives (e.g., the model modules, intranet software, and database configurations—all of them developed, coded, debugged, tested, etc.)

In contrast, at the beginning of this reporting period, the scope and function established for the six of the seven areas above (excluding herring) were “frozen,” that is, there would be minimal further development for the remainder of the project. The focus became the development of model applications in preparation for the final year in which these applications would be tested against the project objectives.

The modelling tasks of the year were still diagnostic, not yet a full, final configuration. However, the models and the diagnostic scenarios for this year had the benefit of much greater realism and completeness. Consequently, results are significant to overall objectives in ways not fully anticipated. The summaries of the project activities and results that follow illustrate several such cases.

The tasks in the areas of database, intranets, and meteorological stations and repeaters also more frequently addressed the use of existing designs and developments rather than requirements for new designs and development. It was a year of providing the needed functions, performance, and services with the present set of resources. For example, a major accomplishment this year was the incorporation of the relational database for fish developed by Willette and Saddler into the SEA database. This is described by Falkenberg in Part II of the Appendix. The SEA intranet expanded to address the new functions required by the SEA synthesis effort, and it responded to never ending demands from this office for faster and more efficient information publishing and exchange. This progress is described by Allen in Part III

of the Appendix. The meteorological station at Applegate Rock is approaching the end of its second year of nearly uninterrupted measurement of one of the regions of the sound needed for the models but not within the coverage of the NOAA navigation aid stations along the tanker lanes. In Part IV Bodnar provides an update on the system, the repeaters, and the archive.

One measure for the year is the degree to which the shape and form of the outcome of this final year of SEA has moved into clearer and sharper focus. The progress described here for the seven areas shows that during 1997 each area has by a large measure moved from open issues and pending development to well-defined functions with specifications that are increasingly stable. The pink salmon fry area closes this period with major enhancements to the problem statement, major additions to the scope of the data used with the model, a reconfiguration of the model, and good evidence that fry model simulations are providing the why and how of previously unexplained features in hatchery net pen survival data.

Pacific herring tasks have not moved fully from development, since the project schedule for herring is delayed by one year relative to pink salmon. Instead, that work has moved from the implementation plan described in January 1997 to a point at which development is nearing completion: the two development milestones for overwinter survival modelling presented in January have been completed, with documentation and algorithms distributed throughout SEA and to ADFG.

The report on the status of the circulation modelling work benefits from the graphical display of recent simulations and the important contributions from the SEA oceanography project.

The natural complement to the foregoing progress is increased efforts to maximally relate the results and progress to the end-users and resource managers. In particular, the EVOS Chief Scientist and the scientific review committee established the rapid prototyping of applications from the model development as a project objective. Therefore, this additional project area has received steadily increasing effort throughout the year. By the end of the year the benefits to the project from the increased contact with stakeholders have begun to accrue, and these exchanges have contributed substantially to wider applicability and relevance and to sharper problem statements in all areas.

Most of this report will be devoted to specific results or milestones. Taken together, however, the collection of these specifics is a source for some optimism and a positive assessment regarding prospects for seeing in one year hence an outcome that fulfills the promise of the efforts begun in the fall of 1993.

OBJECTIVES

1. Numerical model for survival of pink salmon fry during outmigration in PWS.
2. Numerical model for survival of juvenile Pacific herring during winter fasting in PWS.
3. Numerical ocean circulation model (C. N. K. Mooers, RSMAS).
4. Information system supporting collection, analysis, and distribution of the near realtime data required for nowcast/forecast. This includes independently sited and maintained meteorological stations and repeater network providing near realtime data.
5. SEA scientific database.
6. SEA project intraet.
7. Initiatives for rapid transition of model development to applications; this includes intranets supporting model application development conducted jointly with region resource managers and community organizations such as ADFG and RCAC.

METHODS

The methods differ widely among the various objectives, hence information on methods is contained in the sections reporting results for each of the seven objectives.

RESULTS and DISCUSSION: In-depth Reports

In-depth reports are presented for the pink salmon fry model, database, web systems, and weather systems. These reports are covered in individual documents, and these are summarized below. The reports for herring overwinter modelling and for circulation modelling are given in brief summary form in the next section. The in-depth reports are presented in four parts of Appendix 1.

Part I 1997 Progress toward the PWS juvenile fish production models

1997 results for models of pink salmon fry survival in PWS

The results regarding pink salmon fry models for 1997 will be in the form of technical notes. Many of these were prepared throughout the year for distribution of information. Typically the notes were distributed by the SEA intranet. Many were then also published on the SEA-ADFG_Management_Exchange web site, an test intranet used by SEA, John Wilcock, James Brady, and Bill Hauser in an effort to find topics and communication approaches that result in faster movement of findings from independent investigators to agency mission operations.

The following are summaries of the contents of those technical notes, with those items of some note in bold font.

Part I-A **The fry survival model has undergone substantial evolution** and at the end of 1997 is quite different from what it was one year ago. It is sufficiently different that **it is convenient to refer to "1997 extensions"** for there are things covered now that had not been considered prior to this past year. This report is a combination of pieces from earlier in the year and some new development and descriptions.

The first topic is a review of the issue that was the initial catalyst for much of the new developments of the past year. To that end, results are shown from model simulations from earlier in the year run specifically to demonstrate the **sensitivity of fry survival to predator abundance**.

Part I-B (described below) is included by reference. Part I-B is the Technical Note to SEA in which the predation sensitivity was resolved analytically and the nature of the system whereby that effect occurs is characterized.

The EVOS-ADFG-PWSAC fry marking program provides an invaluable window into the ecological production system for fry in PWS. **The fry model with the 1997 extensions makes much greater use of this data resource and in fact is dependent upon it.** . This is reviewed in this note, in part by borrowing liberally from a **Hatchery Data Review to SEA** that was prepared as a web

the development of the zooplankton bloom and the occurrence of a large increase in alternative prey.

It is not uncommon to have a survival **maximum in the middle of the release series. This maximum occurs in model simulations** when preceding and following pre-releases overlap in space during outmigration providing fry self-sheltering as alternative prey, i.e., the so-called **predator swamping**.

During the last quarter of the year the process was begun that will provide end-users with a **specification for the data and the data analysis needed to accomplish the “tracking” objectives**. This notion of “analyzed data”—data wherein substantial value is added by an analysis, data fusion, or an application of a model—can be useful in this context once adequately defined. During the last quarter of 1997 several investigators set out to prepare prototypes of such data sets for use with the simulations described in this report. **Willette provided several such analyzed datasets for 1994: i) temperature for the upper 20m of the water column in the western passages; ii) adult fish species, density, size, and length by space-time strata from the predator net-sampling; and iii) diet data for predators. Cooney and Coyle prepared analyzed datasets for 1994 and 1995 based on a new analysis of the hatchery-watch time series. This provided hitherto unavailable high sampling frequency information on biomass, timing, and stage for euphysiids and pteropods. A third analyzed data set for herring was provided by Stokesbury but has not yet been incorporated into the model.**

1997 progress toward the SEA database

Part II Database. C. S. Falkenberg

C. S. Falkenberg provides a report on the database. The continuing updates and maintenance of those parts of the database that have complete schemas and documentation is an easily overlooked and underappreciated responsibility. More visible are the two new additions. The acoustic surveys conducted with ADFG for the herring and pollock fishery have been included in the SEA database. These data are a key contributor to an analyzed data product regarding predator pressures on fry. Now that data is integrated into the data system. Second, the fish database from M. Willette has been included. This is a major contribution to the data system for that archive had the benefit of many years of refinement and development by Willette and Saddler. The goal is to retain all of the functionality they developed, plus have it compatible with the additional query capabilities of the SEA datasytem.

1997 results and contributions from the SEA intranet

Part III-A Web-based Communications. J. R. Allen

There is one feature that is common to the numerical models, the database, and the SEA intranet: all three are “containers” in which to preserve, present, and make relevant and functional the work of each of the SEA projects. All of us that work on these “containers” have the responsibility to ensure that it is always evident that what is contained is the important contribution. The containers are successful only if the things contained become saved and retrievable in coordinated ways, seen and known in their cumulative, interrelated context, and used to solve problems through their quantitative representation in models. A project management lesson learned from SEA is the value this common feature has as a measure of project performance and status for multi-component projects.

J. R. Allen reports on the progress of the SEA intranet as the inter- and intra-project communication “container” of project results. The report provides a good snapshot of the status of the web on the three key issues at the close of the fourth year: synthesis, models, and relevance. In September the first components were begun for the web resources to “contain” and communicate the development the synthesis document. The model “containers” are increasing in number. Lastly, the means for co-development with the end-users served by SEA has been underway in test mode for some time; The status with that effort is described.

Part III-B Draft manuscript based in part on the paper presented at the 127th Annual Meeting of the American Fisheries Society, Monterey, CA, August 27, 1997: Scientific Visualization Methods for Marine Ecosystem Research: Case Studies Using AVS for Display of Hydroacoustic Data, J. R. Allen, E. V. Patrick, R. Kulkarni, G. L. Thomas, and J. Kirsch.

1997 progress toward the SEA observing system

Part IV Weather Data Systems.

The term “observing system” is another of those terms that has been adopted from another field. It is used in meteorology and oceanography to refer collectively to all observations that must be made and then delivered on some pre-determined schedule to sustain some modelling or analysis objective. The meteorological observing system is the first component of an observing system suitable for the “tracking” models from SEA. This component has gotten first attention because of the immediate need for the support of the circulation. It is also the easiest component to tackle first since near realtime data is a very well established practice in meteorology: for example, all instrument observations from NOAA buoys in PWS are available via the Internet within 30 minutes. Our own Applegate Rock station data is posted via the web every 24 hours solely because of cost and power constraints. S. Bodnar provides the technical update for 1997 on the

operation, maintenance, and performance of Applegate Rock and on related work to automate the data collection from all contributing stations.

RESULTS: Summary Reports

1997 results for models for survival of Pacific herring in PWS during winter fasting.

The model development had two parts. The first of the two was one of the first tasks of 1997, for there was a need to directly resolve a program planning question: Could historical herring fishery data together with historical climate information be useful in a statistical review of overwinter fasting and herring population formation? A second question was addressed in the last part of the year, the question of the model form most appropriate for the task of projecting the impact of a specific winter scenario given a specific measurement protocol.

The problem statement is that prepared for the EVOS Review of SEA-herring in February, 1997. In particular, the model work addressed **first a satisfactory formulation for the simpler problem of inactive fasting.**

An existing Wisconsin-type bioenergetics model for juvenile Baltic herring was used to estimate the consequences of deviation of winter mean ocean temperature from climatological winter mean temperature on the fasting basal metabolism of juvenile Pacific herring. Estimated relative change in metabolism is 5% per degree centigrade. For example, a 2 C increase in the winter mean water temperature results in a decrease in fasting survival time of approximately 10%. Based on this result it is conjectured that climate and winter fasting survival alone, in the absence of information on energy reserves, would exhibit poor correlation.

The linear regression of model of Paul and Paul (1996) can be used as is for a first estimate of the effects of fasting. The question then is what second order effects, if any, need consideration to achieve the SEA objectives. The adjustment to tackle first appears to be the underestimation of overall time for survival. For example, all fish were less than 6.0kJ/gm(wwt). The regression estimate for basal metabolic losses during the 56 day winter test series was 23.3J/gm/da. This implies 100% mortality at 120 days. The companion test for survival time had 38% alive at 120 days. The same loss rate applied to the mean of 5.2KJ/gm(wwt) and the minimum 4.3KJ/gm(wwt) predicts 50% mortality at 86 days and the onset of mortality at 47 days. The study had the first fatality at 50 days, and 80% surviving at 86 days.

The task was to find the suitable next generation formulation for losses during inactive winter fasts. **Models of inactive fasting for juvenile herring were developed using a range of approaches, from the basic Wisconsin model to the two-mass (e.g., structure and reserve mass, or protein and lipids) bioenergetics models of N. Broekhuizen *et al* (1994) and W. S. C. Gurney *et al* (1990).**

1997 results for a Princeton ocean model for Prince William Sound

At the conclusion of 1997 simulations based on 1996 data were being conducted. These were full year simulations using monthly mean forcing. This is one of several validation steps, and brings the validation sequence to about the halfway point. The most recent **runs have for the first time included fresh water input**. This addition has contributed significantly to the model findings. Completion of a suitable freshwater submodel is a first priority in the coming months.

Recent progress has been made with the addition of fresh water input. There is additional progress toward completion of the full complement of forcing data with the design and development of a **“subjective” interpolation method for a gridded analysis of surface wind fields using the existing PWS meteorological stations**. This interpolation is based on local knowledge of the wind field structure for given seasons and atmospheric conditions. An initial set of specifications was provided by Patrick Kearney, pilot with Cordova Air. The longer term requirement is for a much more contemporary approach to surface winds. These longer term considerations benefited from discussions with Dr. J. Tilley of the GeoPhysical Institute at UAF. This is joint work of this project and D. Eslinger.

Two manuscripts accepted during 1997 are attached in Appendix 2.

The paper “A three-dimensional tidal model for Prince William Sound, Alaska” by J. Wang, C. N. K. Mooers, and V. Patrick was accepted for presentation and will appear in the forthcoming volume *Computer Modelling of Seas and Coastal Regions III*.

The journal *Continental Shelf Research* accepted for publication in the JONSMOD '96 Special Issue the manuscript “A two-compartment model for understanding the simulated three-dimensional circulation in Prince William Sound, Alaska” by E. Dellersnijder, C. N. K. Mooers and Jia Wang.

PROJECT BIBLIOGRAPHY

See also bibliographies of manuscripts included as Appendices

Blumberg, A. F. and G. L. Mellor, 1987. A description of a 3-D coastal ocean circulation model. In *Coastal and Estuarine Sciences 4*, N.S. Heaps, ed., Amer. Geophys. Union, Washington D.C. pp 1-16.

Brandt, S. B., D. M. Mason, and E. V. Patrick. 1992. Spatially-explicit models of fish growth rate. *Fisheries*, 17(2) pp 23-35.

Deleersnijder, E., J. Wang and C. N. K. Mooers, 1997. A two compartment model for understanding the simulated three-dimensional circulation in Prince William Sound, Alaska. *Continental Shelf Research*, JONSMOD '96 Special Issue (to appear).

Eslinger, D. L., 1990. The effects of convective and wind-driven mixing on springtime phytoplankton dynamics as simulated by a mixed-layer model, 127pp., Ph. D. Dissertation, Florida State University.

Falkenberg C. S. and R. Kulkarni 1995. Using Spatial Access Methods to Support the Visualization of Environmental Data. In *Proceedings of Visualization '95*, Atlanta GA, November 1995, IEEE Computer Society Press, pp 400-403.

Gallacher, P. C. and P. A. Rochford, 1995. Numerical simulations of the Arabian Sea using tracers as proxies for phytoplankton biomass. *J. Geophys. Res.*, 100, pp 18,565-18,579.

Gerritsen, J., and J. R. Strickler. 1977. Encounter probabilities and community structure in zooplankton: a mathematical model. *J. Fish. Res. Board Can.* 34 pp 73-82.

Godin, J.-G. J. 1981a. Effect of hunger on the daily pattern of feeding rates in juvenile pink salmon, *Oncorhynchus gorbuscha* Walbaum. *J. Fish Biol.* 19 pp 63-71.

Godin, J.-G. J. 1981b. Daily patterns of feeding behavior, daily rations, and diets of juvenile pink salmon (*Oncorhynchus gorbuscha*) in two marine bays of British Columbia. *CJFAS* 38 pp 10-15.

Godin, J.-G. J. 1984. Temporal variation in daily patterns of swimming activity and vertical distribution in juvenile pink salmon (*Oncorhynchus gorbuscha*). *Can. J. Zool.* 62 pp 72-79.

Howick, G. L., and W. J. O'Brien. 1983. Piscivorous feeding behavior of largemouth bass: an experimental analysis. *Trans. Am. Fish. Soc.* 112 pp 508-516.

Mason, D. M., and S. B. Brandt. 1996. Effects of spatial scale, capture efficiency, and the spatial distribution of predators on the predictions made by spatially-explicit models of fish growth rate. *Environmental Biology of Fishes*, 45(3) pp 283-298.

Mason, D. M. and E. V. Patrick. 1993. A model for the space-time dependence of feeding for pelagic fish populations. *Trans. Am. Fisheries Soc.*, 122(5) pp 884-901.

Mooers, C. N. K. and D.-S. Ko. 1994. Nowcast system development for the straits of Florida. *Estuarine and Coastal Modelling III, Proc. of the 3rd Intern. Conf.*, pp 158-171.

Mooers, C. N. K. and Wang, J., 1996. The second generation of the Straits of Florida nowcast/forecast system. In *Conference on Coastal Oceanic and Atmospheric Prediction*, Atlanta, Jan. 28-Feb. 2, American Meteorological Society, Boston, pp 28-35.

Mooers, C. N. K. and Wang, J., 1997. On the Development of a Three-Dimensional Circulation Model for Prince William Sound, Alaska. *Continental Shelf Research*, in press.

Niebauer, H. J., T. C. Royer and T. J. Weingartner, 1994. Circulation of Prince William Sound, Alaska. *J. of Geophysical Research*, 99, pp 14,113-14,126.

Stonebreaker, M. 1994. Sequoia 2000: A Reflection on the First Three Years. *IEEE Computational Science & Engineering* Winter 1994, pp 63-72.

Wang, J. and C. N. K. Mooers, 1996. Modelling Prince William Sound ocean circulation. In *Conference on Coastal Oceanic and Atmospheric Prediction*, Atlanta, Jan. 28-Feb. 2, American Meteorological Society, Boston, pp 36-43.

Wang, J., L.A. Mysak and R.G. Ingram, 1994. A 3-D numerical simulation of Hudson Bay summer circulation: Topographic gyres, separations and coastal jets. *J. Phys. Oceanogr.*, 24, pp 2496-2514.

Wang, J., C. N. .K. Mooers and V. Patrick, (to appear) A Three-dimensional Tidal Model for Prince William Sound, Alaska. *Computer Modelling of Seas and Coastal Regions III*, Proceedings of the third international conference, Computational Mechanics Publications, Southampton.

FIGURES

Figure 1.

Figure 2.

Figure 3.

Figure 4.

Figure 6.

Figure 7.

Figure 8.

Figure 9.

Figure 11.

Figure 12.

Figure 13.

Figure 14.

Figure 15.

initial conditions common for all scenarios: temperature = 9C, fry growth rate = .03 gm/gm, pseudocalanus density is constant = 200 m^{-3}

double both fry and pollock densities

fry density = $0.5 \times 10^{-1} \text{ m}^{-3}$
 pollock density = $0.9 \times 10^{-4} \text{ m}^{-3}$

same

fry density = $0.5 \times 10^{-1} \text{ m}^{-3}$
 pollock density = $0.45 \times 10^{-4} \text{ m}^{-3}$

50%

fry density = $2 \times 0.5 \times 10^{-1} \text{ m}^{-3}$
 pollock density = $2 \times 0.9 \times 10^{-4} \text{ m}^{-3}$

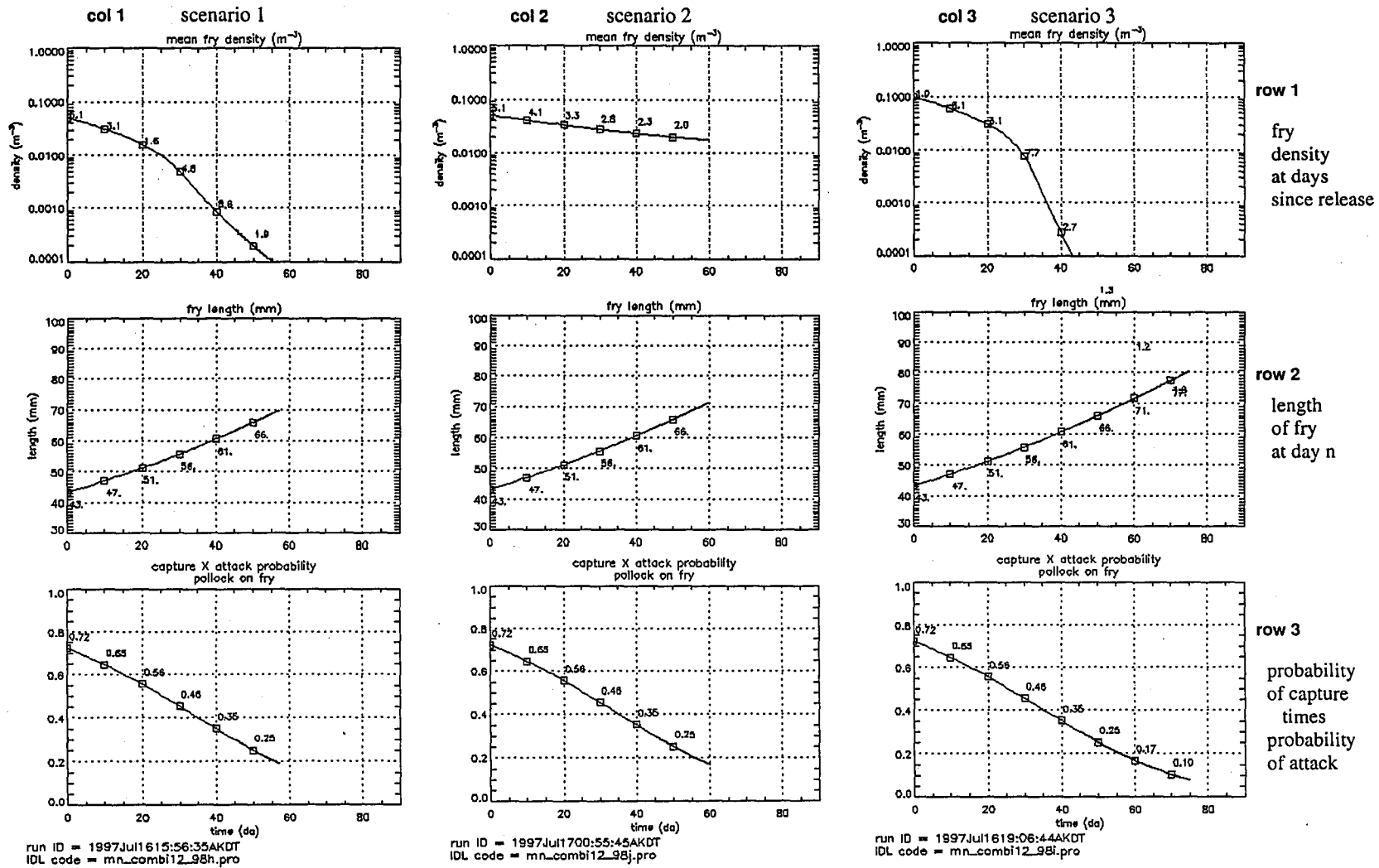


Figure 1. Three diagnostic runs for adult pollock predation on fry. The scenario assumes no prey for pollock other than pink salmon fry. Fry feed on pseudocalanus.

temp = 9C

coupled populations
 time(hr): start = 120.75; interval = 0.25
 present time = 240.00hr = 10.00da
 nodes = 5
 dx = 750.0m

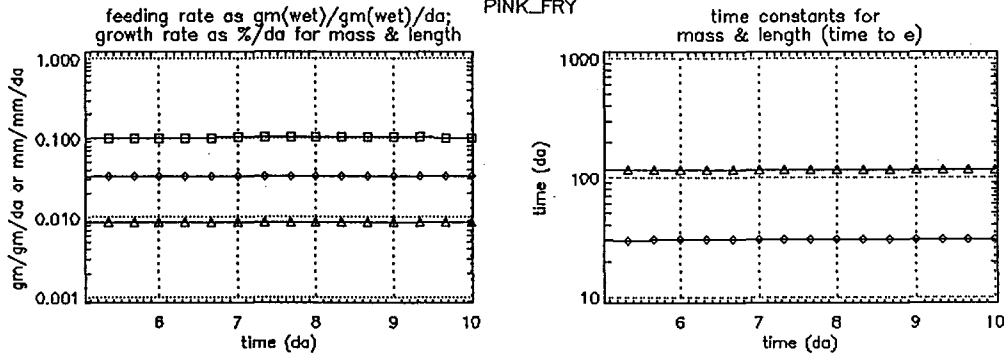
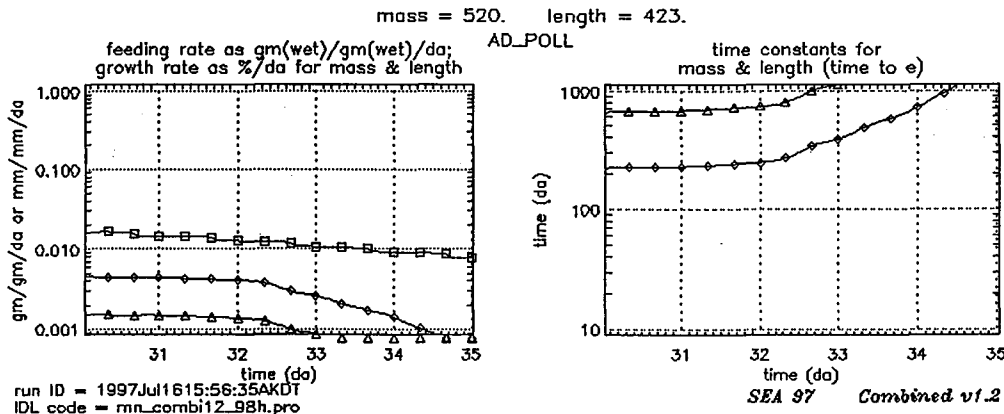
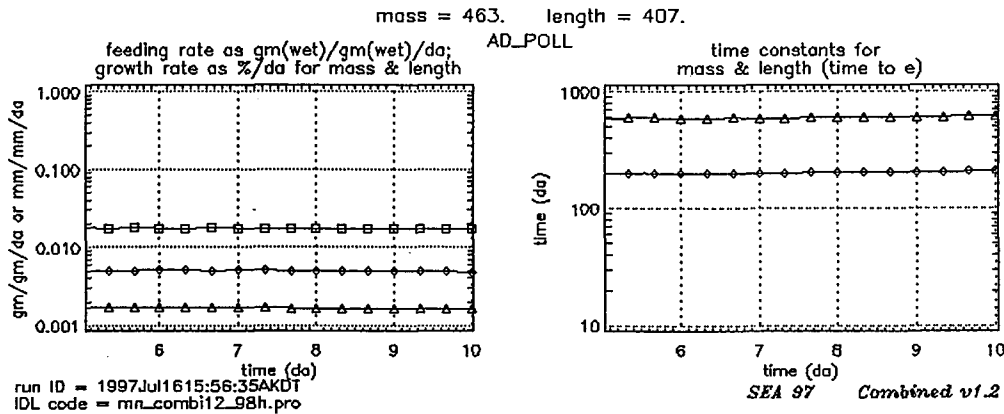
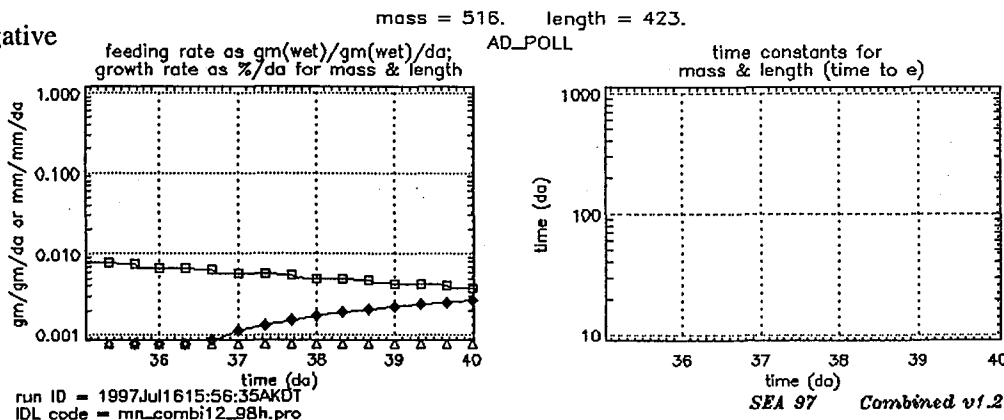


Figure 2.

Rates for consumption, mass change, length change



Note fry density in Figure 1 corresponding to day at which the mass gain goes negative



The SEA problem statement for pink salmon: Survival during outmigration through PWS; Survival in GOA

Fri Sep 5 04:21:47 A KDT 1997

Some recent issues with the fry model, recent discussions regarding synthesis, reminders about sponsor's expectations, and a bit of prior mathematics conditioning all bring to mind the need to continually reexamine and refine the problem statement.

The following is my understanding of the problem statement for pink salmon, and this version should be corrected as needed.

The SEA problem statement for pink salmon is

to forecast the survival of hatchery pink salmon fry during their period of outmigration in PWS using initial conditions for hatchery fry releases provided by the hatcheries and the combined contributions from all of the collaborating disciplines in SEA. These latter provide the physical conditions and the population densities for prey, alternative prey, and predators during outmigration sufficient for the forcing and boundary conditions of the combined model for nowcasting of fry survival.

A further part of the problem statement is

to apply an estimate for survival for the ocean (GOA) phase of pink salmon and thereby forecast an upper bound for adult salmon returns for the following year.

Spatial context of the problem statement

The map at the right shows the spatial context for the problem statement. This map and several companion maps were prepared to describe specific space-time survival issues (hatchery interactions, aggregation in the south in late August, fry density). It is shown here since it seems a simple reminder of both spatial and multidisciplinary aspects of the problem statement. The symbols N_s , N_c , N_w , N_a refer to the total released at Solomon Gulch, Cannery Creek, WHN (Ester), and AFK. The symbols S_{pws} and S_{ocn} refer to survival during PWS and the oceanic periods, respectively.

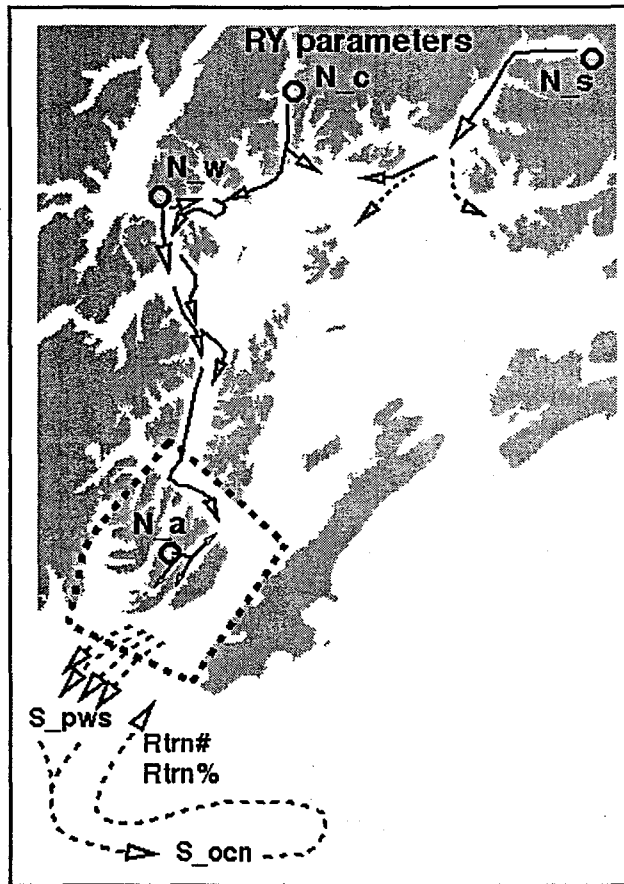


Figure 3. Revisiting the problem statement for pink salmon.



PWS hatchery data

a brief review of data prior to and data since 1994

Fri Sep 5 03:50:00 A KDT 1997

The four pink salmon hatcheries in Prince William Sound provide ADF&G with datasets for their fry releases and the resulting adult returns. Since 1989 a single data record is associated with a unique coded-wire tag group code. Each record has fields for time of release (day, month, year), mean mass at release (gm), duration of release (days), number of fry released, and the percentage of released fry that return the following year.

The SEA problem statement for pink salmon fry is inherently dependent upon the hatchery data for

- a. initial conditions for time, number, and individual mass for hatchery fry released into the system;
- b. accurate survival information for the hatchery component of the fry population, information which is to serve as the final arbitrator of the efficacy and reliability of the SEA coupled models.

This review was motivated initially by modelling issues. During the review, however, the statement above regarding the role of the hatchery data in determining the success of SEA came into greater relief, in part because of recent planning and discussion regarding synthesis. This "report to SEA" is in part shaped by the possible utility in the emerging discussions.

The data reviewed has been provided by Mark Willette. This review is a straightforward assessment of scope and those aspects of the content that (seemingly) require no subtle statistics. Mark has carried out statistical analyses that are not described here. It is hoped that we can get these posted on the web in the near future.

There are two periods to the data. Data for release years 76 through 87 consist solely of release numbers, returns, and survival for the year for each of the four hatcheries based upon estimates without the use of coded wire tags. Data for 88 through 95 is substantially more complex because of the introduction of coded wire tags.

Possibly the greatest motivation for a review is the fact that (to my knowledge) the hatchery data for release years 94 and 95 --- data which became available since the preparation of the SEA Science Plan --- has not been widely reviewed within SEA.

This review of PWS hatchery data consists of:

- **Part 1: yearly means** Sat Sep 6 18:37:54 A KDT 1997
 - cumulative variables for the entire PWS-system;
 - variables for each hatchery;
- variables by *release-day* and by *tag-group*
 - **Part 2a: data summaries; opportunities for synthesis** Sun Sep 7 12:50:09 A KDT 1997
 - **Part 2b: background & misc reviews** Sun Sep 7 22:15:56 A KDT 1997
 - cumulative for the entire PWS-system;
 - variables for each hatchery;
- **Part 3: one view of PWS and GOA survival** Mon Sep 8 07:16:18 A KDT 1997
 - progress of each tag-group under one set of (too simple) assumptions regarding
 - time from release to return
 - the "development time" for observed survival differences.
- **QC Notes: Remarks, further information, clarifications, requested fixes** Thu Sep 11 16:53:57 A KDT 1997

Figure 4. Opening page for web-published overview of PWS hatchery data.

pink salmon
total_return/total_release for PWS hatcheries

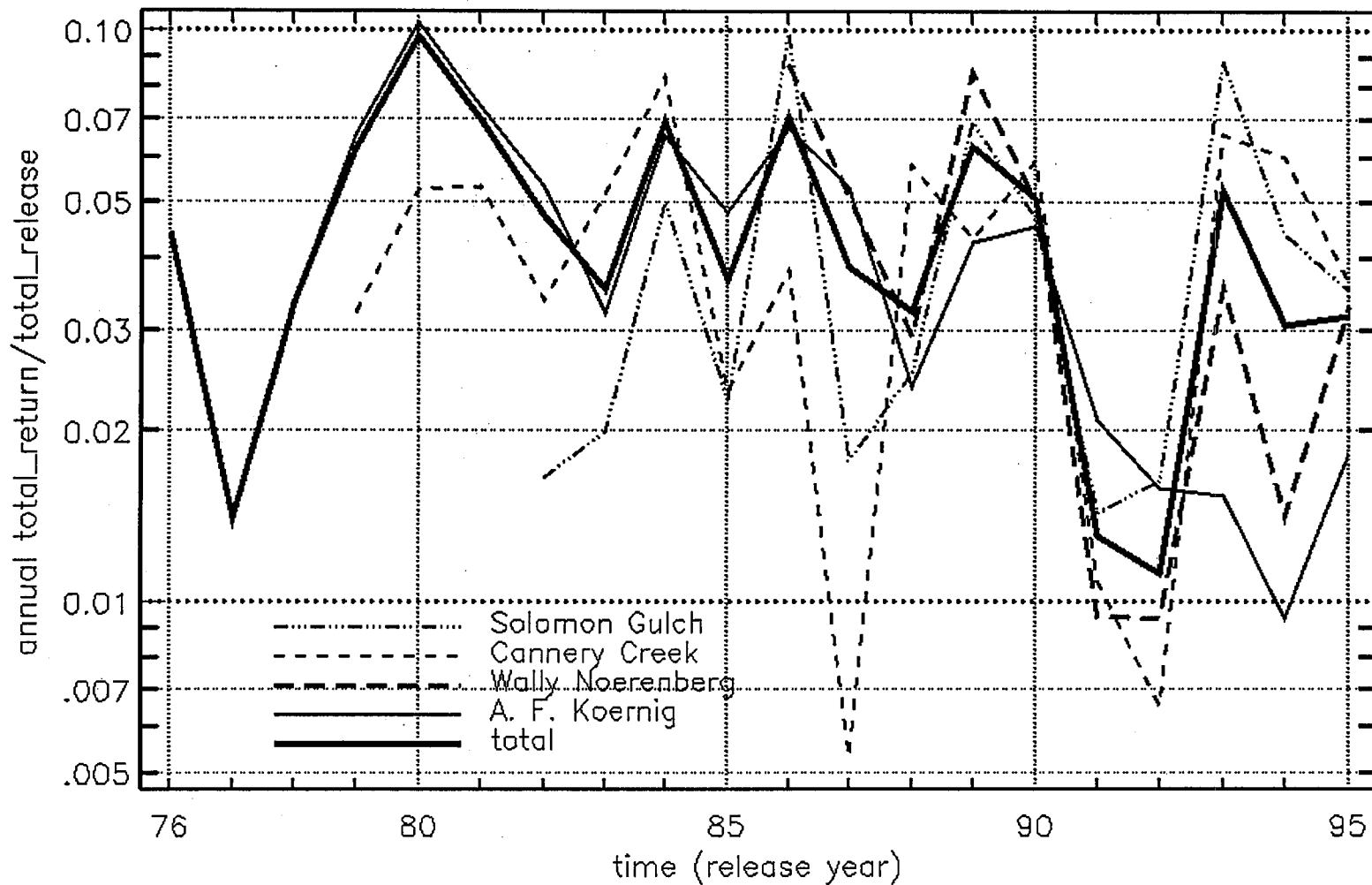


Figure 5. Annual total_return/total_release for each hatchery and for the four PWS hatcheries combined.

Release variables and release/return (for day) for
 o Solomon Gulch

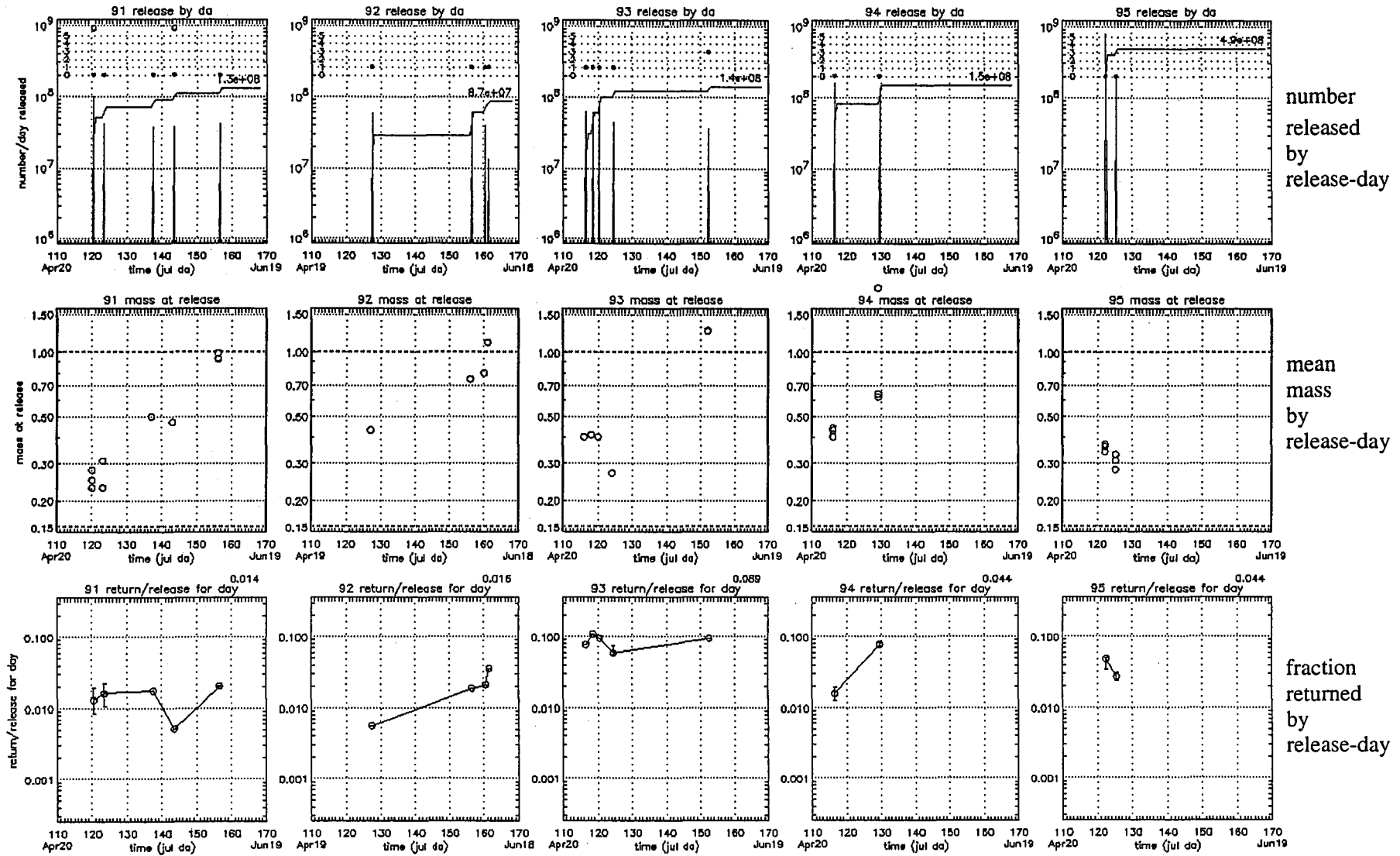


Figure 6. Number released, mass at release, fraction returned for Solomon Gulch, 91-95 release years

Release variables and release/return (for day) for
 □ Cannery Creek

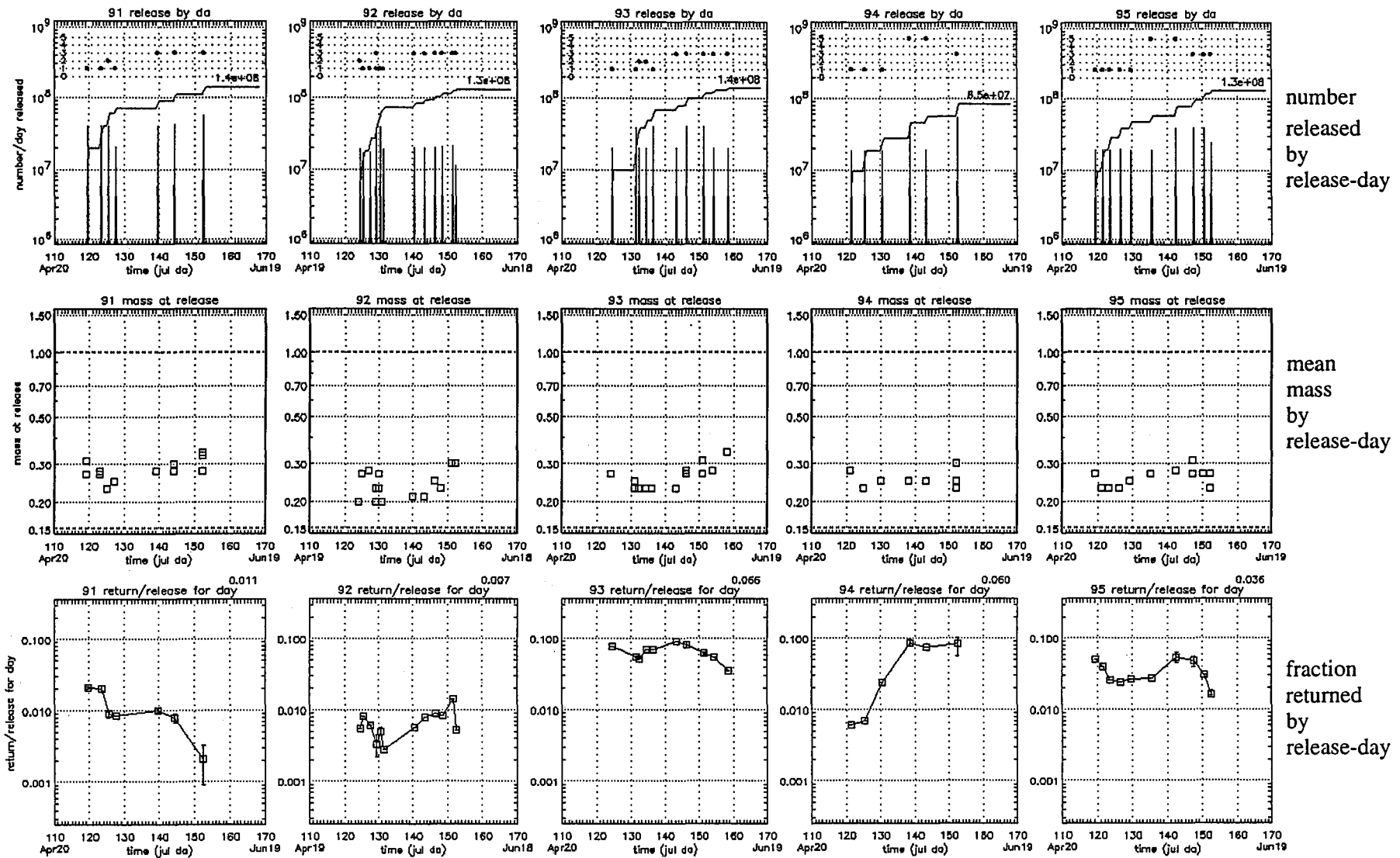


Figure 7. Number released, mass at release, fraction returned for Cannery Creek, 91-95 release years

Release variables and release/return (for day) for
 Δ Wally Naerenberg

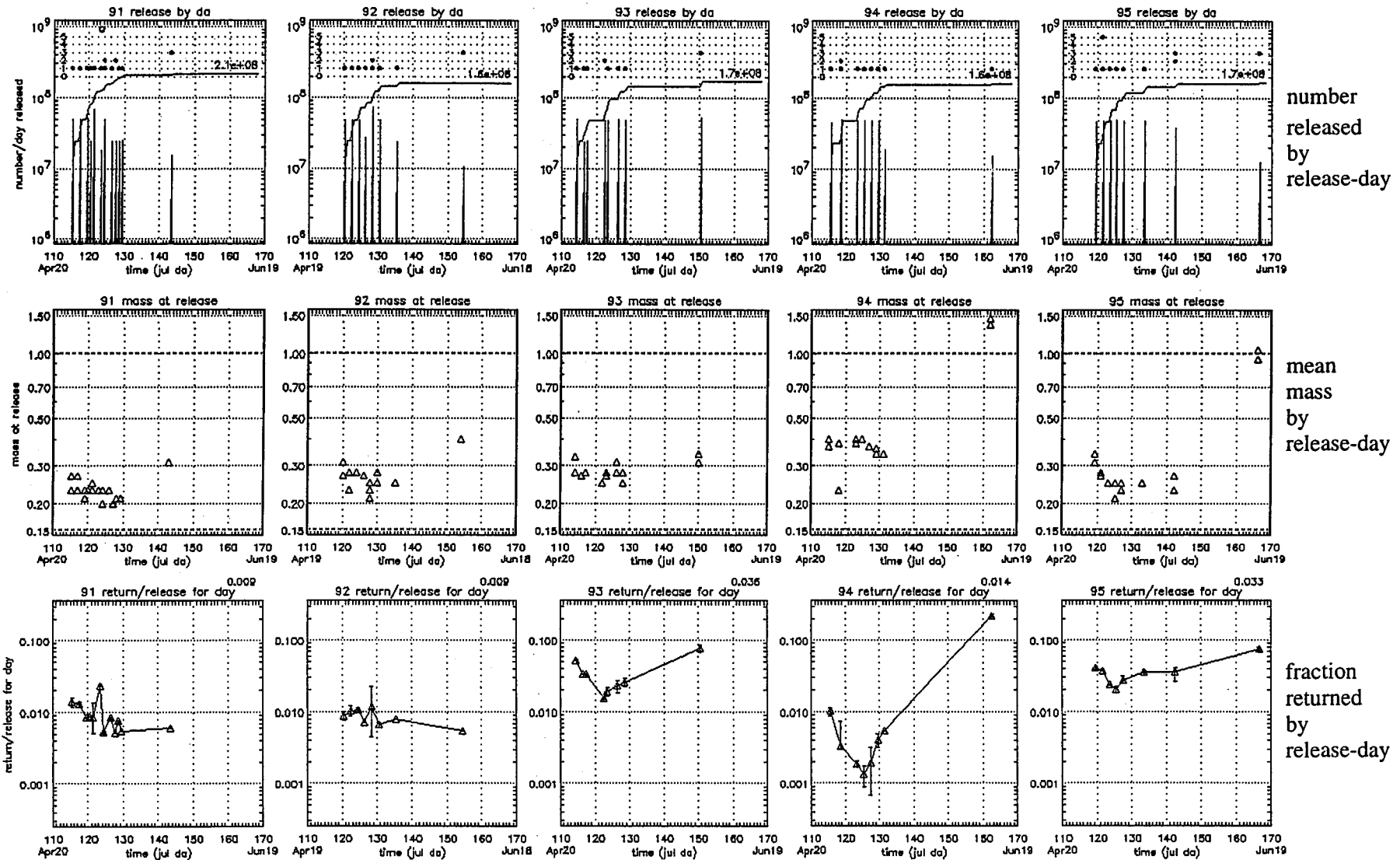


Figure 8. Number released, mass at release, fraction returned for WHN, 91-95 release years

pink salmon hatchery fry
 return/release for return & release summed over day
 error bar indicates day with multiple releases, height corresponds to observed survival range

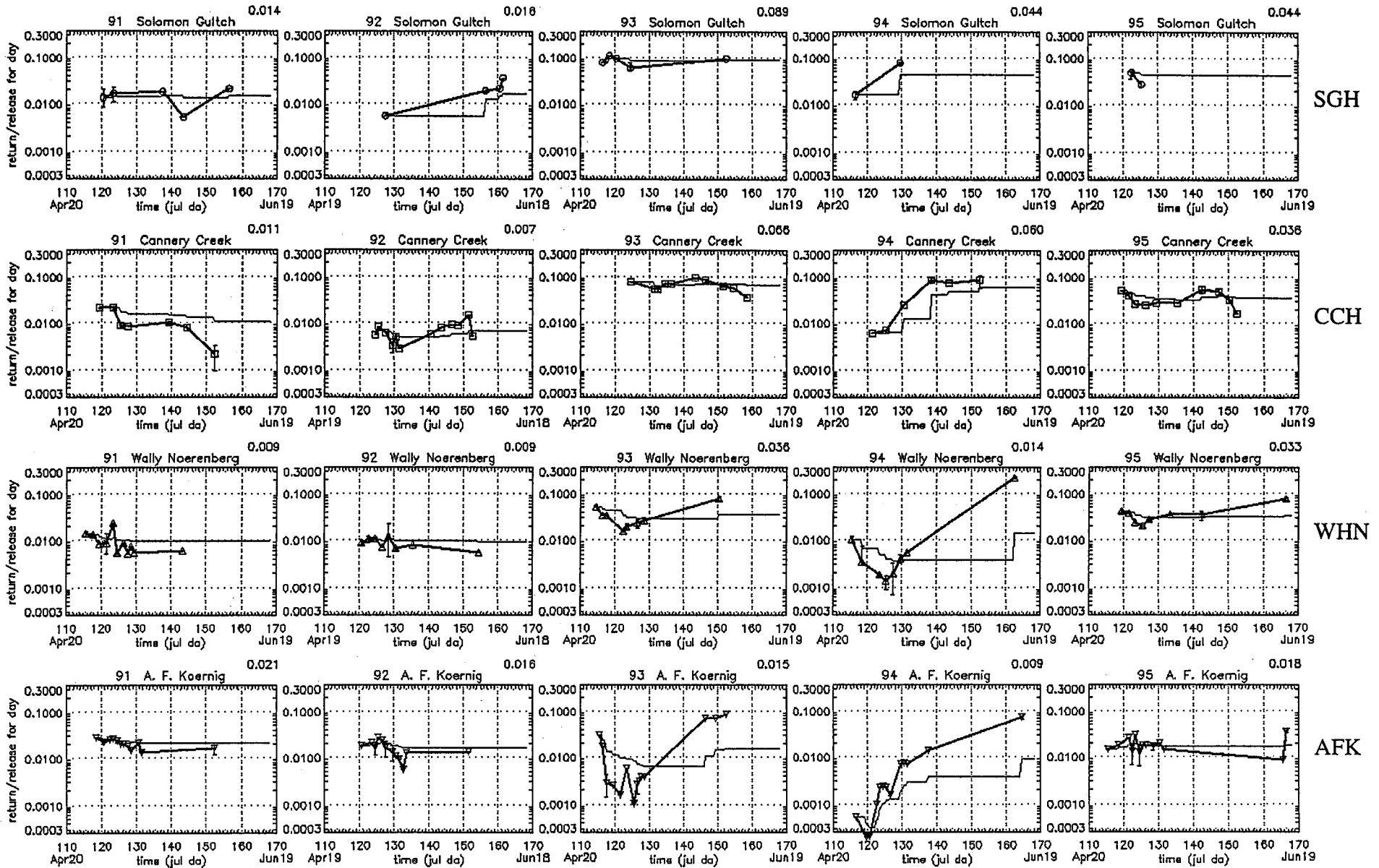


Figure 10. Fraction returned by release-day (bold line between data pairs)
 Running tally of returns/released up through release date (faint line)
 91-95 release-years arranged: north to south = top to bottom

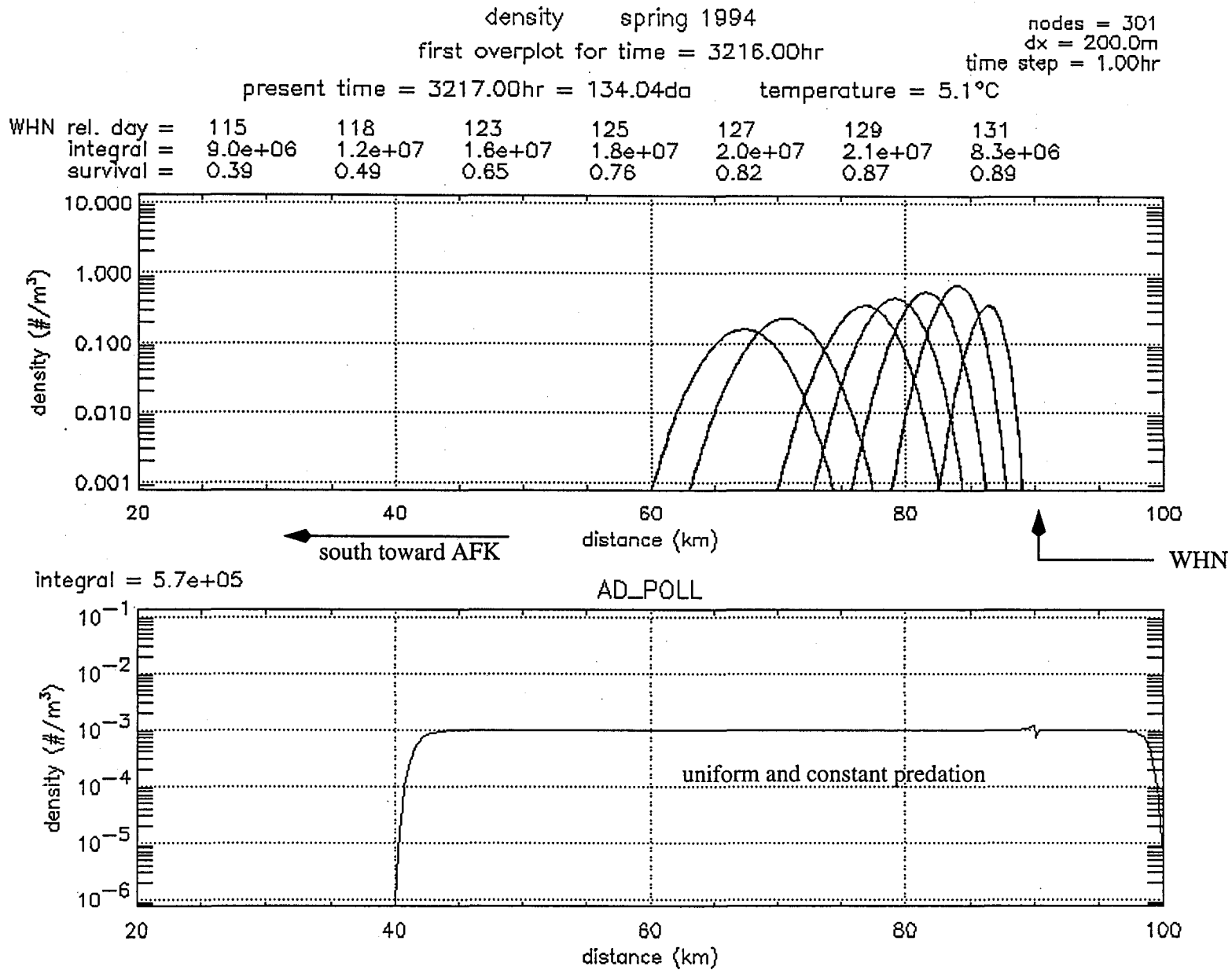


Figure 11. Snapshot of fry survival model "tracking" each group of pens with common release-day.

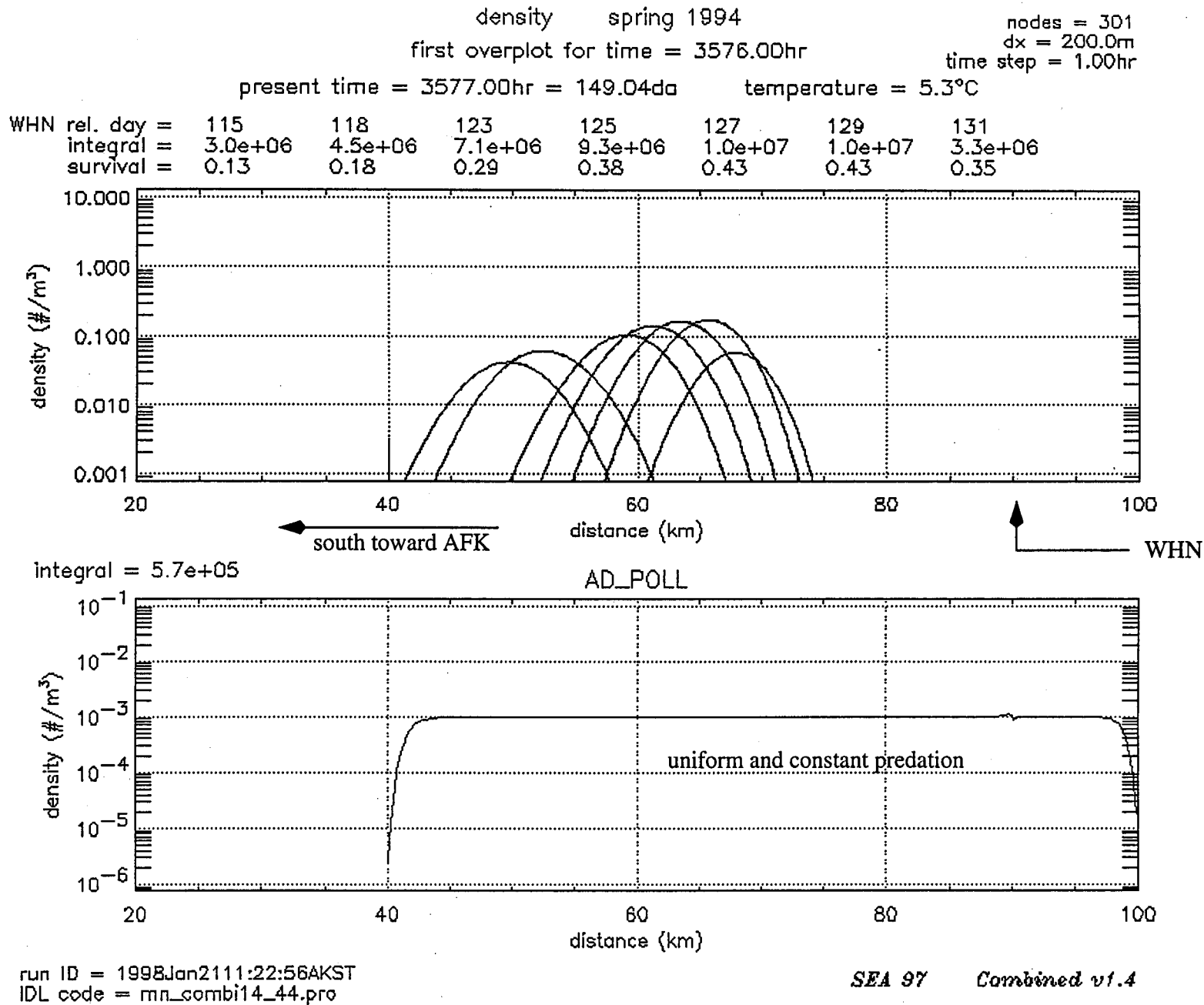
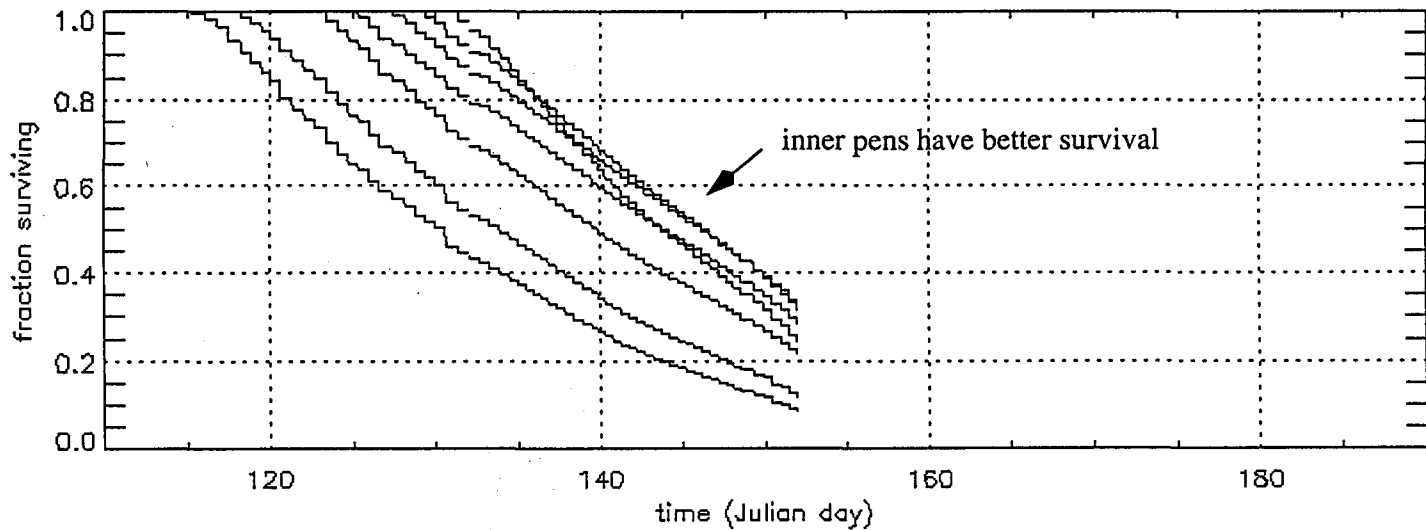
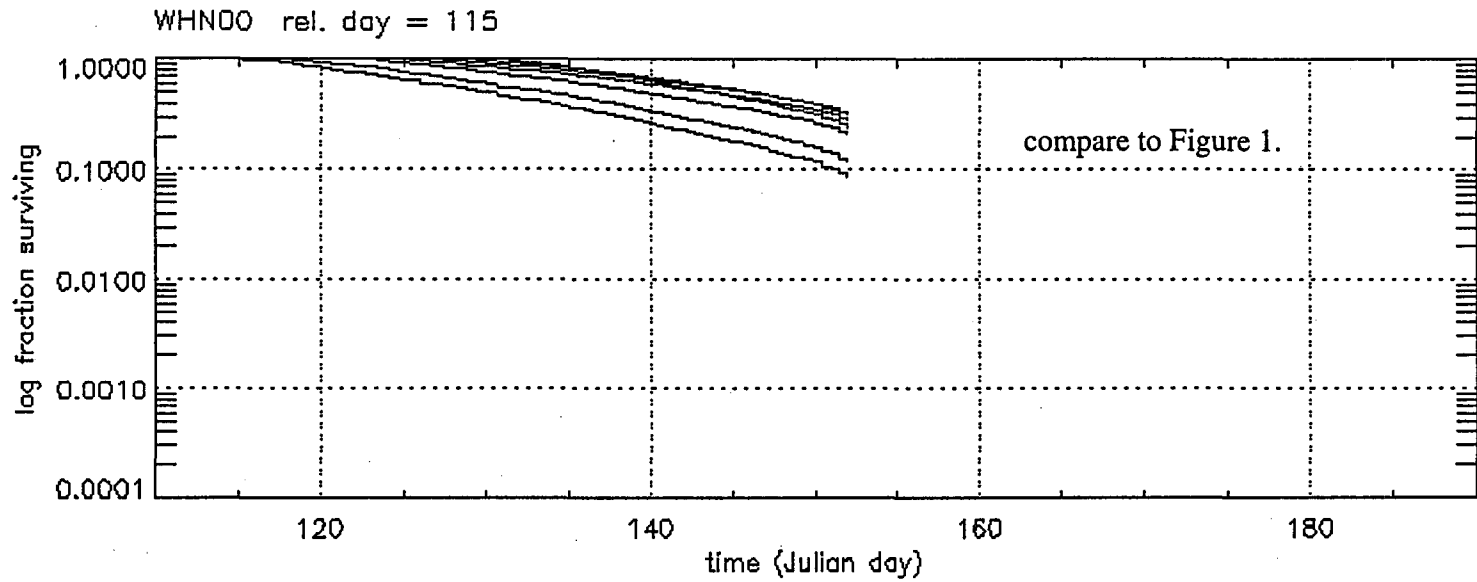


Figure 12. Snapshot of fry survival model "tracking" each group of pens with common release-day. At Julian day 149

survival by release day spring 1994
present time = 3647.00hr = 151.96da

nodes = 301
dx = 200.0m
time step = 1.00hr



run ID = 1998Jan2111:22:56AKST
IDL code = mn_combi14_44.pro

SEA 97 Combined v1.4

Figure 13. The same as Figure 1, but with tracking of each release-day.

Configuration of Systems used in simulations

Initial conditions according to WHN 1994

8 distinct release days

115, 118, 123, 125, 127, 129, 131, 162

fry stock structure = release days

8 discrete fry stocks

initial stock abundance = number released

initial individual mass = mean individual mass at release day.

Scenario for simulations

release site: WHN (at 90km mark)

duration of release: instantaneous

fry diffusivity: $0.088 \text{ m}^2 \text{ sec}^{-1}$

fry forage: pseudocalanus 200 m^{-3}

fry predator(s): equiv. of:

adult pollock 475mm, 700gm

distribution: uniform (wrt. model domain)

diffusivity: $0 \text{ m}^2 \text{ sec}^{-1}$

fry predator forage: fry (only)

(assumes no alternative prey)

Neocalanus: 0 m^{-3}

model manifold: 1d space x time

model 1d coordinate represents:

shore to 500m offshore

upper 20m

along

1d path from Solomon Gulch to AFK

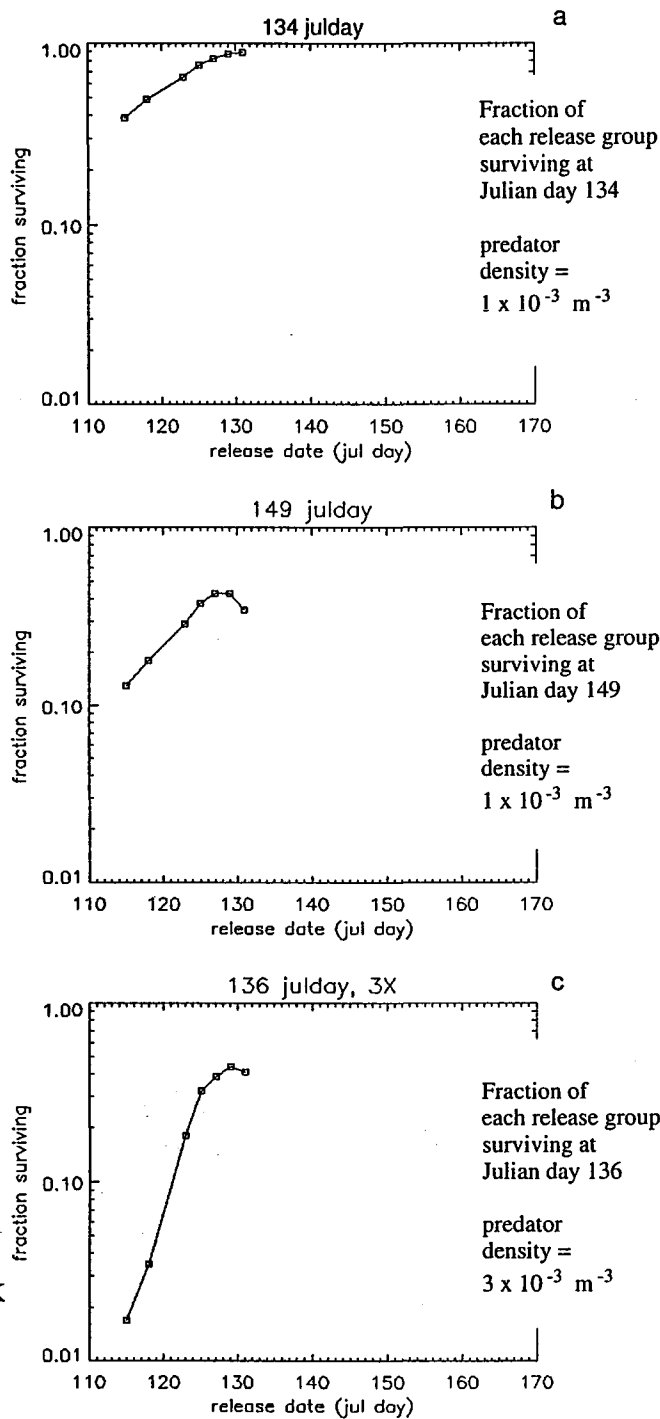


Figure 14. Simulation results from the SEA pink salmon fry model with 1997 extensions.

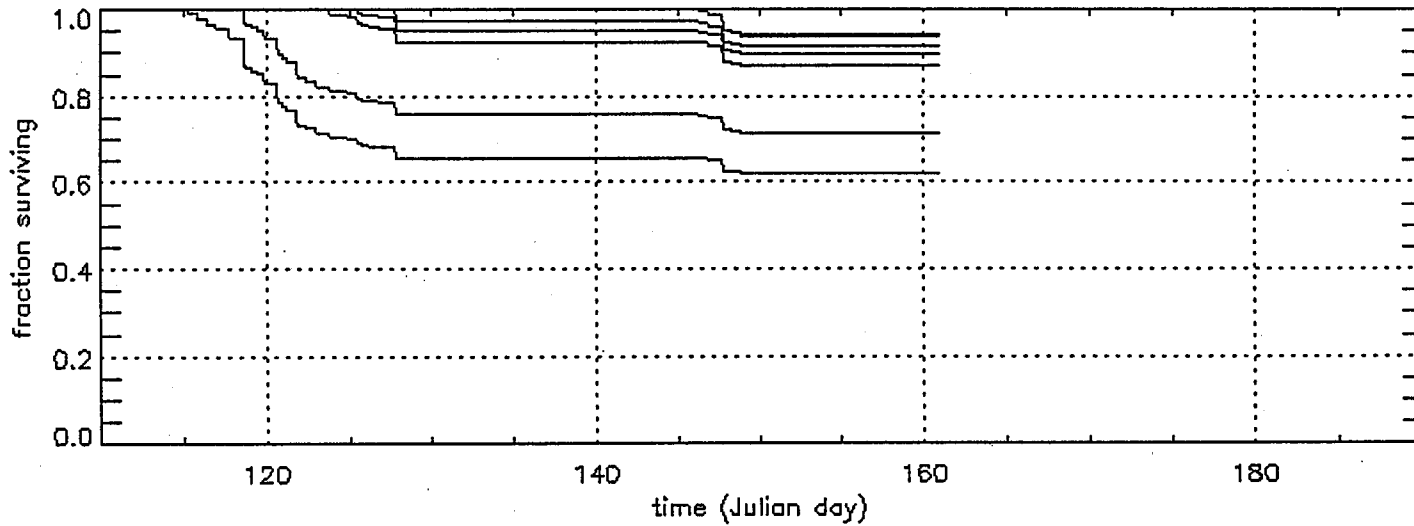
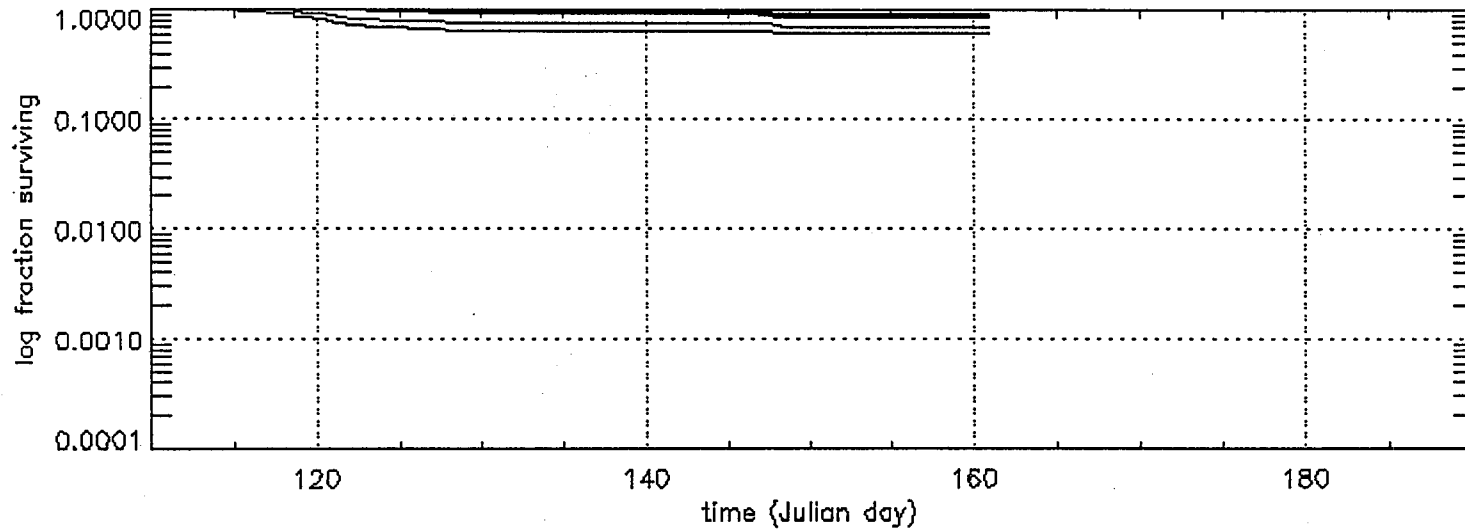
With 1997 extensions the models are capable of tracking production processes for any and all partitions and groupings of fry releases. The 1997 extensions enable production tracking at the maximum resolving power of contemporary fry marking and tagging technologies.

This figure illustrates the function of the new 1998 extensions: PWS ecosystem production processes and PWSAC pre-release hatchery production are modelled jointly, i.e., as a single "plant." With 1998 extensions optimal value problems requiring optimization across both the ecosystem and the hatchery can be considered.

survival by release day spring 1994
present time = 3863.00hr = 160.96da

nodes = 301
dx = 200.0m
time step = 1.00hr

WHN00 rel. day = 115



run ID = 1998Jan2509:11:26AKST
IDL code = mn_combi14_46z.pro

SEA 97 Combined v1.4

Figure 15. The same as Figure 1, but with diversion of predation due to zooplankton bloom development

APPENDIX 1

Part I-A
Technical note to SEA
1997 findings from the EVOS-ADFG-PWSAC fry marking programs and
from models for survival of pink salmon fry during migration thorough PWS

Technical note from SEA
1997 findings from
the EVOS-ADFG-PWSAC fry marking programs
and results from
the models for survival of pink salmon fry
during migration through Prince William Sound, AK *

J. E. H. SEA and M. N. R. SEA¹

Summary

The SEA Project is developing physical-plankton-nekton models for the survival of juvenile fish in Prince William Sound. This reports results from the nekton model for juvenile pink salmon. The model is a space-time model in which models for foraging, gut evaluation, and bioenergetics are embedded within diffusion-taxis models for the dispersion of all interacting nektonic species of the subsystem.

During model testing at the end of 1996, fry survival was found to be non-linearly related to predator density. The nature of this dependence was the starting point of work in 1997, for this dependence is the foundation upon which prey-switching occurs.

This note reports first on how the non-linearity shows up in a simulation of survival. A companion document provides an analysis whereby an approximation is established that explains the behavior. Next, the available data is reviewed for evidence of this effect. The result of that search brings to light new factors that have guided the addition of new extensions to the way the model is used.

* Sponsored by The Exxon Valdez Oil Spill Trustee Council, Anchorage, AK
Restoration Project 97320

¹ J, E, H, M, N, and R identify projects of the Sound Ecosystem Assessment (SEA) Program.
www.pwssc.gen.ak.us/sea/sea.html

1 Fry survival trials with the 1996 SEA model

Fry survival and macrozooplankton

By the end of 1996 all of the nekton responses identified in the SEA hypotheses had been written as model components of the fry survival model. Each of the components had been tested during development. Earlier in the year the numerical solutions for the overall system of equations had been rewritten and recoded and had undergone substantial checking and testing. The newly added model components were relatively straightforward functions within the overall system. With this confidence in the system code and in the code for the new modules, it remained only to begin simulations with all of the parts in place. A full chronology of this period is described in the SEA *FY96 Annual Report*, Ch 7, pp 11-14.

There was much changed within the model during 1996—bioenergetics and dispersion models were combined, it underwent rewrites to allow an arbitrary number of trophic structures, and a hybrid solver replaced the earlier mixed method solver. From the outside, however, the form by which the model represented the PWS ecosystem had changed very little. The model representation that would be used was identical to the representation described by Figures 19–31 of the annual report from a year earlier, from SEA *FY95 Annual Report* (Ch7). The testing domain would be small domains such as the cross-channel domains of Figure 20. The trophic structure was the simple four or five species structure shown in Figure 22: one or two zooplankton species, possibly a juvenile fish other than salmon fry as an alternative prey, a single fry trophic level, and one or two predator species. A frequently used basic test set consisted of pseudocalanus, Neocalanus C4, Neocalanus C5, pink salmon fry, and adult pollock.

A major theme of the model development at the end of 1996 was to insure that the developed model was sufficient to capture in simulation the diet and the shifts in diet seen in the stomach data. Both Willette and Cooney were interested in the diet performance of the model simulations and had made recommendations regarding fry schooling and pollock feeding behavior that should be covered by the model. In effect, the concern was that the model be complete in its representation of pollock foraging in order to accurately represent the observed sensitivity of adult pollock predation to changes in macrozooplankton density.

The typical test of the model began with some choice of initial densities (along a one-dimensional coordinate) for each of the species. These initial densities were then allowed to interact for up to 100 days. Here, of course, there are five things to change. Some have lesser effects on survival. Pseudocalanus are important primarily as food for fry; they are not prey for pollock. The pseudocalanus density for initial tests can be fixed. Also, for a model run late in the bloom, Neocalanus C4 could be lumped with Neocalanus C5.

The model trials at the end of 1996 demonstrated that the models did have sufficient structure for fry survival to be significantly enhanced through the “diversion” or “switching” of pollock predation from juvenile fish to macrozooplankton. A summary of this sensitivity is presented in a table in the SEA *FY96 Annual Report* (Ch 7, p 15). The capability to capture this sensitivity in the combined dispersion-bioenergetics model accomplished a core milestone that was over two years in the making.

Fry survival and predator density

There was a second sensitivity that was first noticed during this testing period at the end of 1996, that of fry survival to changes in the predator density or abundance. This was not anticipated and the information was solely from the model experiments. Because the nature of the sensitivity was not understood, it was necessary to conduct the initial zooplankton tests using a limited range of predator densities. In the SEA *FY96 Annual Report* Ch 7, p14, this fact was noted in the last paragraph:

Throughout these tests the total pollock population "in the domain" is assumed constant, though free to redistribute along the domain. That is, total predator abundance is not changed.

The sensitivity of fry survival to the predator abundance or density was as great, if not greater, than the sensitivity of fry survival to zooplankton density. Unlike the case of zooplankton, there was no prior considerations of the effects of predator density as a source of some non-linear or switching behavior. The properties exhibited by the model with respect to predator density had to be understood hence this issue was the first priority for 1997.

Spatially uniform software option

The sensitivity was almost certainly in the temporal component of the solution solely. Therefore, it would be advantageous to look again at the bioenergetics and foraging parts of the model without the overhead of the diffusion-taxis parts. However, much work had gone into merging the models. Separating them would be additional work, plus additional overhead in tracking two versions. Therefore, the combined code was modified whereby an option flag is used to setup the algorithm at the outset to execute with the smallest possible spatial grid and with all variables identical on this minimal spatial grid. This still retains some of the additional calculations of the spatial code, but with the advantage that the foraging and growth code retain a single revision path with the spatial parts.

The results of three simulations (with the software set for "uniform option on") are shown in Figure 1. The three columns correspond to three different scenarios, labeled 1, 2, and 3. The rows contain differing data reports from the simulation. It is the first row that is of primary interest, for that row contains the record of the fry survival over time. The second row shows the growth of the fry in millimeters. Here this simply documents that the three simulations were identical in terms of fry condition, and that pseudocalanus at a density of 200 m^{-3} are sufficient for essentially optimal growth. The last row contains the graph of the product of the probability of attack and the probability of capture given an attack. This too is solely to show that there is no difference between the fry of the three scenarios.

Significance

In Figure 1 pink salmon fry are the only prey for an adult pollock. (The size of the fry and the pollock at 10 days after fry release is shown in Figure 2.) This situation must obviously be seen as a limit and not a typical situation. In this limiting scenario in column 1, the fry are seemingly reduced to less than 1% of the initial density in less than two months. Figure

2 shows that just after 35 days the energy gain for the predator is negative. Hence, this limit is not so unrealistic, for there is a limiting factor that constrains the fry losses. Still, the fry survival is only 4% after only 35 days—not so good.

In scenario 3, the computer experiment says that the system would respond the same if both fry and predator densities were doubled. Since the predator loses interest at some absolute density, here the survival for the fry would be only about 2% at somewhere after 35 days.

The point of this note is the change seen in scenario 2 for only a decrease of the predator density to 50% of the density in scenario 1. (A doubling of the fry density also works.) That change results in fry survival of 40% at 60 days.

This “swing” from very low survival to extremely good survival in response solely to the predator prey relationship adds another issue in addition to the zooplankton role in predator diversion. Scenario 2 seems to be capable of producing good survival with no need for other mechanisms.

From this limiting case experiment, three factors appeared.

- 1 Although this really is a minimum absolute value with some additional qualifiers, for purposes here it suffices to note that if the “real” interest of predators is part of any model, then things cannot go entirely to zero. Here, adult pollock were not able to make a daily ration for fry approaching 60 mm length and at a density of less than $.0015 \text{ m}^{-3}$. Without benefit of consumption information one can see in scenarios 1 and 3 that the fry losses show an inflection at 35 days that is a useful cue to the minimum.
- 2 For densities that seem quite reasonable, the trajectory for the fry density makes very large swings for relatively small changes in the relative abundances of predator and fry; the end points of these swings seem very low and very high.
- 3 If we recall the historical behavior of salmon survival, it would appear that the salmon production system must have some remarkable feedback features that keep the system from exhibiting the range of values in this example. On the contrary, is it the case that one or the other of the two scenarios never occurs? Is there really only one of the cases that must be “smoothed out?” Is it always the case of “over” predation as in scenario 1? Or is scenario 2 the case except in very rare circumstances.

Much of this could be answered with a better estimate of the actual densities for fry and predators along the outmigration routes. Figure 3 is an effort to focus on the regions that would be the priorities in an effort to get a better estimate of densities.

2 Analysis

The behavior of the model in Figure 1 is the subject of the document in Part 1-B, “Lower bounds for survival of juvenile pink salmon during migration as fry through Prince William Sound, AK.” That analysis provides the relationships between fry and predator densities, fry and predator size, and fry and predator growth rates whereby the survival behaves as scenario 1 or 2 in Figure 1. In that document scenario 1 is referred to as a “crash” condition,

and scenario 2 as a "bloom" condition, and precise definitions are given.

The document also argues on the basis of some rough estimates that scenario 1 is the likely situation that would obtain in the absence of a diverting prey such as macrozooplankton. If this is the case then the system is susceptible to a low survival, this being the underlying situation. The issue then is why values for survival seem so consistent.

3 Review of hatchery data

The question of the potentially low survival in the absence of any predator diversion was good reason to thoroughly review the available hatchery data to fully define the targets for the model. A review with numerous graphical summaries was completed and published on the SEA Intranet. The first page of that review is shown in Figure 4.

The annual survival viewpoint

The driving factor in the review is the picture conveyed in Figure 5, a graph of the annual average survival by hatchery and for all four PWS combined. The survival values sound-wide are remarkable in their consistency. A note in the web-published review points out that the sound-wide annual survival rate is between 0.03 and 0.07 for every year from 1976 to 1995 except for four: 1977, 1980, 1991, and 1992. This consistency seems incompatible with the "crash" or "bloom" scenarios of Figure 1.

On the otherhand, the returns by hatchery are much less consistent. This has several implications that are now part of the modelling effort, but their description cannot be developed in time for this report. It suffices here to note that the individual hatcheries follow the general pattern of the sound-wide survival, but also have considerable individual differences. The immediate conclusion is that the modelling must be on a per-hatchery basis for it seems inappropriate to use one alone to represent "PWS survival."

The hatchery operator viewpoint

Figures 6-9 show just how misleading Figure 5 is. The first row of each of the four figures shows the release schedule each hatchery operator uses. These differ dramatically between hatcheries. The second row shows the mass at release. Once again, huge differences. The third row shows the survival by release-day. If more than one pen or code-group was released in a day then there is an error bar showing the range of survival, and a symbol shows the survival for the release of that day combined.

The most important observation is the degree to which survival can only be computed from a knowledge of the release schedule. To make this more apparent, the survivals for the four hatcheries are plotted together in Figure 10. Along with the survival the cumulative survival is plotted using a faint line. For example, at AFK in 1993, after the first release, the cumulative survival dropped from steadily from 0.03 to about 0.006 due to each release after the first having lower returns than that first one. It was only the late releases that then brought the annual return up to 0.015. In 1994 at AFK each release after Julian day 120 had

increasingly better survival, but things started from a minimum of 0.0003. (All survivals are in fractions, not percentage.)

The consistency in the annual survival plots does not characterize well the processes controlling production of fry in the sound.

The smoking gun

At least tentatively, the EVOS-ADFG-PWSAC coded wire tag data has provided the smoking gun regarding the question of evidence for "crash" occurring in PWS, that is, the low survival values indicated as possible by scenario 1 of Figure 1. The returns for AFK and WHN in 1993 and 1994 certainly have survival values for individual release-days that are consistent with the "crash" conditions. Since the "crash" condition does not persist—prey switching, as indicated in the lower bound analysis—the annual mean does not contain the crash-type survival values.

Part I-B
Technical note to SEA
Lower bounds for survival of juvenile pink salmon
during migration as fry through PWS

Technical note to SEA

Lower bounds for survival of juvenile pink salmon during migration as fry through Prince William Sound, AK *

J. E. H. SEA and M. N. R. SEA¹

Summary

The SEA Project is developing physical-plankton-nekton models for the survival of juvenile fish in Prince William Sound. This reports results from the nekton model for juvenile pink salmon. The model is a space-time model in which models for foraging, gut evaluation, and bioenergetics are embedded within diffusion-taxis models for the dispersion of all interacting nektonic species of the subsystem.

Initial simulations with the nekton model exhibited anticipated time interval of population movement followed by time intervals of reduced movement with sustained, regular population interactions. Based upon these simulations results, the model equations were studied with the intent of identifying the properties of the solutions that were responsible for the interactions during periods of relatively stable distribution. It is assumed here that the realizable foraging rates for all nektonic species exceeds gut evacuation rates, hence consumption is independent of prey density.

Lower bounds for survival of juvenile pink salmon are presented for two cases of prey populations and for arbitrary time-varying physical environments. The first case is that of juvenile pink salmon (or any single prey species) with an arbitrary number of predators. The second case is juvenile pink salmon with a group of alternative prey, again for arbitrary predators. A corollary of the analysis is the classification of conditions in which prey populations either "bloom" or "crash," that is, the prey populations approach limits with either positive values in infinite time or approach zero in finite time, respectively.

* Sponsored by The *Exxon Valdez* Oil Spill Trustee Council, Anchorage, AK
Restoration Project 97320

¹ J, E, H, M, N, and R identify projects of the Sound Ecosystem Assessment (SEA) Program.
www.pwssc.gen.ak.us/sea/sea.html

1 Brief and initial note on results

Starting assumptions; comments on starting assumptions

To be brief and to move quickly to the results, this initial note begins with relationships and distinctions that are specific to the area of application. In particular, the starting point incorporates the assumptions

- 1 smoothed mass intake rate (smoothed meaning averaged over a containing interval of several days) for each predator is
 - 1.1 independent of prey density,
 - 1.2 linear in predator mass, and
 - 1.3 nonlinear in temperature, the temperature dependence having a single maximum.
- 2 temperature is assumed to remain either sufficiently near the maximum or sufficiently constant so that the temperature effects on predator feeding rate can be neglected throughout the time interval in question.

In a separate note these assumed relationships are described using the properties of the forage-bioenergetics model. The assumed relationships develop in the limit as prey densities increase for both episodic and continuous foragers.

Predator foraging

Let φ_f^q denote the foraging rate—that is, the mass flux due for foraging, with units mass per unit time—of predator q on prey type f . A spatial domain is assumed wherein the prey density is everywhere sufficiently high that assumption 1.1 holds everywhere in that domain. For such a spatial domain it follows that, at most, φ_f^q varies with time. By assumptions 1.2 and 2 this time dependence is due exclusively to the time evolution of the mass of the predator. The total foraging mass flux for predator q is

$$\varphi^q = \sum_f \varphi_f^q$$

A routine and general partitioning of feeding conditions consists of the following.

- P-1 $\int_{1 \text{ da}} \varphi^q dt$ is less than that required to meet whole body energy requirements for the 1 da time interval specified in the integral;
- P-2 $\int_{1 \text{ da}} \varphi^q dt$ meets energy requirements but φ^q is insufficient to have the gut attain its maximum capacity;
- P-3 $\int_{1 \text{ da}} \varphi^q dt$ is sufficiently large that the gut reaches capacity and foraging is then either reduced or stopped entirely in order to balance the smoothed mass intake rate and the smoothed assimilative throughput rate.

Throughout the following P-3 is assumed.

A standard approximation for the smoothed mass intake rate $\overline{\varphi^q}$ occurring under assumption P-3 is

$$\overline{\varphi^q}(t) = \frac{1}{\|\mathcal{I}_t\|} \int_{\mathcal{I}_t} \varphi^q(s) ds = \rho_q m_q(t) \quad (1)$$

where \mathcal{I}_t is a time interval of length $\|\mathcal{I}_t\| = (1 + \epsilon) da$, $\epsilon > 0$, with $t \in \mathcal{I}_t$, and where ρ_q depends at most on temperature (hence, possibly on time, but here it does not because of assumptions in 2) and m_q is the time-varying mass of predator type q .

Case 1: single prey population

Let m_f denote the mass of prey species f . By the assumptions in P-3 and by (1), the number of prey of type f consumed per day by any of the type q predators is $\frac{\rho_q m_q}{m_f}$. The number of individuals of type f per unit volume consumed is $\frac{u_q m_q \rho_q}{m_f}$, where u_q is the density (units are number · meter⁻³) of predators of type q . Both f and q are considered to be growing hence m_f and m_q are time dependent; but u_q and ρ_q are assumed constant.

Let u_f denote the population density of the single prey species f for predator q . Combining all of the foregoing provides

$$\frac{du_f}{dt} = - \frac{u_q m_q \rho_q}{m_f} \quad (2)$$

This special case of a single prey is approximately the situation for fry relative to their predators before and after the macrozooplankton bloom. Hence, (2) contains the essential behavior of that predator-prey system for two time intervals during outmigration. We note this by the following lemma for the fry system.

Lemma 1. *For interactions between prey type f and its predator of type q during some time interval \mathcal{I} , if the predator q has only f as prey during \mathcal{I} , and the density of f alone throughout some spatial domain is sufficient for (1) to hold for predator q , then the decline of f during \mathcal{I} is given by (2). In particular, foraging of q and mortality of f are nonlinear in u_f and the decline of u_f is determined by the predator population structure (i.e., number (density u_q) and age and size (mass m_q)) and by the size of individuals in f (i.e., m_f).*

Since the interest is in time intervals of a few to several weeks, the standard approximation for growth suffices, namely

$$\frac{dm_f}{dt} = \gamma_f m_f, \quad \frac{dm_q}{dt} = \gamma_q m_q, \quad \gamma_f \text{ and } \gamma_q \text{ constants, with } \gamma_f > \gamma_q \quad (3)$$

Only $\gamma_f > \gamma_q$ is considered in this Note.*

* It is left as an exercise to determine whether these results suffice to determine the consequences for f if a predator q occurs with $\gamma_f < \gamma_q$.

Let $t = 0$ be the initial time and let $u_f(0)$ denote the initial density for prey f . (2) and (3) provide

$$\frac{d}{dt} \left(\frac{u_f}{u_f(0)} \right) = + \frac{u_q m_q(0)}{u_f(0) m_f(0)} \frac{\rho_q}{(\gamma_f - \gamma_q)} \frac{d}{dt} \left(e^{-(\gamma_f - \gamma_q)t} \right) \quad (4a)$$

$$= K_f^q \frac{d}{dt} \left(e^{-(\gamma_f - \gamma_q)t} \right) \quad (4b)$$

where

$$K_f^q = \frac{u_q m_q(0)}{u_f(0) m_f(0)} \frac{\rho_q}{(\gamma_f - \gamma_q)}. \quad (4c)$$

For reasons that will be apparent, K_f^q is called here the “crash” constant. It is convenient to distinguish two functions appearing in (4): U and E are defined to be

$$U(t) = \frac{u_f(t)}{u_f(0)} \quad \text{and} \quad E(t) = e^{-(\gamma_f - \gamma_q)t}, \quad (5a)$$

and the significance of (4) is the relationship between U and E ,

$$\begin{aligned} U(0) &= E(0) = 1 \\ \dot{U} &= K_f^q \dot{E} \end{aligned} \quad (5b)$$

Only predation mortality for f is considered. That is, changes to u_f due to population flux into or out of the spatial domain are not included. The results, then, are applicable to each of a series of bounded time intervals such that during any one the “zero flux” assumption is suitable. It is with this approximation in mind that we can state that “by construction” $\dot{U} < 0$.

From (3) and (5) $\dot{E} < 0$ by construction, E is decreasing exponentially at the rate $-(\gamma_f - \gamma_q)$, that is, declining somewhat less fast than the rate at which the mass of members of f are growing. If $K_f^q = 1$ then $U = E$ by the basic uniqueness theorem of ODEs. A short calculation shows that the “biomass” $m_f(t) u_f(0) U(t)$ of f is not constant but rather increasing at a rate that just keeps up with the increase of the biomass of q , for the case $K_f^q = 1$.

But if $K_f^q \neq 1$, then by (4) U is decreasing either faster or more slowly than E . Precisely how the evolution of U differs from E for $K_f^q \neq 1$ is the subject of Lemma 2. Lemma 2 is the most important result of this Note. Everything that follows is an application or extension of this simple “Crash-Bloom Lemma.” The “crash or bloom” response is exhibited by the prey for any system wherein prey are sufficient to keep predator consumption in the neighborhood of its upper bound. Predator consumption so constrained then satisfies (1) which in turn is the source of the nonlinear relation (2) and the consequent “crash-bloom” response.

Lemma 2. (Crash-Bloom Lemma) Let f denote a single prey population and q its predator population as in Lemma 1. Restrict considerations to a time interval \mathcal{I} for which (1) holds. Let K_f^q , U , and E be as defined in (4) and (5). Then, the trajectory of $U(t)$, $t \in \mathcal{I}$ “crashes” or “blooms” according to whether K_f^q is greater or less than 1, with the trajectory of U following paths described by the following summary.

$$\begin{aligned} K_f^q > 1 &\implies U(t) < E(t), \quad U(t^*) = 0, \quad t^* = \frac{1}{(\gamma_f - \gamma_q)} \ln \left(\frac{K_f^q}{K_f^q - 1} \right) && \text{crash} \\ K_f^q = 1 &\implies U(t) = E(t), \quad U(t) = e^{-(\gamma_f - \gamma_q)t} \xrightarrow{t \rightarrow \infty} 0 && \text{predator} \leq \text{product} \\ K_f^q < 1 &\implies U(t) > E(t), \quad U(t) > \lim_{t \rightarrow \infty} U(t) = 1 - K_f^q > 0 && \text{bloom} \end{aligned}$$

Proof: The analytic solution to (4) or (5) is straightforward.

$$U(t) = \frac{u_f(t)}{u_f(0)} = 1 - K_f^q \left(1 - e^{-(\gamma_f - \gamma_q)t} \right) = 1 - K_f^q (1 - E(t)) \quad (6)$$

□

Corollary to Lemma 2. In the “crash-bloom” system of Lemma 2, the prey population f declines according to the scaling and affine shift of a single exponential,

$$\frac{u_f(t)}{u_f(0)} = (1 - K_f^q) + K_f^q e^{-(\gamma_f - \gamma_q)t}.$$

In particular, the decline is a family of functions parameterized by the “crash” constant K_f^q .

The prey population never declines exponentially for some approximately constant mortality rate. In particular, mortality rate μ is never constant but rather is related to the “crash” constant by

$$\mu(t) = \frac{d \ln(u_f)}{dt} = - \frac{(\gamma_f - \gamma_q) K_f^q E(t)}{1 - K_f^q + K_f^q E(t)};$$

$\mu(0) = -(\gamma_f - \gamma_q)$ initially; thereafter μ is monotonically increasing to ∞ or decreasing to 0 according to whether $K_f^q > 1$ or $K_f^q < 1$, respectively.

The foregoing closed form solutions, the limits, and the zero crossings must all be viewed as indicative of the shape and trend but not the actual outcome. The density u_f does not actually approach 0 in the sense of a zero-crossing, for as u_f gets small the assumption regarding predator foraging described in P-3 no longer holds. Similarly, for time t large the mass m_f gets sufficiently large so that prey f is no longer within the predation range of q . These two, prey density and prey size, act jointly in the sense that increasing individual size increases the threshold density that f must exceed to sustain predation in P-3 mode and functioning according to (1).

In contrast to the limits shown in Lemma 2, the inequality relationships between U and E presented in Lemma 2 do not require the foregoing precautions. The inequalities develop instantaneously. Whether U is above or below E can be used to characterize the “crash” and “bloom” scenarios without appealing to the limits.

Case 1 applied to pink salmon fry in PWS: Case 1 for fry is "crash"

Conjecture 1. Available evidence indicates that for time intervals in which pink salmon fry are a single prey for one or more of their predators and occurring at densities sufficient for predator foraging according to assumption P-3 and (1), then they will be in "crash" mode. Attaining fry densities or growth sufficient for "bloom" seems problematic.

The following numerical examples provide the basis for Conjecture 1. Briefly we consider fry as single prey for any of adult pollock, adult salmon, and juvenile pollock. The following parameters for K_f^q are used for all three predators.

temp (C)	γ_f	m_f (g)
9	0.04	0.03

adult pollock A range of mass for adult pollock is 300–440 g. For $\gamma_q = 0.005$ and $\rho_q = 0.02$ then

$$K_f^q \leq 1 \iff u_f \geq \frac{300}{0.3} \frac{0.02}{0.035} u_q \approx 570 u_q$$

A pollock biomass of 30 kM, with mean mass $m_q = 300$ g, is equivalent to 10^7 predators. Wild and hatchery fry combined are approximately 10^9 . Hence, $u_f/u_q \approx 100$. This estimate places u_f substantially below the value needed to be at the threshold of "bloom".

For $u_f/u_q = 100$, then $5.7 < K_f^q < 8.4$, and $3.6 < t^* < 5.7$, where t^* is the time-to-zero during a "crash".

adult salmon Returning adult pink salmon are typically greater than 3% of the released fry, and of those returning approximately 25% are early (June) returning pink salmon. Here again $u_f/u_q \approx 100$ using only early returning adults.

Mass for a returning adult pink is approximately 1500 g. For $\gamma_q = 0.0$ and $\rho_q = 0.01$ then

$$K_f^q \leq 1 \iff u_f \geq \frac{1500}{0.3} \frac{0.01}{0.04} u_q \approx 1250 u_q$$

This is an upper bound, for it uses the fry release mass. For fry growth to .6g or even to 1.0g the $400 < u_f/u_q < 600$. If the full 25% of the 3% returning adults constitutes a predator population, then u_f/u_q is at least a factor of 4 above the switch to "bloom." The involvement of returning adult salmon is not well developed.

juvenile pollock For juvenile pollock (age 1,2) of, say, 55g, then

$$K_f^q \leq 1 \iff u_f \geq 105 g.$$

This illustrates that the "depth" of the "crash" condition can be substantially less for equivalent population densities with differing population structures.

Case 1: single prey, multiple predators

Only a minor change is needed to extend Case 1 to multiple predators. For this case q is now a set of indices $\{q_j, j = 1, \dots, n\}$. Summations over the predators is denoted by summation over the set q of indices.

For a set of predators, the rate of decline for f is simply the result obtained by linear superposition applied to the right side of (2). Results analogous to (4) and (5) follow directly,

$$\frac{d}{dt} \left(\frac{u_f}{u_f(0)} \right) = \sum_q K_f^q \frac{d}{dt} \left(e^{-(\gamma_f - \gamma_q)t} \right) \quad (7a)$$

which has the solution

$$\frac{u_f(t)}{u_f(0)} = 1 - \sum_q K_f^q \left(1 - e^{-(\gamma_f - \gamma_q)t} \right). \quad (7b)$$

The foregoing definition of “crash” and “bloom” is used: the scenario is “crash” if u_f goes to zero in finite time and “bloom” if $\lim_{t \rightarrow \infty} u_f = u_0 > 0$. From (7b) “crash” is the case for $\sum_q K_f^q > 1$ and “bloom” for $\sum_q K_f^q < 1$.

An approximation for (7a) in the form of (4b) can be useful. Let $\bar{\gamma}_q = \max_q \{\gamma_q\}$ and $\underline{\gamma}_q = \min_q \{\gamma_q\}$. Then from (7a)

$$\left(\sum_q K_f^q \right) \frac{d}{dt} \left(e^{-(\gamma_f - \bar{\gamma}_q)t} \right) > \frac{d}{dt} \left(\frac{u_f}{u_f(0)} \right) > \left(\sum_q K_f^q \right) \frac{d}{dt} \left(e^{-(\gamma_f - \underline{\gamma}_q)t} \right). \quad (8)$$

Neocalanus in PWS: testing the consequences of macrozooplankton as a single prey having multiple predators.

It is a SEA conjecture that during the macrozooplankton bloom *Neocalanus spp.* C4 and C5 instars become the preferred or dominant prey for all predators that feed upon both zooplankton and fish. To the extent this holds, the *Neocalanus* meet the criteria for the foregoing case of one prey, many predators.

For *Neocalanus* in PWS, the mass changes by a factor of approximately 3 during the C4 instar. For an interval of 15 days between molts, the growth rate per unit mass during C4 is approximately 0.20. The initial mass is estimated as 8×10^{-4} g. With these and previous values for pink salmon fry and for adult pollock, estimates for the conditions needed for $K_f^q < 1$ are

$$\begin{aligned} \text{adult pollock } K_z^q \leq 1 & \iff u_z \geq \frac{440}{8 \times 10^{-4}} \frac{0.02}{0.2} u_q \approx 55 \times 10^3 u_q \\ \text{pink salmon fry } K_z^f \leq 1 & \iff u_z \geq \frac{0.3}{8 \times 10^{-4}} \frac{0.10}{0.16} u_f \approx 235 u_f \end{aligned}$$

This suggests that for $u_q \approx 10^{-3}$ and $u_f \approx 0.1$ then $K_z^g + K_z^f < 1$. However, if $u_f \rightarrow 1.0$ or $u_q \rightarrow 10^{-2}$, then, at least locally, the density for macrozooplankton will approach zero.

In the following it will be assumed that $\sum_q K_z^g < 1$ and, hence

$$\frac{d}{dt} \left(\frac{u_z}{u_z(0)} \right) > \frac{d}{dt} \left(e^{-(\gamma_z - \min_q \gamma_q)t} \right),$$

at least during some interval during the (apparent) zooplankton bloom.

3 Bibliography

Part I-C
Summary of 1997 progress
The pink salmon fry survival model with 1997 extensions:
ecosystem production processes and their record in code-group survival

Technical note from SEA
The pink salmon fry survival model
with 1997 extensions:
ecosystem production processes
and
their record in code-group survival *

J. E. H. SEA and M. N. R. SEA¹

Summary

The SEA Project is developing physical-plankton-nekton models for the survival of juvenile fish in Prince William Sound. This reports results from the nekton model for juvenile pink salmon. The model is a space-time model in which models for foraging, gut evaluation, and bioenergetics are embedded within diffusion-taxis models for the dispersion of all interacting nektonic species of the subsystem.

Analyses of both the models and the coded wire tag data for Prince William Sound hatcheries have shown that successful tracking of the production processes requires the tracking of each release group. There is no "mean" fry outmigration.

The SEA fry model has been extended in the sense that each release group for each hatchery is modeled as a separate stock. The model specification fully encompasses this extension. The model is configured with a taxis providing the migration velocity, with calibration provided by 1994 measurements from Willette.

This reports on a simulation of WHN for 1994 with eight separate release days and the results from the model for the case of no macrozooplankton. This case is to simulate a pre-bloom condition and a multiple release version of previous simulations.

A second simulation is shown wherein analyzed data sets, one from Willette and one from Cooney and Coyle. were used to simulate the actual bloom onset.

* Sponsored by The *Exxon Valdez* Oil Spill Trustee Council, Anchorage, AK
Restoration Project 97320

¹ J, E, H, M, N, and R identify projects of the Sound Ecosystem Assessment (SEA) Program.
www.pwssc.gen.ak.us/sea/sea.html

1 An example with 1997 extensions

1994 WHN and the model configuration

The release schedule for WHN for 1994 is shown in Figure 8. The actual release days are shown along the top of Figure 11. The focus will be on the first seven release days for this discussion.

The model holds each "pen" until the release day, and then deposits instantaneously all fry into a one dimensional domain representing the outmigration path from WHN to the southwest entrance to the sound. The one dimensional domain represents a 500m wide by 20m deep shoreline domain of 90km length. The one-dimensional coordinate is oriented so that 0km is at the southwest entrance just south of AFK, WHN is at 90km, Cannery Creek is at a greater distance, and Solomon Gulch at the end, essentially as shown in Figure 3. Upon a release at WHN, there is a pulse at 90km with area equal to the release for the day.

The diffusion-taxis model is configured for a constant southward migration by advection plus a diffusive spreading. The diffusivity and the advection velocity were jointly calibrated so that the leading edge of the pulse was consistent with the measurements of Willette. At this time no further migration responses are included, such as zooplankton density, tidal velocity, and the like.

Two scenarios for predators have been tested. First, the predators were configured to move in response to releases. This had several consequences of interest in terms of processes, but the magnitude of the impact warranted using the simpler uniform predation shown in Figure 11. This uniform predation density is used to begin an "inverse" assessment of predation densities consistent with recorded survivals, especially the release-day sequence of survival values.

Progress of outmigration

Figure 11 is a snapshot of the release-day groups on day 134, that is, 3 days after the seventh release-day (131) and 19 days after the first release-day (115). The plot shows the extent of spreading of each of the releases in the time since release, the distance southward traveled by the group, and the extent of the mortality to the group. The actual integral of each group is shown across the top, along with the survival, that is the ratio of the integral to the initial release.

The example in Figure 11 has the same predator density as Figure 1, however, it uses more realistic values from the data analysis provided by Willette: the temperature at day 134 was 5.1C for the upper 20m, and the predator size is 475mm, 700g. See also Figure 14 for values.

A second snapshot at day 149 is shown in Figure 12. The first release group after 34 days has its leading edge approximately 45km south from WHN.

2 Results from a test case

Crash or Bloom?

To compare the simulation with Figure 1, the survival for each group is plotted in Figure 13 in a manner similar to that used in Figure 1. However, the results of the Lower Bound note cannot be applied directly for now each of the groups is acting as alternative prey for each of the other groups. However, in general, the shape of the plots in Figure 13 indicate that in finite time survival will tend toward zero, hence this is crash.

In addition to the alternative prey issue, the diffusion of fry reduces the fry density during the migration. This spreading, in terms of the lower bound, moves them closer to crash.

The point here is that the lower bound is the qualitative description but the actual simulation is needed for any specific case. Even this simple scenario has numerous examples of how many factors contribute to a specific outcome.

Predator swamping

An often mentioned "rule" is that more fry should yield better survival due to "predator swamping." This is precisely the content of the lower bound lemmas.

However, the simulation reveals that in addition to a general effect there is a local effect due to fry as self-alternative prey. The linear plot of Figure 13 shows that the last release is dropping faster than the ones preceding it, and indeed is approaching the earlier releases, even though the last has been out for a very much shorter time period. This is because the pen releases in the middle are the ones with self-alternatives, whereas the first and the last are short changed. This "dooming" or local maximum for survival in the middle pen releases occurs in the hatchery data.

Pre-bloom predation

The last result from this simulation without *Neocalanus* is to approximate the consequences of predation during a period prior to the development of a significant diversion due to macrozooplankton. In Figure 14 the survival shown in Figure 11 is simply plotted against the day of release—precisely as was done with the PWS hatchery data in Figure 10. The resulting survival vs. release-day curve would have resulted if the WHN release had progressed to the state in Figure 11 and thereafter the predation was substantially reduced by the bloom. The survival pattern due to the first period without refuge would still be retained in the population, and would appear as shown in the top panel of Figure 14.

If instead the bloom did not cease predation until day 149, then the pattern in Figure 12 would be retained—as shown in the middle panel of Figure 14. If the predation were three times greater and stopped at day 136, the pattern in the lower panel would be obtained.

Tentatively, this identifies how one of the system production processes is recorded in the coded wire tag records of survival, and the records for 1994 for all hatcheries have records with this pattern.

3 Results from test case with analyzed data

A first simulation with analyzed data sets provided by Willette (temperature and predators) and Cooney and Coyle (zooplankton) was completed during 1997. The results plotted in the manner of Figure 13 are shown in Figure 15. Although it appears that predation is not adequate or zooplankton switching too great relative to the record for WHN for 1994, the pattern of initial predation decline in the manner reflecting the crash scenario followed by the sharp reduction of predation losses is clear.

Part II
Report on 1997 progress
Database
C. S. Falkenberg



Part II: DATABASE

Charles S. Falkenberg
April 15, 1998

Summary

As with FY96 the database development effort in FY97 was split between data management activities and the development of the software tools to access those data. However, with the successful implementation of the web based retrieval tools in FY96, the focus of FY97 was on data management and ingestion in order to expand the data content of the SEA DataWeb. This included adding new datasets or "data types" as well as augmenting the data archived in for existing datasets. Several special project were also undertaken in FY97 to reformat existing data to make it more usable by the researchers within SEA. Together these data management tasks combined to form the bulk of the FY97 database development.

Although software tool development was secondary, the usability of the existing tools was improved and new user interfaces were added to support the added datasets. Part of this work included the initial development of an interface to the predator fish data. This web based interface is more elaborate then the ones used for the other SEA datasets. In addition to the integrated retrieval with other SEA datasets, this interface allows a small, specific, subset of the predator fish data to be displayed and downloaded.

The funding for the database effort in FY97 was .5 FTE or six months. Of this time nearly 40% was allocated to data management and ingestion, 30% was devoted to software tool development and 20% was devoted to EVOS reporting requirements and conference attendance. This last 20% included the AAAS conference in Valdez and the EVOS annual workshop. In addition several unfunded activities in FY97 bore an impact on the development of the SEA DataWeb. These included an investigation of the NASA EOS data archiving system and the development of the Shepard Point Region Environmental Assessment Database (SPREAD) for the Prince William Sound Science Center.

Expanding the content of the SEA DataWeb

The primary focus of FY97 was to expand the data content of the DataWeb and to provide data reformatting where it was needed. This included three basic activities: adding new types of data, reformatting existing data so it was more usable, and augmenting existing datasets with data from recent field seasons. Some of these new data types required the development of new retrieval tools which will be discussed in the next section.

Two new SEA datasets were ingested into the SEA DataWeb. Echo acoustic data on herring

abundance was ingested over the summer and predator fish data was ingested in the fall. The CTD and zooplankton datasets were augmented with data from recent field season and the zooplankton data was reformatted for use by the cross channel nekton modeling application.

The data ingestion process includes creating a description of the data and constructing the necessary database tables to allow the data to be retrieved. In the case of the herring acoustic data these tables look similar to the tables which are used by other SEA datasets. The predator fish data has a much more complicated structure, however, and required new processing and indexing techniques. These fish data are imported from another DBMS and although the volume is not high, multiple database tables are needed to capture all of the information. In the SEA DataWeb, the basic schema of the original tables is augmented with new data elements that allow these fish data to be viewed in an integrated way with the other DataWeb datasets.

Reformatting existing data was a secondary but important data management task for FY97. This is a data preparation step which allows data from the DataWeb to be made available to users in a more accessible format. Three different datasets were reformatted, the ocean circulation data, the bathymetry data and the herring acoustic data.

Of these the ocean circulation reformat was perhaps the most significant. In order to make these large data files available for the variety of platforms used by SEA researches, the circulation data were reformatted into the HDF scientific file format. This is a self-describing, transportable data format which keeps data in a binary representation and which can be read by programs running on different workstations architectures like SGI, Sun, or DEC or on PC's running Windows. The reformatting utility included several routines which can be used by the SEA researchers to read the data in the HDF file. Once reformatted these data were made available to various SEA researchers.

The bathymetry data of Prince William Sound was reformatted and converted to allow the creation of contour maps of the Sound and to integrate depth into several of the modeling applications. These bathymetry data were reprojected and subsampled into the required grids and coordinate system. Finally, several acoustic datasets were reformatted for use with the SEA visualization software.

Part of the FY97 data management activity was the acquisition and reformatting of external data which is relevant to the SEA project. These external data include both weather and tide data collected at stations around Prince William Sound and archived by NOAA. Software utilities which can automatically download both types of data from NOAA were created. The tide data have been downloaded, reformatted and are available through the DataWeb. The weather data are highly coded and need additional work but are currently being downloaded and archived.

Improving the DataWeb Software

The focus of FY96 was the implementation of the WWW software for the SEA DataWeb. This was a secondary focus for FY97 but several improvements were made in the basic tools, and the functionality was extended to incorporate new datasets. The interface to Directory Services was improved and expanded, and a new interface was created for both the echo acoustic data and the

predator fish data. In addition, several improvements were made in the software development environment in order to support the DataWeb mirroring.

A limited file name search capability was added to Directory Services as well as the ability to download a single zip file containing multiple data files. The new bathymetry data and the tide data were added to Directory Services in addition to the zooplankton and CTD data from the new field seasons. The initial choice page was also modified to allow access to Directory Services, Query Services, and Modeling Services.

Query Services was updated with a new user interface to the echo acoustic and predator fish data. The interface to echo acoustic data is similar to the other dataset selection pages but allows for echo acoustic specific selection criteria to be entered. A new page was also added for displaying all of the columns of echo acoustic data from the tables in the database.

Accessing the predator fish data is somewhat different than the other SEA datasets. The predator fish data is contained in eight different database tables that could be considered eight different datasets. However, the data from the different tables is linked closely and so it being made available together in Query Services. The interface to the predator fish data allows the entry of selection criteria and then a subset of the data matching those criteria from all selected tables is displayed. This required new utilities and display pages and is a new paradigm for retrieving SEA data.

The predator fish data are also available, in an integrated way, along with the other SEA datasets through the standard, cross dataset, selection page. The location of the fish catches will be displayed on the interactive map tool along with the other SEA datasets and a dataset containing the length and weight of the predator fish in a single catch can be downloaded along with the other SEA datasets in the group. Work on the final interface to the predator fish data will continue into FY98.

The utility used to download the tide data is not part of the access tools for the SEA DataWeb but the development of this tool has potential long term value for SEA. This utility is written in the Java programming language and uses the features built into this language to open a connection to a web site, download data and write out a local archive file without using a browser interface. The advantage of this utility is that it can be triggered on a regular basis to retrieve external data into a local archive.

One of the features of this utility is that it bypasses the form fill-in page and supplies all of the parameters which would the web server expects from that page. The server then responds by supplying the data which is normally returned in response to the submission of the HTML form. Although this utility was written to download tide data several of the objects which make up this utility can be reused for downloading data from similar web site. Taken together these changes represent a significant improvement in the capability of the DataWeb Tools.

Conferences and Related Projects

In addition to expanding the data content and extending the functionality of the SEA DataWeb

several related activities were undertaken during FY97. These included the attendance at several relevant conferences and the creation of a data system similar to the SEA DataWeb. Some of these activities, although relevant to the long term mission of building a the SEA DataWeb, were not funded as part of FY97 EVOS funding. The funded activities included a presentation at the AAAS conference in Valdez and attendance at the EVOS yearly workshop. Unfunded activities include involvement with the data archiving systems for the NASA Earth Observing System NASA-EOS, updates to the Informix DBMS, and a data system for the Shepard Point regional environmental assessment.

Two conferences were included in the FY97 database development funding. The first was the AAAS conference in Valdez and the second was the EVOS annual restoration workshop. The content and structure of the DataWeb was presented at the AAAS conference and the feedback was positive. This status of the SEA DataWeb was also presented at the associated SEA planning meeting in Valdez.

Unfunded activities which are of particular importance to the evolution of the SEA DataWeb included participation in the NASA workshop devoted to the data archiving tools needed to support the large volume EOS database. Several tools which allow spatial selection and reformatting of EOS data may be available and quite useful to the SEA DataWeb.

In addition, insight into the evolution of the Informix DBMS was gained during a multi-day meeting at the headquarters of the Informix technical team in Oakland Ca. Informix remains committed to the concept of extensible database management systems and it has greatly expanded its spatial data management offerings. These offerings come from partnerships with two GIS vendors, ESRI who makes the Arc/Info product and MapInfo. It is clear from these different partnerships, and from the spatial products that are supported by Informix itself, that Informix will continue to support several options for the management of spatial data.

Finally a data system similar in some aspects to the SEA DataWeb was developed to support the Shepard Point Road Environmental Impact Statement. This work was funded by the Prince William Sound Science Center is designed to allow public access to the data collected as part of the environmental impact statement. The data system supported a the selection and display of data from a wide range of database tables using time, date, location and species as possible selection data. This system provided some of the concepts used to implement the interface to the predator fish data.

Future work on the DataWeb

The goals for FY98 will again include both the management and ingest of the SEA data and the development of user tools to retrieve those data. FY98 will see the wrap up of the tool development into a final user interface to SEA data. This will include some significant improvements to the spatial selection and display and should include a new map display. Additional datasets will also be added to the DataWeb as the individual projects wrap up the processing that is necessary before the data are submitted to the archive.

Part III-A
Report on 1997 progress
Web-based Communications
J. R. Allen



Part III: WEB-BASED COMMUNICATIONS

Jennifer R. Allen
April 15, 1998

ABSTRACT

The SEA internal web site (Intranet) has been functional since September, 1995, providing electronic mechanisms to facilitate collaborative interactions critical to the mission of SEA. This annual report addresses features added or expanded in the last year. These include a Synthesis work area; Modeling Progress area; Management Collaboration area; and the State of the Sound report, which is a compilation of near realtime data for Prince William Sound. Detailed usage statistics for the system are also presented.

INTRODUCTION

The rationale and design of the SEA internal web site (Intranet) were reported to EVOSTC last year (Allen et al., 1997) and were the subject of a presentation to the AAAS Arctic Division Science Conference in Valdez, AK, in September 1997 (Allen and Patrick, 1997). Briefly, the purpose of this work is to provide electronic collaboration mechanisms to the multi-disciplinary, geographically dispersed SEA research team. Tasks served include scheduling, data sharing, joint assessment of data across disciplinary boundaries; preparation of joint presentations and manuscripts; and liaison between the field and modeling efforts. The ongoing quest is to help integrate the observations, expertise and knowledge of each investigator into a joint system-wide synthesis, with translation into management and monitoring applications.

Previously reported features include a dynamic results archive, threaded discussion server, interactive papers collaboration work area, platform-independent file upload and exchange tools, as well as general informational documents such as calendars, maps, cruise plans, cruise reports, and announcements. The present report addresses new developments made during FY97. Detailed usage statistics for the internal web site are also presented (Appendix 1).

FY97 ACTIVITIES

In addition to maintenance of existing Intranet functions, development work continued during FY97. The new additions and expanded features reflect the shifting emphasis in SEA from field work to synthesis activities. Areas in the Intranet that were new or expanded during FY97 include:

1. Synthesis work area
2. Modeling Progress area
3. Management Collaboration area
4. Near Realtime Data delivery work

Each of these will be described individually, following a brief synopsis of general activities.

General Activities

The areas and their relationships within the SEA Intranet are diagrammed in Figure 1. A new feature, this diagram is posted on the web site in the form of a clickable map and gives direct access to each of the named regions. The map is instantly reachable via the "SITEMAP" icon found on every page.

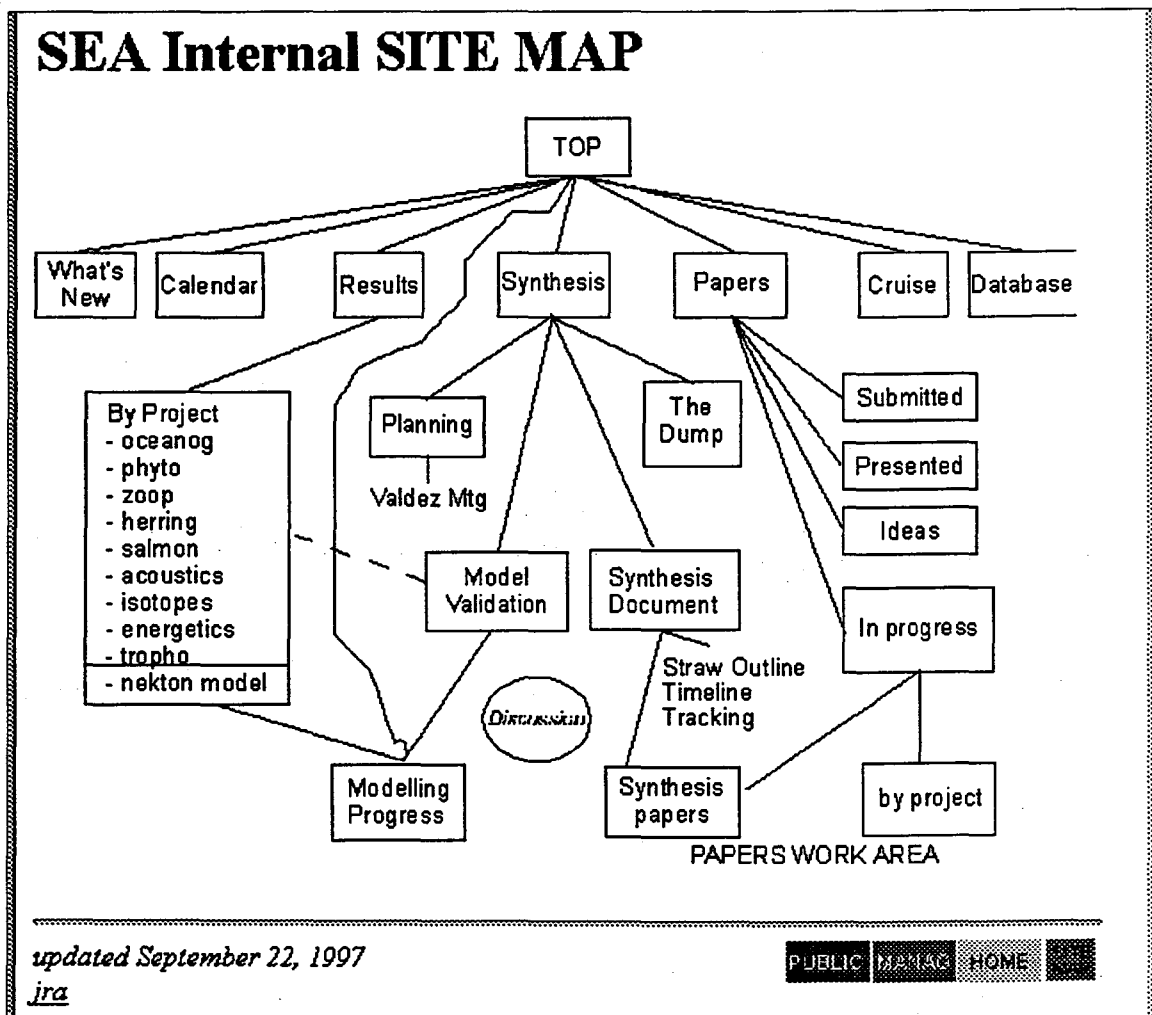


Figure 1: Layout and area relationships in the SEA Intranet

The opening page of the SEA Intranet (Figure 2) is password-protected and provides secure access to the rest of the internal functions, including the database. The structure and functionality of this opening page was updated in FY97 to reflect the increasing emphasis on modeling and synthesis and to promote interrelationship between the SEA internal areas and the Management Collaboration area.

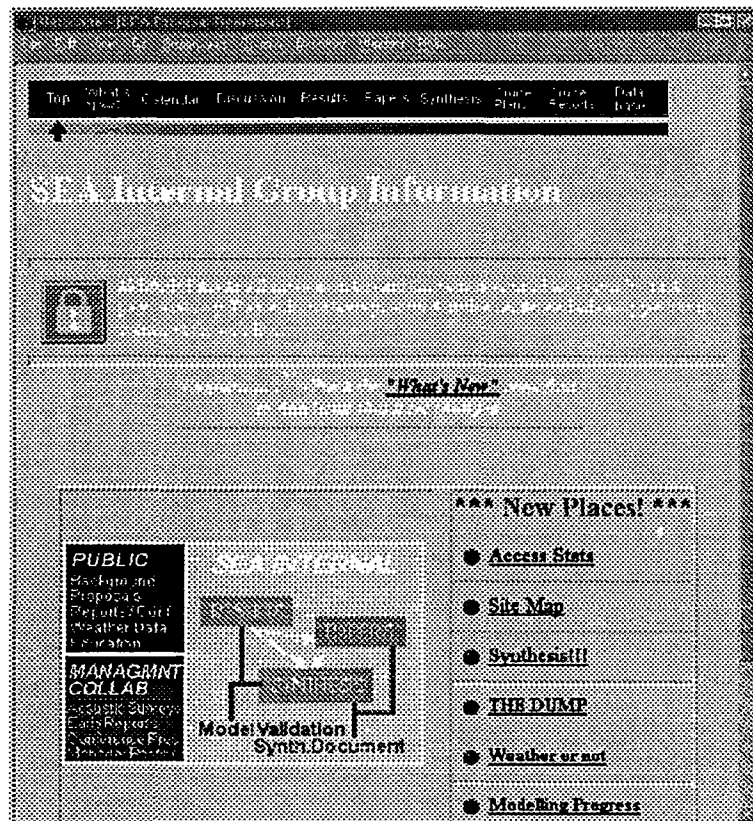


Figure 2. SEA Internal Web - reorganized opening page

The schematic in the lower left quadrant (Figure 2) is a simplified version of the sitemap, showing the Intranet divisions into major areas. This diagram also is hyperlinked and clickable, providing quick access to the various work areas. The text list at lower right is used to introduce new features as they are added to the site. The clickable cross-site menu bar, visible at the top of Figure 2, is present on most pages of the web site and incorporates a graphic indicator of current location.

Other changes in FY97 included an expansion of the number of draft papers online, and an increase in web authoring by individual researchers and staff, and improvement in access tracking. Software was obtained (Analog v2.11 for Unix) and written (PERL scripts) to allow convenient analysis of access logs with summaries both by user and by area accessed. Daily updates of these

summaries are automatically posted to the internal website. Finally, the file upload area or "dump" site has proven successful and is a frequently used mechanism of file exchange, particularly in the case of files that are too large to transmit as email attachments or which are of general interest to multiple SEA team members. This application, which was written in the PERL language, was described in more detail in the FY96 report.

Synthesis Work Area

The SEA Synthesis Work Area was established as a result of a SEA synthesis planning meeting held in September 1997. Its purpose is to support the dual ongoing tasks related to synthesis: model validation and preparation of a joint multi-chapter report detailing the new ecosystem level results and understanding which have resulted from SEA research. The site was also used for assembly of materials during preparation of the 1997 SEA presentation made to the January 1998 Restoration Workshop. Figure 3 shows the entry page to the synthesis area.

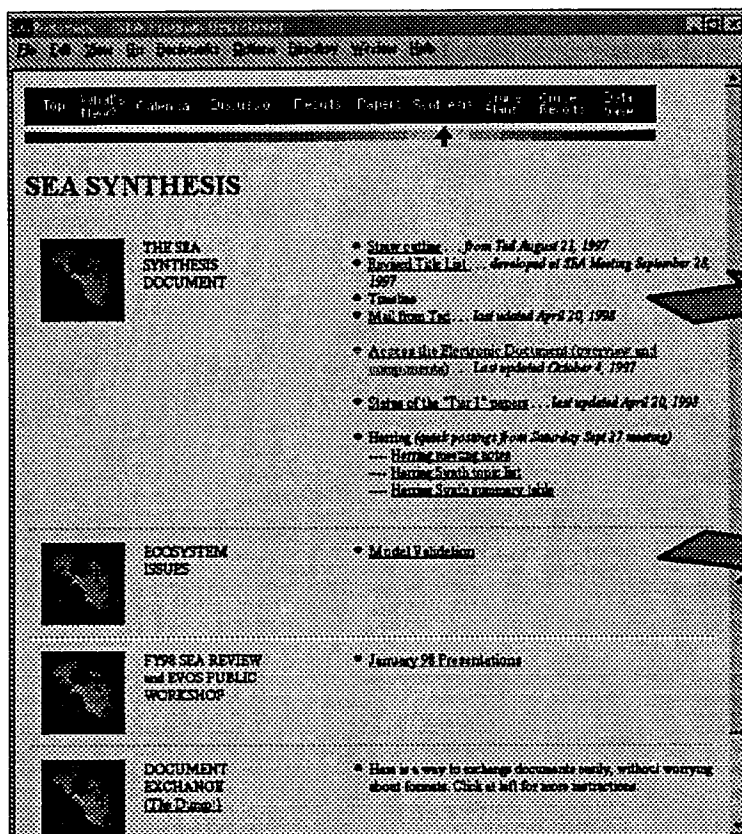


Figure 3 (left)
SEA Synthesis area opening page

A. Synthesis document work area (detail below)

B. Model validation work area (detail in following section)

Figure 4 (below)
SEA Synthesis Document Work Area
(first row of 12 rows)

SEA SYNTHESIS DOCUMENT

Monday, 27-Apr-98 18:52:17 AKDT

HELP ... How This Page Works ...
Display help file in:
[This Window](#) | [Separate Window](#)

Look Bold/red "Look" in the table indicates component has web-browsable material available for online viewing.

Overview Table

CHAPTER	WHO	Key "Tier 1" Papers to be cited	TARGET/STATUS				Comments
			Data	Outline or Key Points	Draft	Figures	
I. Introduction: What is SEA?	Cooney, Thomas, Tonic Baker, et al.		Data Target date: Status:	Outline Target date: Status: Next draft date:	Draft Target date: Status:	Figures Target date: Status:	<input type="button" value="Add a Comment"/> <input type="button" value="Reset Comments"/> Number of messages: 1

The Synthesis Document work area (Figure 4, previous page) is laid out as a table, in which each row is a chapter and each column is an attribute or target for that chapter. The basic structure is shown in Figure 4, which has been cropped to display the layout for the first row only. This table provides an at a glance summary of the status of work and also gives entry to deeper levels of detail on each chapter. Hyperlinks in each row provide access to related papers in preparation, bibliographies, data summaries where applicable, drafts and figures. The three buttons below each row deliver a status update or allow users to send and retrieve binary files, respectively. The two buttons in the right-hand column provide access to notes and discussion on the chapter: users can add comments to the dialog as well as review previous comments which are logged chronologically. It is anticipated that this work area will be heavily used during the final synthesis year of the SEA program.

The synthesis entry page (Figure 3) also gives entry (arrow B) to a new section for model validation work (Figure 5, at left). This area has been built to house model simulation output and corresponding comparative field data during the model validation and refinement process. It is also a repository for results of a planned set of scenario simulations under selected realistic input parameter settings, and will provide an online focus for emerging findings and discussion. This page also links to the extensive Modeling Progress area maintained by Vince Patrick (see next section).

SEA Synthesis: MODEL VALIDATION
(A. Pink Salmon)

► Objectives/Overview

- * The objective of the model validation task is to simulate salmon survival figures from previous years based on observed data from those years for the environmental factors of interest. The first iteration will be very general, looking for trends and patterns consistent with the model's predictions, and based on power's inputs.
- * Successors iterations will be used to progressively refine the model parameters and will require increasingly detailed (spatially and temporally) inputs, drawn from the SEA database.
- * This web area will be used as a gathering house to display the data used as inputs and to illustrate and describe the model's responses. Input from YOU in the form of reality checks at any time will help the process.

► Current State of the Model

► Data on Fish Population Size or Recruitment

► Salmon Release and Return Numbers

Data from Mack - thanks.

- Salmon release numbers and survival % by year (1988-9) return) and release site. clicking on the link or page will bring up a separate window. clicking on the name displays the information in the present window.
- Tag-in variables %
- Tag-in return of fish data

► Data on Herring Biomass Estimates

Data also from Mack. These data are estimates of adult herring biomass (ASA) model for PWS for 1988-96. The ASA model returns different kinds of data.

- Text file of age-structured analysis estimates

► Process Measurements

- **Summary Table - Characteristics of the Years**
- **Temperature**
- **Circulation**
- **Phytoplankton bloom timing, magnitude**
- **Zooplankton timing, abundance**
- **Producer Density**

► Model Validation Runs

TGCD	HSKC	BSTR	SPCD	RLNO	RLWT	SCEN	BODY	ENEN	ENDY	RLTR	
1301010104	114	87	440	89280153	0.21	4	25	5	17	88	
1301010105	114	87	440	9439753	0.21	5	10	5	10	88	
1301010106	114	87	440	11522113	0.23	5	31	6	1	88	
	310000	115	87	440	1513	-9.99	5	16	5	16	88
1301010109	115	87	440	35322711	0.21	5	10	6	5	88	
1301010114	115	87	440	40251430	0.21	5	9	5	16	88	
1301010110	120	87	440	37200196	0.25	5	6	5	6	88	
1301010111	120	87	440	17002558	0.37	5	17	5	17	88	
1301010112	120	87	440	33213406	0.33	5	14	5	14	88	
1301010113	120	87	440	43414107	0.37	5	17	5	17	88	
1301010107	122	87	440	184277200	0.25	5	1	5	14	88	
1301010108	122	87	440	11342361	0.23	4	29	5	16	88	
1301010301	114	88	440	40793295	0.25	4	24	4	29	89	
1301010302	114	88	440	32598861	0.28	5	15	5	25	89	
1301010303	114	88	440	43331812	0.23	4	27	5	15	89	
1301010309	114	88	440	43772606	0.25	5	1	5	31	89	
1301010306	115	88	440	10033836	0.21	5	5	5	5	89	
1301010307	115	88	440	20702880	0.23	5	5	5	7	89	
1301010308	115	88	440	28235320	0.25	5	25	6	1	89	
1301010207	120	88	440	21405470	0.31	4	25	4	25	89	
1301010208	120	88	440	19903146	0.34	4	26	4	28	89	
1301010209	120	88	440	20284352	0.31	5	19	5	19	89	
1301010210	120	88	440	14412130	0.28	4	28	4	28	89	
1301010211	120	88	440	32610684	0.50	5	16	5	16	89	
1301010212	120	88	440	9208873	0.40	5	4	5	4	89	
1301010213	120	88	440	10693597	0.40	5	4	5	4	89	
1301010304	122	88	440	112244525	0.23	4	23	4	30	89	

Figure 5. Model Validation work area

Modeling Progress area

The Modeling Progress area is an extensive subsection of the Intranet which is maintained by Vince Patrick and modeling colleagues as a medium for communication of emerging modeling findings to other SEA researchers. It can be accessed directly from the top level page as well as from the synthesis page and model validation sections. Maintained in chronological order, this section traces findings and posts items for review and discussion. A few representative posting examples are illustrated below (Figure 6a-c).

Most recent result from the qualitative analysis of fry model equations

Simulations with the full space-time fry survival model had shown that fry survival could be quite sensitive to initial values for predator and fry population densities. The source of this sensitivity was not immediately obvious.

During the last months a priority has been a qualitative analysis of the solutions to the model equations sufficient for an explanation of the properties exhibited by those simulations. The most recent result of that analysis is presented.

The simulations typically show a first time interval of population movement, then a second time interval with locally homogeneous populations assumed here.

The conditions assumed (spatially uniform, constant populations, with each population assumed to remain invulnerable to the other population either "before" or "after" a few days)).

An unanticipated finding was that the mean length of population in established populations in established populations is the mean length of population in established populations.

The report is a sequence of pages:

- [title page](#)
- [abstract page 1](#)
- [abstract page 2](#)
- [page 1](#)
- [page 2](#)
- [page 3](#)
- [page 4](#)
- [page 5](#)
- [page 6](#)
- [page 7](#)

Brief report of results ("flash" report)

This brief report will use relationships that are rooted in the applied disciplines and will forego the linking of relationships to the SEA foraging - bioenergetics model (units of gm/ha)

Let ψ_f^q denote the foraging rate of predator q on prey f . A spatial domain of approximately uniform density is assumed so that, at most, ψ_f^q varies with

Figure 6a. Use of Intranet for posting of emerging findings in real time, allowing rapid dissemination of results for feedback and discussion.

A further part of the problem statement is

to apply an estimate for survival for the ocean (GOA) phase of pink salmon and thereby forecast an upper bound for adult salmon returns for the following year.

Spatial context of the problem statement

The map at the right shows the spatial context for the problem statement. This map and several companion maps were prepared to describe specific space-time survival issues (hatchery interactions, aggregation in the south in late August, fry density). It is shown here since it seems a simple reminder of both spatial and multidisciplinary aspects of the problem statement. The symbols N_s, N_c, N_w, N_a refer to the total released at Solomon Gulch, Cannery Creek, WHN (Ester), and AFK. The symbols S_pws and S_ocn refer to survival during PWS and the oceanic periods, respectively.

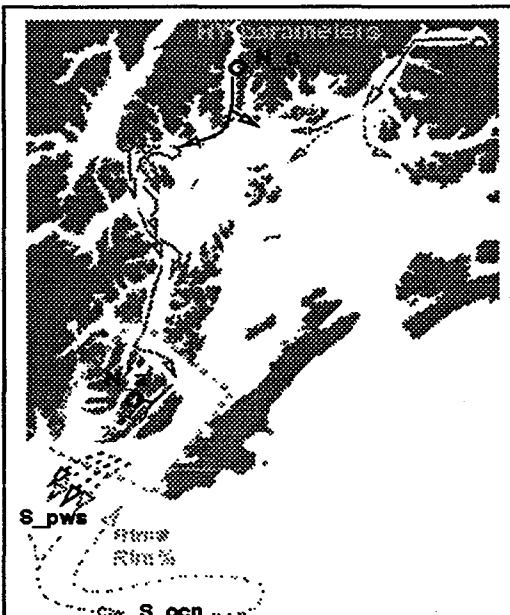


Figure 6b (left)
Use of Intranet for archival postings of SEA's developing description of the system

returns, and survival for the year for each of the four hatcheries based upon estimates without the use of coded wire tags. Data for 88 through 95 is substantially more complex because of the introduction of coded wire tags.

Possibly the greatest m... years 94 and 95 - data widely reviewed within

This review of PWS has:

- Part 1: yearly
 - o cumulative
 - o variable
- variables by ref
- Part 2a: data
- Part 2b: backg
 - o cumulative
 - o variable
- Part 3: main review progress of each
 - o time from
 - o the "dev"
- QC Notes: Rev 1997

Tue Aug 26 08:...

Model for over First formulat

The text is not yet "T2"

first formulation:

Tue Sep 16 16:5...

Most recent re

Simulations with the fu...

(hatchery, release day, release site, treatment, tag group, release mass)

(release day, release site, treatment, tag group, release mass)

slant font = object (e.g., plot) presenting basis for conclusions

total_release
HatchPart_release_tbrnd76-95
HatchPart_release76-95

release/total_release
HatchPart_re2total76-95

77-88 50X incr.
exp change: $2^{(yr-77)/2}$

76-87 AFK dominates

79-89 20X incr.

88-94 constant
500-600million

94-95 1.8X increase
from 500 to 900million

total_return
HatchPart_return_tbrnd76-95
HatchPart_return76-95

79-89 20X incr.
tracks release

91-92 decr. to 0.2X

historical upper bound
31million

total_return/total_release
HatchPart_re2total76-95

historical range 03-07

pink salmon release for PWS hatcheries

annual release

Solomon Gulch
Cannery Creek
Wally Macomber
A. F. Koernig
total

from 87 to 94 releases were quite consistently between 500 and 600 million total;
but in 95 releases almost doubled, reaching 900 million.

Figure 6c (below)
Use of Intranet for sharing in-depth reviews of data relevant to modeling results

Management Collaboration work area

The management collaboration work area was established with the intent of providing an online forum for exchange between SEA researchers and PWS resource managers. It currently exists in functional prototype form although is not yet in routine use. Features to date include postings of early release data, compilations of acoustic survey results, pre-release draft reports, and an index to abstracts presentations of all SEA presentations. There are also facilities for upload of postings from managers and for email feedback.

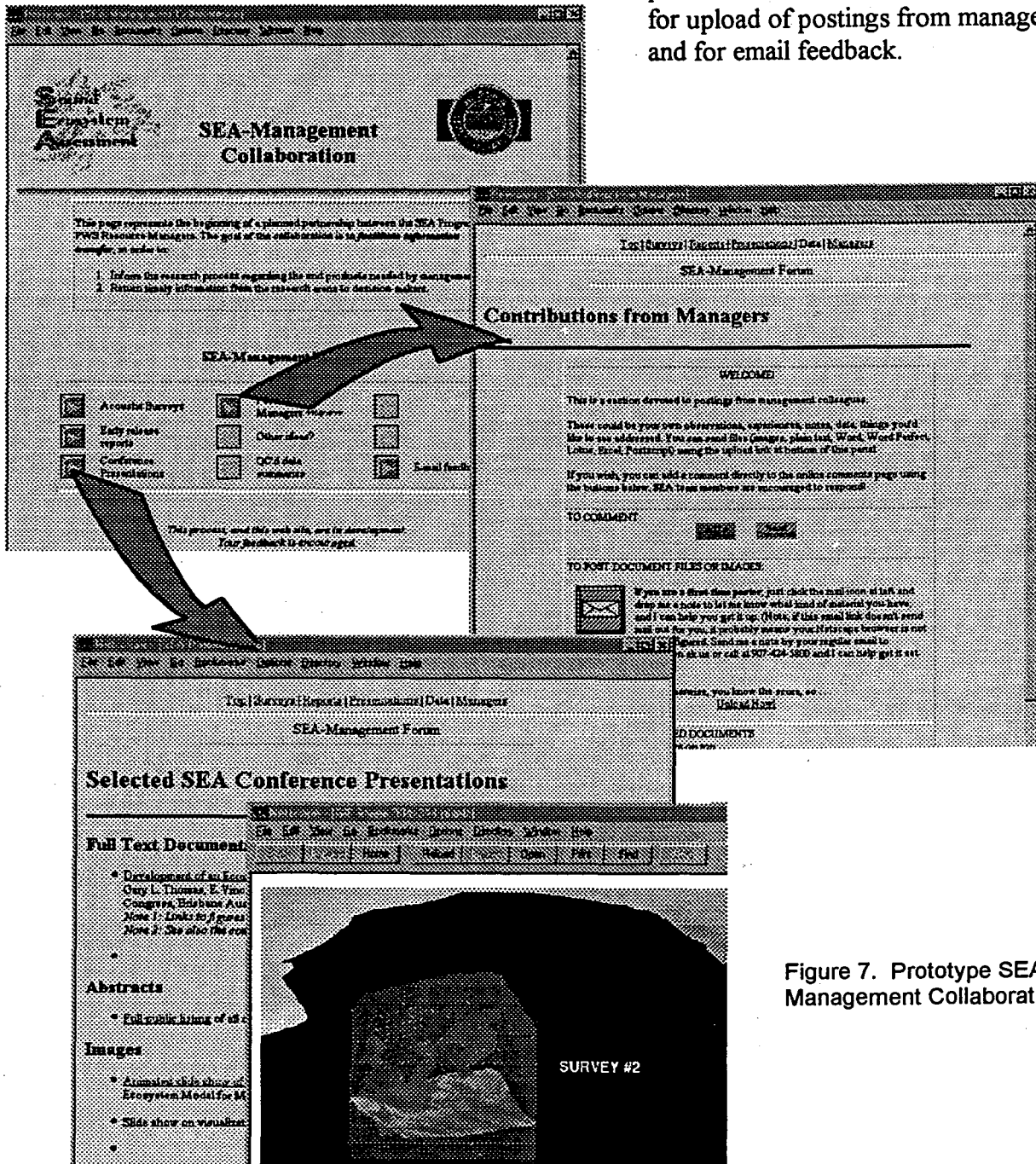


Figure 7. Prototype SEA-Management Collaboration area

REFERENCES

Allen, J.R., Patrick, E.V. and Cooney, R.T. (1997) The SEA Intranet: Scientific collaboration in a shared information space by a multidisciplinary, geographically distributed research team. In preparation.

Allen, J.R. and Patrick E.V. (1997) The SEA Intranet: Story of a long-distance collaboration. Presented at 48th AAAS Arctic Division Science Conference, Valdez Alaska, September, 1997.

Stein, L. D. (1998) Web Security: Reference Guide. Addison Wesley Longman, Inc., Reading Massachusetts. Part II: Client side security. Part III: Server side security.

APPENDIX 1: Usage Statistics for SEA Internal Web Site

- A. June 96 to present, summary of accesses by Investigator**
- B. June 96 to October 97: detailed report.**
- C. October 97 to present: detailed report.**

Please note: these reports cover the SEA internal (restricted access) area only.

Activity in the public SEA web site will be tabulated separately.

A. Usage Statistics for SEA Internal Web Site, by Investigator

Please note: this report tabulates only whole pages accessed. It does not count multiple items retrieved from a single page. This was a design decision intended to best capture actual usage intensity. The numbers below are therefore lower than produced by standard access counters which log every mouse click and every graphic logo, line or button delivered as a "hit".

[Image]
 [Image]
 Back to Stats Menu

SEA Intranet Access Statistics ANALYSIS BY USER

- o June 96 to Today
- o Last 30 Days
- o Last 24 Hours

REPORT PREPARED: Sat Apr 25 04:00:35 AKDT 1998

Total Requests

FOR PERIOD: June 1996 to TODAY

Person	# of Pages Accessed	
		(* = 23 accesses or part thereof)
-----	-----	
allen	3727	*****//
baker	44	**
bishop	34	**
bodnar	34	**
brady	2	*
brown	72	****
clapsadl	140	*****
cooney	172	*****
eslinger	212	*****
falkenberg	127	*****
foy	92	****
gay	17	*
guest	5	*
hauser	52	***
kirsch	189	*****
kline	138	*****
mason	608	*****
mcroy	68	***
mooers	11	*
osgood	358	*****
patrick	580	*****
peters	185	*****
scheel	25	**
seitz	60	***
steinhart	365	*****
stokesbury	85	****
thomas	57	***
thornton	426	*****
tuttle	897	*****
vaughan	252	*****
wilcock	46	**
willette	46	**
williams	395	*****

Back to top

/continued....

=====

REPORT PREPARED: Sat Apr 25 04:00:35 AKDT 1998

=====

Last 30 Days

FOR PERIOD: Mar 25 1998 to Apr 25 1998

Person	# of Pages Accessed		(* = 5 accesses or part thereof)
allen	78	*****	
baker			
bishop			
bodnar			
brady			
brown			
clapsadl			
cooney	15	***	
eslinger	10	**	
falkenberg	3	*	
foy	37	*****	
gay	9	**	
guest			
gunther			
hauser	36	*****	
kirsch			
kline	37	*****	
mason	119	*****	
mcroy	38	*****	
moers			
osgood	48	*****	
patrick	38	*****	
peters	10	**	
scheel	6	**	
seitz			
steinhart	107	*****	
stokesbury	4	*	
thomas			
thornton	14	***	
tuttle	154	*****	
vaughan			
wilcock			
willette			
williams	70	*****	

Back to top

=====

Access counts are for HTML pages and menu requests.
GIF files are not counted.

=====

Analysis by in-house SEA software, code available on request [Image]
jra October 10, 1997

B. Detailed Usage Statistics for SEA Internal Web Site 6-19-96 to 10-15-97
(file-level tabulation is omitted from this printout)

Program started at Thu-16-Oct-1997 14:38 local time.
Analysed requests from Wed-19-Jun-1996 18:03 to Wed-15-Oct-1997 17:59
(483.0 days).

Total successful requests: 30 167 (628)
Average successful requests per day: 63 (89)
Total successful requests for pages: 20 916 (361)
Average successful requests for pages per day: 43 (51)
Total failed requests: 3 557 (73)
Total redirected requests: 3 060 (91)
Number of distinct files requested: 2 420 (90)
Number of distinct hosts served: 89 (11)
Number of new hosts served in last 7 days: 0
Corrupt logfile lines: 8
Unwanted logfile entries: 470 500
Total data transferred: 443 836 kbytes (5 788 kbytes)
Average data transferred per day: 940 973 bytes (846 644 bytes)
(Figures in parentheses refer to the last 7 days).

(Go To: Monthly Report: Daily Summary: Hourly Summary: Domain Report: Host Report: Directory Report: Request Report)

Monthly Report

(Go To: Top: Daily Summary: Hourly Summary: Domain Report: Host Report: Directory Report: Request Report)

Each unit ([+]) represents 60 requests for pages, or part thereof.

month: pages:

Jun 1996: 63: [++]
Jul 1996: 160: [+++]
Aug 1996: 919: [+++++]
Sep 1996: 738: [+++++]
Oct 1996: 2249: [+++++]
Nov 1996: 2326: [+++++]
Dec 1996: 2131: [+++++]
Jan 1997: 2555: [+++++]
Feb 1997: 192: [++++]
Mar 1997: 1581: [+++++]
Apr 1997: 1289: [+++++]
May 1997: 431: [+++++]
Jun 1997: 850: [+++++]
Jul 1997: 1405: [+++++]
Aug 1997: 475: [+++++]
Sep 1997: 1568: [+++++]
Oct 1997: 1984: [+++++]

Daily Summary

(Go To: Top: Monthly Report: Hourly Summary: Domain Report: Host Report: Directory Report: Request Report)

Each unit ([+]) represents 100 requests for pages, or part thereof.

day: pages:

Sun: 2982: [+++++]

```

Mon: 4888: [+++++]
Tue: 3218: [+++++]
Wed: 2980: [+++++]
Thu: 2861: [+++++]
Fri: 2335: [+++++]
Sat: 1652: [+++++]

```

Hourly Summary

(Go To: Top: Monthly Report: Daily Summary: Domain Report: Host Report:
Directory Report: Request Report)

Each unit ([+]) represents 30 requests for pages, or part thereof.

hr: pages:

```

0: 871: [+++++]
1: 873: [+++++]
2: 606: [+++++]
3: 499: [+++++]
4: 246: [+++++]
5: 471: [+++++]
6: 224: [+++++]
7: 220: [+++++]
8: 483: [+++++]
9: 647: [+++++]
10: 826: [+++++]
11: 960: [+++++]
12: 1339: [+++++]
13: 1315: [+++++]
14: 1484: [+++++]
15: 1584: [+++++]
16: 1367: [+++++]
17: 1032: [+++++]
18: 1109: [+++++]
19: 1095: [+++++]
20: 885: [+++++]
21: 968: [+++++]
22: 1011: [+++++]
23: 801: [+++++]

```

Domain Report

(Go To: Top: Monthly Report: Daily Summary: Hourly Summary: Host Report:
Directory Report: Request Report)

Printing all domains with at least 20 requests, sorted by number of requests.

```

#reqs: %bytes: domain
-----
25469: 84.30%: .us (United States)
4010: 14.68%: .edu (USA Educational)
334: 0.52%: .ca (Canada)
185: 0.31%: [unresolved numerical addresses]
142: 0.14%: .net (Network)
27: 0.05%: .com (Commercial, mainly USA)

```

Host Report

(Go To: Top: Monthly Report: Daily Summary: Hourly Summary: Domain Report:
Directory Report: Request Report)

Printing all hosts with at least 20 requests, sorted alphabetically.

#reqs:	%bytes:	host
302:	0.45%:	cyclops.erin.utoronto.ca
62:	0.17%:	banana.ims.alaska.edu
658:	1.70%:	cooney.ims.alaska.edu
29:	0.03%:	filth.ims.alaska.edu
49:	0.18%:	halibut.ims.alaska.edu
27:	0.04%:	murre.ims.alaska.edu
79:	0.21%:	sarah.ims.alaska.edu
78:	0.54%:	scoter.ims.alaska.edu
528:	1.71%:	skua.ims.alaska.edu
134:	0.21%:	sole.ims.alaska.edu
86:	0.31%:	twister.rsmas.miami.edu
62:	0.09%:	venus.rsmas.miami.edu
71:	0.12%:	blackbirch.fnr.purdue.edu
88:	0.24%:	norspruce.fnr.purdue.edu
46:	0.23%:	cooney.ims.uaf.edu
46:	0.05%:	ebrown.ims.uaf.edu
22:	0.03%:	foy.ims.uaf.edu
91:	0.77%:	iron.ims.uaf.edu
49:	0.26%:	murre.ims.uaf.edu
42:	0.08%:	pppl.ims.uaf.edu
52:	0.20%:	sarah.ims.uaf.edu
101:	0.26%:	skua.ims.uaf.edu
34:	0.09%:	sole.ims.uaf.edu
630:	3.21%:	europa.avl.umd.edu
303:	2.21%:	io.avl.umd.edu
487:	1.43%:	limnosun.limnology.wisc.edu
47:	0.08%:	f181-184.net.wisc.edu
21:	0.09%:	f181-196.net.wisc.edu
112:	0.10%:	pwssc.alaska.net
485:	1.25%:	abot.pwssc.gen.ak.us
404:	0.88%:	clupea.pwssc.gen.ak.us
168:	0.56%:	copepod.pwssc.gen.ak.us
25:	0.02%:	curly.pwssc.gen.ak.us
2340:	1.53%:	daffy.pwssc.gen.ak.us
74:	0.22%:	donald.pwssc.gen.ak.us
303:	3.16%:	eagle.pwssc.gen.ak.us
11250:	34.70%:	grizzly.pwssc.gen.ak.us
431:	2.69%:	husky.pwssc.gen.ak.us
411:	1.00%:	ichthys.pwssc.gen.ak.us
111:	0.06%:	larry.pwssc.gen.ak.us
473:	1.58%:	lumpsucker.pwssc.gen.ak.us
316:	0.96%:	marmot.pwssc.gen.ak.us
54:	0.14%:	moose.pwssc.gen.ak.us
509:	1.12%:	nemo.pwssc.gen.ak.us
1316:	6.39%:	onerka.pwssc.gen.ak.us
40:	0.13%:	ophiodon.pwssc.gen.ak.us
139:	0.34%:	orca.pwssc.gen.ak.us
94:	0.11%:	sea6.pwssc.gen.ak.us
6351:	27.30%:	sebastes.pwssc.gen.ak.us
133:	0.08%:	wolverine.pwssc.gen.ak.us
101:	0.21%:	137.229.41.61
23:	0.04%:	146.63.245.240
37:	0.05%:	152.163.195.240

Directory Report

(Go To: Top: Monthly Report: Daily Summary: Hourly Summary: Domain Report:

Host Report: Request Report)

Printing all directories with at least 20 requests, sorted alphabetically.
Printing directories to depth 4.

```
#reqs: %bytes: directory
-----
2215: 1.04%: /sea/block/
500: 0.24%: /sea/block/progop/cal/
817: 1.49%: /sea/block/progop/cruise/
1278: 6.39%: /sea/block/progop/dump/
77: 0.26%: /sea/block/progop/misc_collab/
20: 0.05%: /sea/block/progop/mysterypic/
9542: 15.14%: /sea/block/progop/papers.inprog/
21: 0.01%: /sea/block/progop/proposals.inprog/
5252: 27.53%: /sea/block/progop/rslts_disc/
1927: 2.89%: /sea/block/progop/synthesis/
735: 1.92%: /sea/block/progop/whatsnew/
1611: 8.23%: /sea/block/progop/wip/
1260: 9.94%: /seaDB/
29: 0.07%: /seaDB/Webdriver/
30: 0.05%: /seaDB/cspARFile/ctd/cruise.hdr/
85: 0.25%: /seaDB/cspARFile/ctd/datafiles/
86: 0.38%: /seaDB/cspARFile/zoops/datafiles/
132: 0.02%: /seaDB/cspARFile/zoops/modelfiles/
34: 1.63%: /seaDB/cspARZipFile/
38: 0.05%: /seaDB/page/
252: 0.13%: /seaDBH/
137: 0.06%: /seaDBHtest/
2830: 16.53%: /seaDBtest/
34: 0.24%: /seaDBtest/cspARFile/tide/OLLD/
34: 0.88%: /seaDBtest/cspARFile/zoops/datafiles/
34: 0.01%: /seaDBtest/cspARFile/zoops/modelfiles/
50: 0.37%: /seaDBtest/cspARZipFile/
168: 0.17%: /seaDBtest/page/
306: 1.03%: /synthdoc/
160: 0.02%: /synthdoc/comments/
166: 0.08%: /synthdoc/update/
30: 0.02%: /synthdoc/update/ch01/
30: : /synthdraft/ch01/
24: 0.01%: /synthdraft/ch06/
```


This analysis was produced by analog2.11/Unix.
Running time: 45 seconds.

(Go To: Top: Monthly Report: Daily Summary: Hourly Summary: Domain Report:
Host Report: Directory Report: Request Report)

C. Detailed Usage Statistics for SEA Internal Web Site 10-6-97 to 4-20-98

(file-level tabulation is omitted from this printout)

Program started at Tue-21-Apr-1998 00:16 local time.
Analysed requests from Mon-06-Oct-1997 13:56 to Mon-20-Apr-1998 16:41
(196.1 days).

Total successful requests: 8 285 (78)
Average successful requests per day: 42 (11)
Total successful requests for pages: 4 594 (65)
Average successful requests for pages per day: 24 (9)
Total failed requests: 1 472 (18)
Total redirected requests: 965 (7)
Number of distinct files requested: 725 (37)
Number of distinct hosts served: 59 (7)
Number of new hosts served in last 7 days: 1
Corrupt logfile lines: 33
Total data transferred: 208 651 kbytes (643 481 bytes)
Average data transferred per day: 1 064 kbytes (91 926 bytes)
(Figures in parentheses refer to the last 7 days).

(Go To: Monthly Report: Daily Summary: Hourly Summary: Domain Report: Host Report: Directory Report: Request Report)

Monthly Report

(Go To: Top: Daily Summary: Hourly Summary: Domain Report: Host Report: Directory Report: Request Report)

Each unit ([+]) represents 25 requests for pages, or part thereof.

month:	pages:	
Oct 1997:	1089:	[+++++++]
Nov 1997:	1070:	[+++++++]
Dec 1997:	775:	[+++++++]
Jan 1998:	759:	[+++++++]
Feb 1998:	239:	[+++++++]
Mar 1998:	425:	[+++++++]
Apr 1998:	237:	[+++++++]

Daily Summary

(Go To: Top: Monthly Report: Hourly Summary: Domain Report: Host Report: Directory Report: Request Report)

Each unit ([+]) represents 20 requests for pages, or part thereof.

day:	pages:	
Sun:	346:	[+++++++]
Mon:	1005:	[+++++++]
Tue:	970:	[+++++++]
Wed:	784:	[+++++++]
Thu:	838:	[+++++++]
Fri:	454:	[+++++++]
Sat:	197:	[+++++++]

Hourly Summary

(Go To: Top: Monthly Report: Daily Summary: Domain Report: Host Report: Directory Report: Request Report)

Directory Report: Request Report)

Each unit ([+]) represents 8 requests for pages, or part thereof.

hr: pages:

```

--  -----
0:   47: [++++++]
1:    8: [+]
2:   96: [+++++]
3:  129: [+++++]
4:   71: [+++++]
5:   65: [+++++]
6:   62: [+++++]
7:   55: [+++++]
8:  126: [+++++]
9:  264: [+++++]
10: 358: [+++++]
11: 259: [+++++]
12: 294: [+++++]
13: 296: [+++++]
14: 401: [+++++]
15: 399: [+++++]
16: 330: [+++++]
17: 290: [+++++]
18: 200: [+++++]
19: 168: [+++++]
20: 260: [+++++]
21: 149: [+++++]
22: 113: [+++++]
23: 154: [+++++]

```

Domain Report

(Go To: Top: Monthly Report: Daily Summary: Hourly Summary: Host Report: Directory Report: Request Report)

Printing all domains with at least 20 requests, sorted by number of requests.

```

#reqs: %bytes: domain
-----
6402: 73.25%: .us (United States)
1695: 25.64%: .edu (USA Educational)
  72:  0.23%: .net (Network)
  65:  0.60%: [unresolved numerical addresses]
  34:  0.24%: .com (Commercial, mainly USA)

```

Host Report

(Go To: Top: Monthly Report: Daily Summary: Hourly Summary: Domain Report: Directory Report: Request Report)

Printing all hosts with at least 20 requests, sorted alphabetically.

```

#reqs: %bytes: host
-----
  28:  0.76%:      idefix.rsmas.miami.edu
568: 10.29%: blackbirch.fnr.purdue.edu
  27:  0.44%:      auklet.ims.uaf.edu
  35:  0.33%:      banana.ims.uaf.edu
163:  3.65%:      cooney.ims.uaf.edu
  66:  0.38%:      ebrown.ims.uaf.edu
  32:  0.20%:      engle.ims.uaf.edu
  89:  0.35%:      foy.ims.uaf.edu
  52:  0.35%:      pppl.ims.uaf.edu
345:  3.68%:      sarah.ims.uaf.edu

```

```

100: 0.90%:          skua.ims.uaf.edu
 55: 0.15%:          sole.ims.uaf.edu
109: 4.03%:          europa.avl.umd.edu
 25: 0.11%:          anc-p29-165.alaska.net
 31: 0.10%: dialups-31.cordova.ptialaska.net
 25: 0.04%:          abot.pwssc.gen.ak.us
 23: 0.05%:          commfish.pwssc.gen.ak.us
737: 5.57%:          copepod.pwssc.gen.ak.us
299: 0.71%:          daffy.pwssc.gen.ak.us
121: 0.82%:          eagle.pwssc.gen.ak.us
 47: 0.26%:          evelyn.pwssc.gen.ak.us
2235: 11.29%:         grizzly.pwssc.gen.ak.us
381: 4.33%:          husky.pwssc.gen.ak.us
246: 1.75%:          ictchys.pwssc.gen.ak.us
236: 1.08%:          larry.pwssc.gen.ak.us
112: 1.12%:         lumpsucker.pwssc.gen.ak.us
 41: 0.23%:          mark.pwssc.gen.ak.us
209: 9.84%:          marmot.pwssc.gen.ak.us
134: 0.84%:          nemo.pwssc.gen.ak.us
553: 11.59%:         onerka.pwssc.gen.ak.us
 55: 0.19%:          ophiodon.pwssc.gen.ak.us
155: 2.21%:          orca.pwssc.gen.ak.us
 49: 0.25%:          pwssc-01.pwssc.gen.ak.us
306: 7.92%:          sea6.pwssc.gen.ak.us
404: 12.86%:         sebastes.pwssc.gen.ak.us
 22: 0.09%: 146.63.245.240

```

Directory Report

(Go To: Top: Monthly Report: Daily Summary: Hourly Summary: Domain Report:
Host Report: Request Report)

Printing all directories with at least 20 requests, sorted alphabetically.
Printing directories to depth 4.

```

#reqs: %bytes: directory
-----
 875: 0.84%: /sea/block/
  56: 0.06%: /sea/block/progop/cal/
 127: 0.48%: /sea/block/progop/cruise/
 562: 31.91%: /sea/block/progop/dump/
 470: 2.99%: /sea/block/progop/papers.inprog/
 287: 2.74%: /sea/block/progop/rslts_disc/
3641: 32.73%: /sea/block/progop/synthesis/
 217: 1.83%: /sea/block/progop/whatsnew/
 384: 2.62%: /sea/block/progop/wip/
 586: 12.61%: /seaDB/
  42: 0.32%: /seaDB/cspARFile/echodens/datafiles/
  63: 6.54%: /seaDB/cspARFile/zoops/datafiles/
  23: 0.07%: /seaDB/page/
 127: 0.17%: /seaDBH/
 323: 2.29%: /synthdoc/
  82: 0.03%: /synthdoc/comments/
  40: 0.03%: /synthdoc/draft/ch01/
 162: 0.16%: /synthdoc/update/
  33: 0.05%: /synthdoc/update/ch01/

```

(Go To: Top: Monthly Report: Daily Summary: Hourly Summary: Domain Report:
Host Report: Directory Report)

This analysis was produced by analog2.11/Unix.
Running time: 24 seconds.

Part III-B

**Scientific Visualization Methods for Marine Ecosystem Research:
Case Studies Using AVS for Display of Hydroacoustic Data**

J. R. Allen, E. V. Patrick, R. Kulkarni, G. L. Thomas, and J. Kirsch

Scientific Visualization Methods for Marine Ecosystem Research:

Case Studies Using AVS for Display of Hydroacoustic Data

Jennifer R. Allen¹, E.V. Patrick¹, R. Kulkarni²,
G.L.Thomas¹ and J. Kirsch¹

¹ Prince William Sound Science Center
P.O. Box 705, Cordova AK 99574

² Advanced Visualization Laboratory
University of Maryland
College Park, MD 20746

Running title: Visualization of Marine Systems

Partial Text of a Paper Presented at the
127th Annual Meeting of the American Fisheries Society
Monterey CA, August 27, 1997

INTRODUCTION

Background

The Sound Ecosystem Assessment (SEA) program is a five year, multidisciplinary study initiated in 1994 to examine pink salmon and Pacific herring populations in Prince William Sound (PWS), Alaska. At that time pink salmon and herring were classified as injured and non-recovering species following the 1989 *Exxon Valdez* oil spill. The SEA objective is to develop predictive models of juvenile survival and to separate natural from anthropogenic causes of population fluctuations. The research team includes investigators from the fields of oceanography, remote sensing, phytoplankton, zooplankton, herring and salmon biology, energetics, isotope tracing of foodwebs, and numerical modeling. The ecosystem approach taken by SEA depends upon gaining insight into sound-wide physical processes, as well as an understanding of the spatial and temporal distributions of the fish, their predators, prey, and the biological processes that occur in the areas of overlap. The value of computer visualization in aiding communication of individual results during such efforts at building an ecosystem understanding has been recognized (Lam et al., 1994).

Role of Visualization

Scientific visualization is a form of communication involving both cognitive and computing elements. Functionally it is the process of re-mapping numeric data into a visual representation, in order to facilitate improved understanding of the data structure. This process takes advantage of analytical and pattern recognition capabilities of the human eye-brain system in ways not possible with purely numeric data (DeFanti et al., 1989). In most cases, the visual representation has been found to be more intuitive or accessible than numerical or mathematical portrayals of the same data (Arrott, 1992). The ability to visualize complex datasets, models and results from simulations is increasingly regarded as essential in provoking insights, enabling communication to colleagues, and confirming the integrity of observations (Kaufman, 1994). Figure 1 shows an example with a marine systems application which illustrates the power of the visual approach. Figure 1a is a partial table of data from an acoustic Doppler current profiler (ADCP). This is a 15-line snapshot from a data set which is over 8,000 lines long and occupies several megabytes. Figure 1b shows a 3-dimensional (3-D) still shot from a 4-D tide cycle animation of this data. After re-mapping the 3-D vector data into 3-space and animating it over time, it is possible to visualize current flow patterns in eastern PWS in a way that is not possible from the table of data or even 2-D cross sections or profile plots. The full animation is available for viewing at <http://www.pwssc.gen.ak.us/sea/movies/adcp.mpeg>.

In SEA, high level visualization procedures are being used to help assess dynamic distributions, give some insight into patterns of overlap, and facilitate joint representation of cross-disciplinary observations. The aim is to assist in a visual understanding of the structure of the data as a tool for gaining insight into the underlying biological phenomena. The present communication summarizes visualization techniques employed in this effort and presents some specific examples of hydroacoustics applications.

METHODS

Visualization Software

Most of the visualizations in SEA are performed using the Application Visualization System (AVS) (Advanced Visual Systems, Inc., Waltham, MA). This system uses a data flow paradigm and graphical programming interface to provide an extensible and customizable visualization environment. Libraries of interchangeable modular components are assembled into flow networks. Flow networks are constructed via a graphical user interface (GUI) known as the Network Editor (Figure 2). Additional user-authored modules can be written in either C or FORTRAN, with optional assistance from the AVS module generator. For the SEA work, some customized modules for displaying individual transect data were coded in C. Animations were created using the AVS animator, which provides sophisticated and efficient key-frame interpolation. Animated output was converted to MPEG format for portable, platform-independent, web capable display of dynamic products.

Pixel-based versus Geometry-based Visualization.

Pixel-based visualization is a 2-D process based on a relatively direct one-to-one representation of each data point as a color-coded pixel in an image. By contrast, the work described in this report concerns multidimensional, geometry-based visualization. In geometry-based visualization, data points are mapped into the vertices of geometric objects, and the data values are used to assign color and other characteristics to the geometry. Using AVS, low level graphics software and rendering hardware then render the objects for display to the screen in the AVS geometry viewer. Advanced features available include transparency, texture mapping, volume rendering, particle advection, isosurfaces and slice planes. In addition, use of geometry-based techniques provides a display that is not static, but can be interrogated interactively. Objects in the geometry viewer can be viewed dynamically using the mouse to pan, zoom, rotate the object, change the viewing angle, lighting direction, perspective and other attributes. An animation showing the power of these features is available for viewing on the web at <http://www.pwssc.gen.ak.us/sea/movies/flyby1.mpeg>

Data Model

The data model provides the rules for mapping of the data array into the display coordinate space. The AVS data model supports a number of aggregate data types, of which two were used in the work reported here: unstructured cell data (UCD) and field data. UCD is based on representation of data by a geometric model built from individual cells that are defined by nodes. It provides a useful mechanism for representing volume data that is not sufficiently structured to be represented as a field data type. The UCD data type was employed for some of the acoustic visualization processes, particularly those involving interpolation.

The field structure is typically used for image and volume data. Field Data are in the form of an n-dimensional array with an m-dimensional vector of observations at each location. AVS recognizes uniform, rectilinear and irregular fields. These differ primarily in the method of mapping from the computational space into the coordinate space (see Figure 3). In uniform fields, the elements are equally spaced; in rectilinear fields the between-element spacing can vary but is constant along each axis; whereas in irregular fields there is no implicit mapping between the computational space and the coordinate space, and no restriction that the number of dimensions in the coordinate space be the same as the number of dimensions in the computational space. Because of these useful properties of irregular fields, much of the SEA data is handled as the irregular field type. Figure 3 shows some examples of AVS mappings of irregular fields, showing 1-D data that is re-mapped into 1-, 2- or 3-space, as might occur in visualizing a CTD cast, a single acoustic transect, or a series of acoustic transects, respectively.

Figure 4 shows a composite example in which 2-D acoustic transects re-mapped into 3-D coordinate space; along with several examples of 1-D data sets: CTD casts showing temperature, aerial survey flight paths, and a 1-D data stream from an towed aquashuttle measuring zooplankton counts.

Bathymetry Data

The PWS bathymetry data renderings used as the basis for all visualizations presented here are a product of the SEADATA group from FY94 and also involved collaboration beyond SEA. The original data source was the National Ocean Service (NOS) database, obtained on tape in both raw and 15' gridded versions. Substantial processing performed at the Alaska Department of Natural Resources (ADNR) helped remedy the patchiness of the original NOS coverage. This work yielded several Arcinfo coverages that included 20m depth contours. The present gridded data set was created by David Scheel and Vince Patrick using the 20m contour coverages and Arcinfo coastlines provided by Randal Hagenstein, formerly of Pacific GIS. The last conversion used Delauney triangulation and quintic interpolation in the Arc procedures TIN and GRID, respectively. Additional documentation on this data set is available on request.

Acoustics Data

The data for the acoustic visualization examples presented here are drawn from acoustic surveys in PWS performed by Gary Thomas and Jay Kirsch as part of the SEA program and in stock assessment work with the Alaska Department of Fish and Game (ADF&G). Surveys used a dual beam echo sounder with echo integrator. Accompanying trawl or seine samples provided species composition and size distribution. Post-processing was performed using in-house software developed by Jay Kirsch. Species of interest were identified and separated interactively based on a priori knowledge of acoustic appearance and behavior plus information from the catch data. An estimate of mean backscattering cross-section (target strength) was computed from length/weight measurements in the catch data. Biomass density was then calculated by multiplying the acoustic backscatter (echosquare integration, calibrated) by the target constant of average weight divided by the mean backscattering cross-section. Georeferenced arrays of either volume backscatter (dB) or biomass (kg/m³) were exported for re-mapping and visualization.

CASE STUDIES

1. Spatial distribution patterns of pollock in western PWS.

Re-mapping of acoustic data into 3-space as described above provided early insights into the nature of the time-varying spatial distribution of pollock, an important system predator. Figure 6 shows data from multiple surveys during the spring and summer of 1994 in the western corridor of PWS. Figure 6a shows survey transect locations in May (red) and July (blue); Figure 6b shows the locations where pollock were present. Figure 6b is zoomed and rotated to about 45 degrees from the vertical to reveal the depth distribution. This method of display makes it easy to discern that pollock are collected at the northern and southern ends of the passage at both observation times, but that in July the distribution is more aggregated or contagious than in May. There is also a tendency for pollock in the southern areas (lower Knight Island Passage and Montague Strait) to be deeper in the water column, particularly in July, compared with the northern end where they are concentrated near the surface. This pattern could be related to food

supply, as pollock in the north are likely feeding on newly released fry from the Wally Noerenberg hatchery. In contrast, by the time they reach the southern end of the migration corridor the fry are more dispersed and larger, and the pollock may be turning to alternative sources of food. It should be noted that this picture is just showing presence or absence, i.e. the pattern of the distribution, but gives no indication of density. Figure 7 shows the same pollock distribution data enhanced by addition of a quantitative representation. Here biomass density is coded by color. In this and all subsequent images, density scales range from blue (lowest density) to red (highest). This figure confirms that in the northern part of the channel the pollock aggregation was concentrated near the surface, while moving down the channel the densities decrease and the higher concentrations were deeper in the water column.

2. Case Study: Pollock and Plankton Co-Distribution

This set of figures provides an example of overlaying distributions of organisms from two different trophic levels, in this case pollock and zooplankton, in order to examine their codistribution patterns in time and space. Figures 8a and 8b show pollock and plankton densities assessed acoustically in the same region of PWS as the preceding case. In these figures, pollock density is indicated by color on a scale of 10^{-6} to 10^{-3} kg/m³. The slightly compressed scale is used to shorten the scale of contrast and thereby highlight patches in the pollock distribution. Zooplankton are indicated by black dots, classified here on a 4-point qualitative scale from 0 to 3. Only levels 3 and 4 are plotted; the larger black dots indicate the highest density level. The inset in Figure 8a shows an example of an AVS widget: in this case the color map interface. The viewer can use these controls to adjust the lower and upper bounds, and other properties, of the color scale, in order to narrow or broaden the focus on the density region of interest. Similar dynamic techniques are used in medical imaging to interrogate density-based 2-dimensional images such as CT and MRI scans. From these data, in May, there appears to be some concordance between the high density pollock and the plankton clumps, but only imperfect agreement. It is easy to find aggregations of pollock where not associated with plankton aggregations. On the other hand, in July, the remaining dense clumps of pollock are associated fairly consistently with high density zooplankton patches.

3. Case Study: School characteristics of adult herring and pollock and repeatability of herring acoustic surveys.

The third example illustrates some more advanced visualization techniques and ways they can be applied to acoustic data once it has been re-gridded into 3D coordinate space. The example focuses on repeated surveys of herring schools, conducted on a pre-spawning aggregation of tightly grouped adult herring in Stockdale harbor in March 1996. Stockdale harbor is a shallow bay with a sloping shore (Figure 9). This enables the herring to move onshore into quite shallow water and can make covering a school with an acoustic survey difficult.

a. 1-D Remapping into 3-space (scatter dot cloud)

Figure 10a shows a top-down view giving the orientation of the survey transects. Figures 10b through d show progressive rotation of the geometry about the vertical axis from 20 to about 85

degrees (d), by which point the viewpoint is into the bay at an angle almost perpendicular to the horizontal face of the transects. Each colored dot in this image corresponds to an actual data point from the echo-integration data. Viewed together, the 3-D dispersion of the from all transects forms a “scatter dot cloud” that to the human eye takes on the appearance of an almost solid object.

b. Volume interpolation

In Figure 11a, the size of the dots has been reduced and a semitransparent interpolated volume has been overlaid. The boundaries of this colored volume represents the actual sampled water volume in the survey and its colors correspond to the log of fish density (expressed here as volume backscatter in dB). The volume interpolation in this study was achieved by reconfiguring the data into a UCD format and then applying an interpolation by Delauney triangulation using several UCD-processing module from the AVS libraries. The fuzzy 3-D region delimited by the red-orange-yellow region within the interpolated volume corresponds to the most dense area of the herring school.

c. Slice planes and Isosurfaces

Having achieved a volume interpolation of herring density, two further manipulations are useful for assessing school distribution. The first is to pass a slice plane through the volume (Figure 11b). This plane can be placed at any orientation and at any depth within the volume. In this case a horizontal plane, i.e. parallel to the water surface, has been positioned at a depth of about 15m. The colors on the slice correspond to herring density encountered at that slice plane, ranging from blue (empty water) to red (highest herring density). The widget illustrated in Figure 11b is a control panel that allows the viewer to interactively position the plane. Plane angle, offset and depth are all user adjustable. The viewer can thus dynamically interrogate the data, by moving the slice plane through the volume and visualizing the changing shape of the density pattern. Doing this rapidly on a live screen gives the viewer a good “feel” for the structure of the fish school. Figure 12a-12d shows a series of 4 such horizontal slices passing through the school at progressively increasing depths. This series indicates that the herring are crowded towards the shoreline at the inner margin of the surveyed volume. The last slice in the series contains blue-green densities only, indicating that the school was, however, fully encompassed in the vertical direction in this survey.

The second useful manipulation is to delineate sub-volume structure by means of isosurfaces. The AVS isosurface module takes UCD data as input and produces a 3-D surface passing through all points at the specified density level and enclosing points at higher densities. Figure 13a and b show two representative surfaces at -45 and -37 dB respectively. Again, interactive widgets enable the viewer to dynamically interrogate the data by sweeping the isosurface threshold through a range of values, thereby visually delineating the shape of the school. The image movement which accompanies dynamic use at the computer also facilitates appreciation of the 3-D orientation of the school which is more difficult to convey in 2-D still shots here. In this survey the herring school has a single center of aggregation and this core is located relatively deep within the sampled volume. Although the school depth and location are variable, this pattern of

unifocal aggregation is typical of adults in the prespawning period. However the schooling patterns differ among species. For example, Figure 14a and 14b show results of a survey of adult prespawning pollock in March 1997 in Port Bainbridge. This visualization was generated in the same way as described above. The color scale indicates biomass, with bounds set to encompass the range from empty water to densest fish aggregations seen. In this survey the pollock isosurfaces tend to be rather fragmented, indicating that these pollock were not aggregated into a single concentrated school were dispersed more diffusely. (It should be noted that this is not a constant finding for pollock, since a survey the preceding year did not show this appearance but instead revealed more aggregation, with the pollock isosurfaces enclosing large coalesced volumes that appeared more like the herring pictures.) The visualization techniques used in this example are providing information about the fish schooling behavior that is difficult to discern simply from looking at the individual 2-D transects.

d. Time animation of herring school movements

The fourth component of this study consisted of repeating the above procedures for each of five surveys conducted over the Stockdale harbor herring school during a single night. In particular, the isosurface demarcating the body of the herring school was generated for each survey. The results were then animated over time, yielding a display which illustrates the temporal and spatial dynamics of this single large school. In addition, visualization results for each survey were used to assess the completeness of coverage of the school by the survey. This technique thereby provides information that can be used to (a) assess the repeatability of survey methods, and (b) help determine the validity of inclusion of particular surveys in biomass estimate determinations, by means of providing a visual assessment of the degree of truncation of the school. In this case, the herring school was found to be quite mobile, with both its depth and its concentration on or off shore varying during the course of the night. Of the five surveys, #2 and #3 were considered successful in capturing the bulk of the school, whereas #1, #4 and #5 all exhibited varying degrees of truncation of the school. The animation showing school movements is available for viewing at <http://www.pwssc.gen.ak.us/sea/movies/herring1.mpeg>

DISCUSSION

The exponentially increasing power of computers and graphics systems has made it possible for computer scientists and engineers to exploit advanced data visualization techniques using realtime interactive display. It was predicted early in this decade that interactive visualization would "offer the possibility of profoundly changing the way we assimilate and process new information" (Arrott, 1992) and to a great degree that has proven true. However the high level of programming expertise required has tended to limit the use of these techniques by scientists in general. In this respect AVS is a compromise which allows the scientist to develop powerful customized visualization applications, but at the same time reduces the programming required. This combination is beginning to bring visualization techniques into more generalist use. For example, Socha et al. (1996) developed a customized data-handling module as part of a post-processing system for AVS-based analysis of acoustic data, with display in 2-D image format. The

extendability of AVS have been investigated by Pagendam and Choudry (1993), who found creation of user modules for AVS to be feasible and comfortable. In addition, large numbers of modules are available for the system, both in the marketed application and via the international user group web site.

The present work with multidisciplinary data from a marine ecosystem study confirms the some of the usefulness of visualization applications that has been reported from other fields. In the present study, many relationships of interest involve multidimensional quantities both in domain and range; variables measured at multiple spatial scales, changing over both space and time. In addition, many measurement technologies, such as remote sensing, hydroacoustic and many oceanographic techniques, give rise to extremely large volumes of digital data. While such large collections of numerical values contain great deal of information, effectively conveying the information requires a form of communication with a high bandwidth and an effective interface (Nielson, 1989). Visualization techniques such as those described here provided a means of conveying information compactly and effectively. Although the display is somewhat subjective, it nevertheless was useful in revealing patterns that often suggested avenues of further analysis or further questions to be addressed. The value of interactivity for evaluating visually presented data has been stressed repeatedly by others (Nielson, 1989; Arrott, 1992; Kaufman, 1994) and this was also borne out by the present work using such interrogation operators as the slice plane and isosurface threshold to delineate fish school boundaries. Interactivity, and its consequence, motion, were particularly valuable in enhancing three-dimensional comprehension of the data structure. Abilities in 3-D perception were noticeably variable between individuals, but in all cases lack of 3-D comprehension was overcome by the introduction of movement, as this enabled the viewer to establish 3-D reference points and relationships. Interactivity also, as reported by Neilson (1989), "allows the researcher to cooperate with the computer, increasing the chance for insight and understanding". Animation sequences were also found to be effective at revealing the time evolution of changes and also were particularly valuable in communicating results.

Advanced visualization methods have not previously been reported in application to fisheries acoustics data. Greene et al. (1996) described the use of visualization methods for assessment of patchiness in plankton populations. They found that interactive exploration of 3-D acoustic datasets provided enhanced insights into zooplankton and micronekton dynamics and spatial structure. The present work suggests similar benefits arise from application of visualization procedures to fisheries acoustics data. Active areas of visualization research, continuing both in SEA and elsewhere, include development of graphical computer interfaces to design simulation and modeling environments that are more accessible to decision-makers (Wagner et al., 1996); integration of scientific visualization systems with geographic information systems in order to realize simultaneously the complementary strengths of each (Hay and Knapp, 1996); and use of the Java language and web-based protocols to permit platform-independent data visualization across collaborative groups (Byeongseob and Klasky, 1997).

ACKNOWLEDGMENTS

We thank Mark Willette, Kevin Stokesbury, and John Wilcock for assistance in data interpretation. This work was performed as part of the Sound Ecosystem Assessment (SEA) Program funded by the *Exxon-Valdez* Oil Spill Trustee Council.

REFERENCES

- Arrott, M. and Latta, Sara (1992) Perspectives on visualization. *IEEE Spectrum*, September 1992, pp. 61-65.
- Byeongseob, K. and Klasky, S. (1997) Collaborative scientific data visualization. *Concurrency Pract. Exp.* 9(11):1249-1259.
- DeFanti, A., Brown, M.D. and McCormick, B.H. (1989) Visualization: Expanding scientific and engineering research opportunities. *IEEE Computer* 22:12-25.
- Domik, G. (1996) Computer visualization: Concepts, trends and current research. *Proceedings 23rd International Symposium on Current Trends in Theory and Practice of Informatics*. Milovy, Czechoslovakia, November 1996.
- Globus, A. and Raible, E. (1994) Fourteen ways to say nothing with scientific visualization. *IEEE Computer* 27(7):86-88.
- Hay, L. and Knapp, L. (1996) Integrating a geographic information system, a scientific visualization system, and an orographic precipitation model. *Proceedings of International Conference on Application of Geographic Information Systems in Hydrology and Water Resources Management*, Vienna, Austria, April 1996. pp. 123-131.
- Greene, C.H., Wiebe, P.H. and Zamon, J.E. (1994) Acoustic visualization of patch dynamics in oceanic ecosystems. *Oceanography* 7(1): 4-12.
- Kaufman, A.E. (1994) Visualization (guest editorial). *IEEE Computer* 27:18-19.
- Lam, D.C.L., Wong, I., Swayne, D.A. and Fong, P. (1994) Data and knowledge visualization in an environmental information system. *J. Biol. Syst.* 2(4):481-497.
- Nielson, G.M. (1989) Visualization in Scientific Computing. *IEEE Computer*, 22:10-11.
- Pagendarm, H.-G. and Choudry, S.I. (1993) Visualization of hypersonic flows: Exploring the opportunities to extend AVS. *Proc. 4th EuroGraphics Workshop in Visualization in Scientific Computing*, Abington, UK, April 1993.
- Socha, D.G., Watkins, J.L and Brierly, A.S. (1996) A visualization-based post-processing system for analysis of acoustic data. *ICES Journal of Marine Sciences* 53(2):335.
- Wagner, P.R., Freitas, C.M.D.S. and Wagner, F.R. (1996) A new paradigm for visual interactive modeling and simulation. *8th European Simulation Symposium*, Genoa, Italy, October 1996. Vol.1 pp. 142-145.

FIGURES

All figures and animations accompanying this report are available for viewing on the web at <http://www.pwssc.gen.ak.us/evos97rpt/>

FIGURES

Figure 1: Acoustic Doppler current profiler (ADCP) vector animation in eastern PWS. **A.** Form of the stored data; first 15 lines of a multi thousand line file. **B.** The 3-D visualization. This view looks north in PWS through Hinchinbrook Entrance. The arrows indicate direction and magnitude of current flow. Red arrows are closest to the surface, blue arrows to the bottom. The data are animated over 8 stages of the tide. Full animation available for viewing at <http://www.pwssc.gen.ak.us/sea/movies/adcp.mpeg>.

Figure 2: AVS network editor interface. This example shows the AVS network that generated one of the visualizations presented in Case Study #3. The screen consists of a library of modules (top) and a work area for flow network construction (below). Each box in the work area is a module which performs a specific function data handling or graphic manipulation function. The point-and click interface allows the user to select modules from the libraries, drag them to the work area, and connect them together to specify routes of data flow through the network. Data enter the network at the top, pass through being acted upon by each module in turn under control of the flow executive, finally being output as the graphic product. AVS also provides for co-routines (modules that act spontaneously) and upstream flow control for specialized feedback loop requirements. In addition to the data input and output ports for data flow, most modules accept input parameters to adjust functional settings at run-time. These are presented in the form of graphical widgets: dials, buttons, slider bars, that allow the user to configure or interactively adjust the visualization during the data display process.

Figure 3: Steps in generation of geometry-based visualization using AVS. Georeferenced data are acted on by “filter” modules to produce representations in terms of the AVS data model, and then passed through “mapper” modules to create geometric objects which in turn can be acted upon in various manipulations such as slicing and contouring.

Figure 4: Examples of AVS mappings for irregular fields. Computational space refers to the dimensionality of the data (AVS assumes that the computational space is logically rectangular, with each dimension forming a perpendicular axis beginning at the origin, with the interval between elements equal to 1 for each element in the array). Coordinate space is the physical space into which the data array is mapped. Regridding is accomplished by explicitly defining the mapping that translates each data point into a specific location in physical space. This allows, for example, a 2D plane such as an acoustic transect to be re-mapped into 3D space. Because of the nature of the sparse sampling in large marine systems, it can often be convenient to handle data as a 1D array of points remapped into 3-space, as this avoids the requirement of having an observation for every possible combination of x,y,and z locations within the data array.

Figure 5: Simultaneous display of multidisciplinary ecosystem data sampled at different spatial scales. This example includes 2-D acoustic transects re-mapped into 3-D coordinate space (the vertical planes); along with several examples of 1-D data sets: CTD casts showing temperature, (cylinders); aerial survey flight paths (red lines), and a 1-D data stream from an towed aquashuttle measuring zooplankton counts (sinusoidal track).

Figure 6: Pollock surveys 1994. **A.** Location of survey transects in May (red) and July (blue). **B.** Location of pollock. For more explanation, see text - Case Study #1.

Figure 7: Quantitative representation of pollock distribution in northwestern PWS, May. Wally Noerenberg hatchery is at top left of image. For more explanation, see text - Case Study #1.

Figure 8: Co-distribution of plankton (black dots) and pollock (colored areas) in northwestern PWS in May (**A**) and July (**B**). This figure also shows AVS widgets for interactive adjustment of color scale. For more explanation, see text - Case Study #2.

Figure 9: Location and bathymetric features of Stockdale Harbor, a prominent location for aggregation of pre-spawning adult herring in PWS.

Figure 10: Preliminary step in herring survey visualization in Stockdale Harbor. **A.** Top-down view of transect locations. **B.** through **D.** progressive rotation toward a front-on view, illustrating the appearance of the “scatter dot cloud”. For more explanation, see text - Case Study #3.

Figure 11: Volume interpolation used in herring survey visualization in Stockdale Harbor. **A.** The interpolated volume is displayed as the semitransparent structure seen here, color coded by herring biomass density. **B.** A horizontal slice passed through the interpolated volume at approximately 15 m depth. The widget shown in this figure allows interactive movement of the plane through the region of the herring school. For more explanation, see text - Case Study #3.

Figure 12: Sequence of 4 slices moving through the interpolated volume, beginning near the surface and passing through the herring school. For more explanation, see text - Case Study #3.

Figure 13: Isosurfaces through interpolated volume in herring survey visualization. **A.** Surface at -45dB **B.** Surface at -37dB, delineating the core of the herring school. For more explanation, see text - Case Study #3.

Figure 14: Isosurfaces through interpolated volume in pollock survey visualization, showing more fragmented distribution than seen for the herring. For more explanation, see text - Case Study #3.

A.

400	400	400	30	8	47	4						
94	9	19	19	21	39	96	1	6	5.680	-1.400	58.320	11.630
-207.90		-111.10					-0.90	0.10	-32768	-32768	-32768	-32768
	205.80	209.88	196.81									199.79
191.66		81.23					91.03		168.64		191.64	
	60.5840625	-145.9955711					-201.60		-66.30		173.9	
-1571.0		-82.5					-228.5			0.0	0.0	0.0
	0.0	0.0	0.0									
30 cm BT	dB	0.43	0.038									
13.98		7.57	224.465	-5.3	-5.4	2.6	2.2	75.8	77.1	76.3	7	
5.4	100	-5.51										
17.98		15.68	238.033	-13.3	-8.3	1.3	6.4	76.8	80.2	78.1	7	
5.9	100	-2.65										
21.98		18.98	227.990	-14.1	-12.7	1.0	3.7	76.8	79.4	77.7	7	
6.4	100	-6.88										
25.98		24.47	224.669	-17.2	-17.4	1.4	-1.0	77.7	79.4	79.0	7	
6.8	100	-10.75										
29.98		26.05	234.846	-21.3	-15.0	1.1	3.1	77.0	78.7	78.3	7	
6.5	100	-4.84										
9.0	100	-14.01	223.708	-19.5	-20.4	1.2	6.9	77.7	79.9	77.7	7	
37.98		31.76	226.148	-22.9	-22.0	0.6	5.9	80.0	85.2	82.2	8	
3.9	100	-11.78										
41.98		44.83	209.539	-22.1	-39.0	2.6	11.6	82.2	90.8	86.5	8	
8.2	100	-33.42										
45.98		28.00	225.000	-19.8	-19.8	-1.6	-1.0	86.4	97.6	90.7	9	
2.4	83	-4.28										
49.98		10.15	212.125	-5.4	-8.6	-0.3	0.2	93.1	97.0	93.6	9	
5.3	100	-7.99										
53.98		7.44	120.700	6.4	-3.8	0.6	2.3	97.2	99.4	95.9	10	
1.1	100	-11.40										
57.98		15.48	127.388	12.3	-9.4	-0.4	3.9	99.5	101.7	100.4	10	
1.7	100	-20.63										
61.98		14.45	152.371	6.7	-12.8	-0.4	-0.6	99.6	100.5	103.9	9	
8.7	100	-19.66										
65.98		13.10	138.403	8.7	-9.8	0.2	6.9	98.4	100.1	100.1	10	
0.1	100	-18.76										
69.98		17.40	109.477	16.4	-5.8	0.9	5.6	99.7	101.8	101.4	9	
9.2	100	-18.41										
73.98		15.34	85.888	15.3	1.1	0.7	5.0	97.1	100.1	100.9	9	
4.5	100	-8.16										
77.98		11.85	78.311	11.6	2.4	0.6	5.8	94.9	97.9	97.9		

B.



Figure 1.

Color versions are available for viewing at www.pwssc.gen.ak.us/evos97rpt/

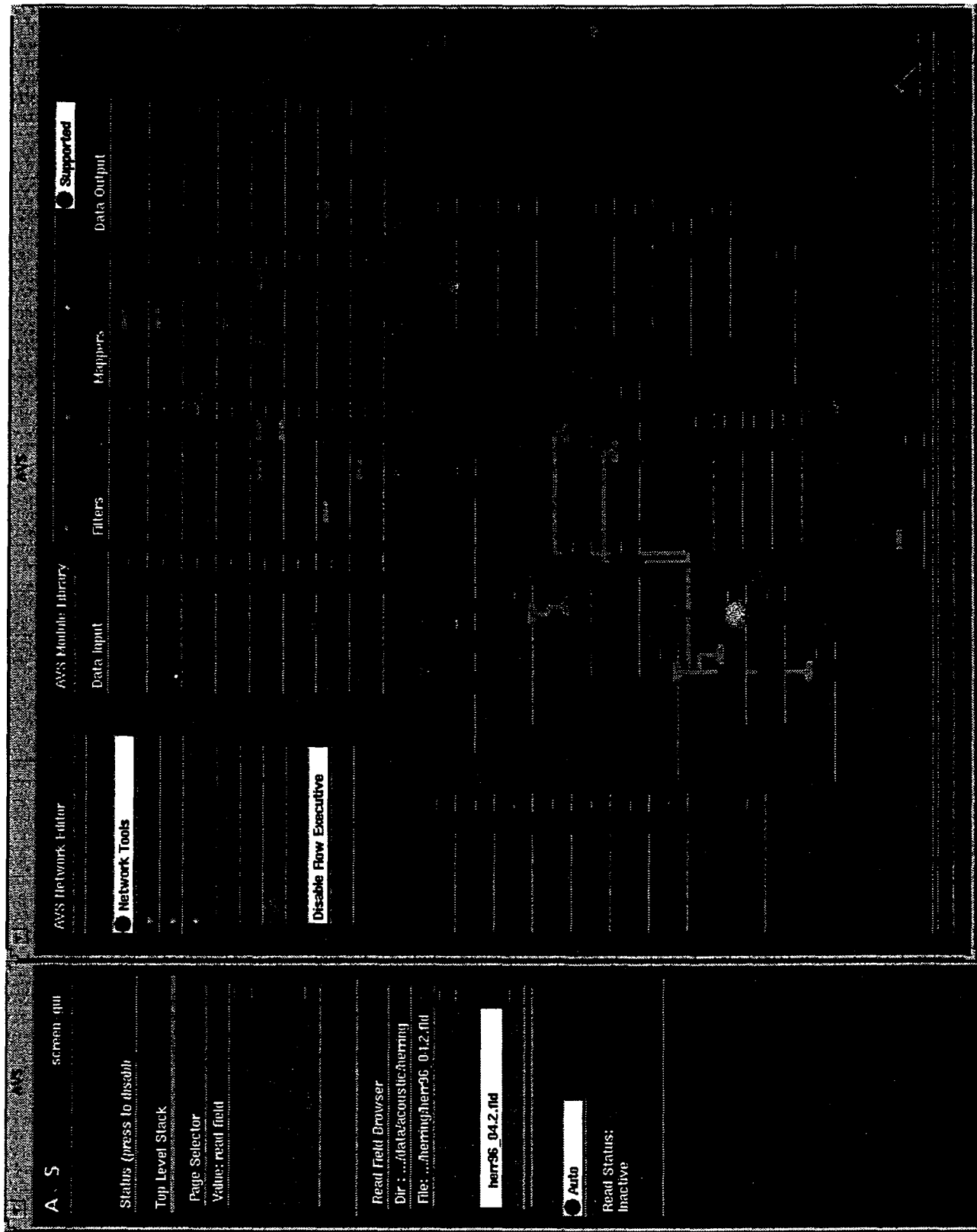


Figure 2.

Color versions available for viewing at www.pwssc.gen.ak.us/sea/evos97rpt/

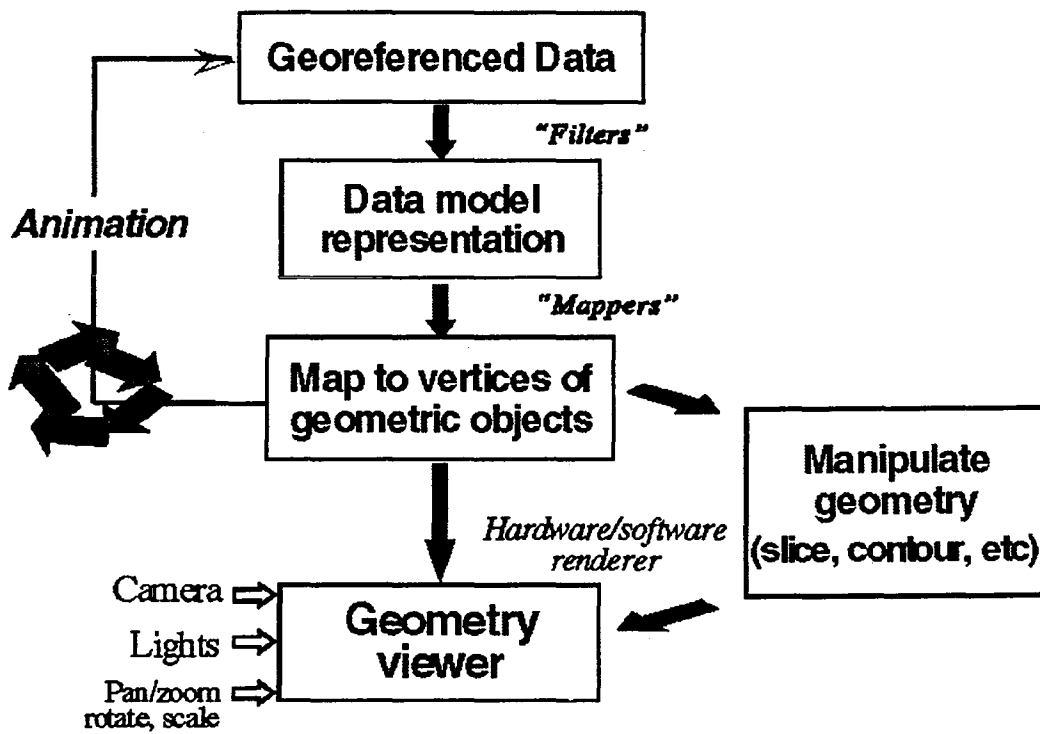


Figure 3

Examples of AVS Mapping for Irregular Fields







	Computational Space	Coordinate Space
	1	1
	1	2
	1	3 *
	2	2
	2	3 *
	3	3 *

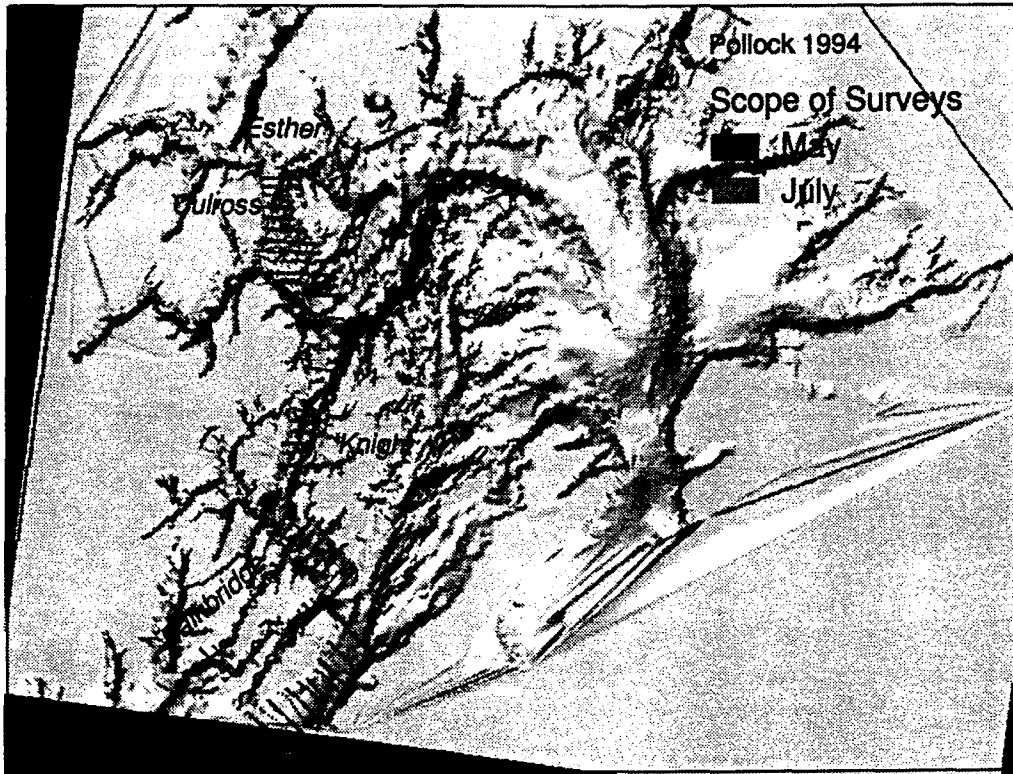
Figure 4



Figure 5.

Color versions available for viewing at www.pwssc.gen.ak.us/sea/evos97rpt/

A



B

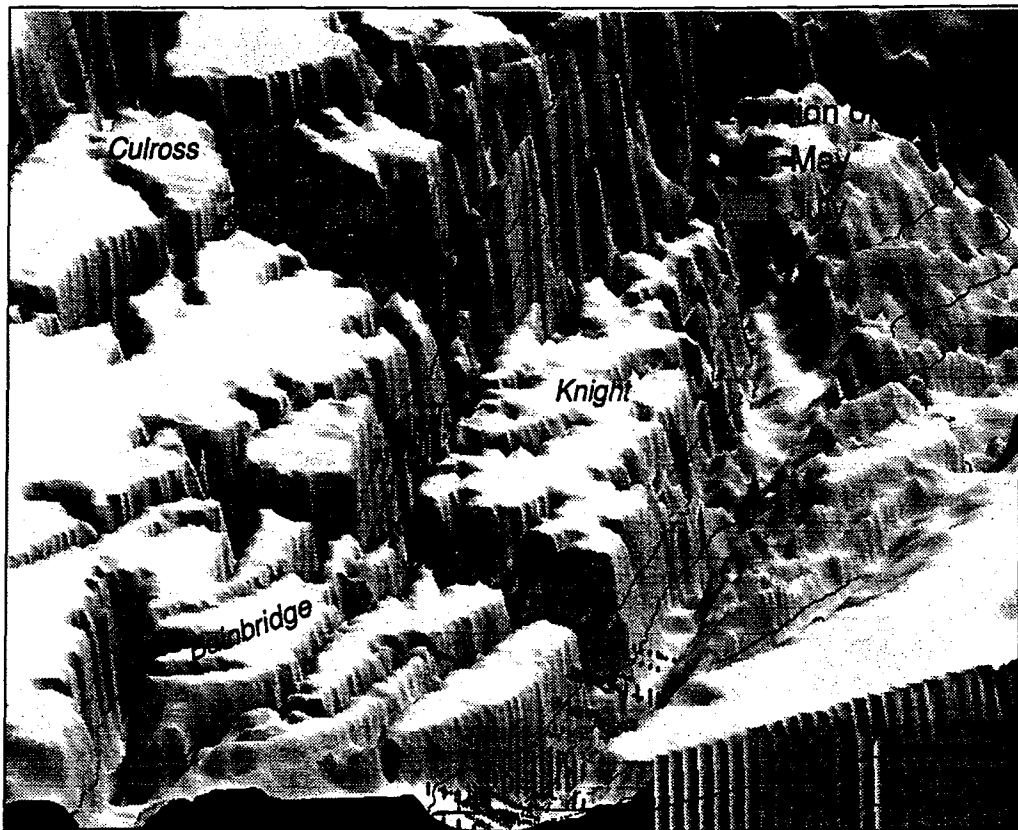


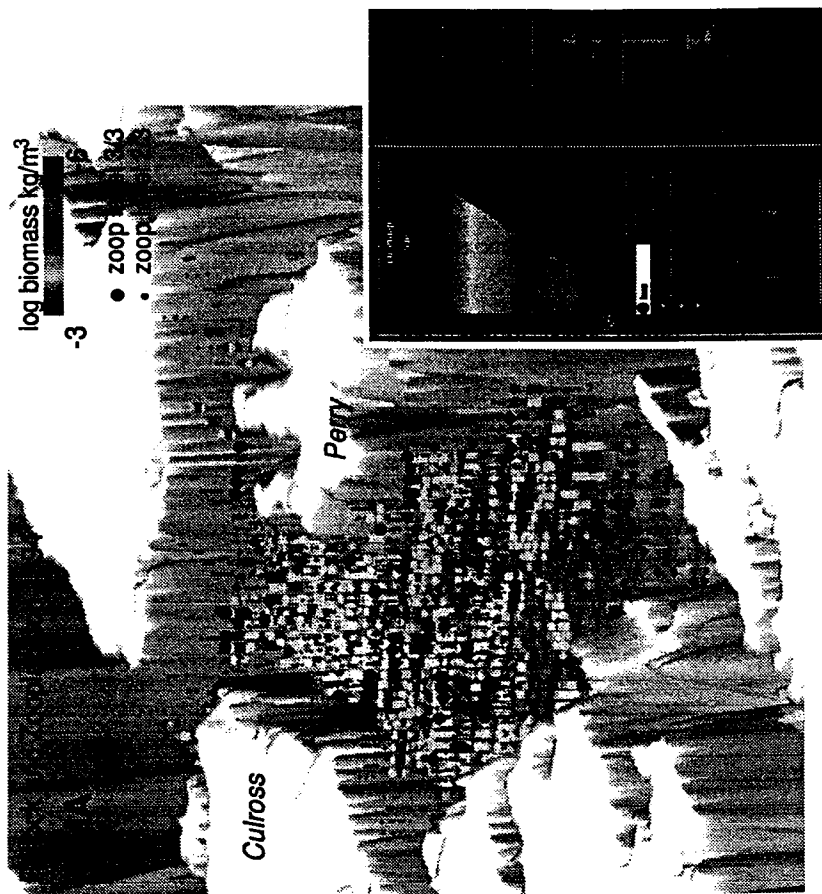
Figure 6

Color versions available for viewing at www.pwssc.gen.ak.us/sea/evos97rpt/



Figure 7.

Color versions available for viewing at www.pwssc.gen.ak.us/sea/evos97rpt/



A



B

Figure 8

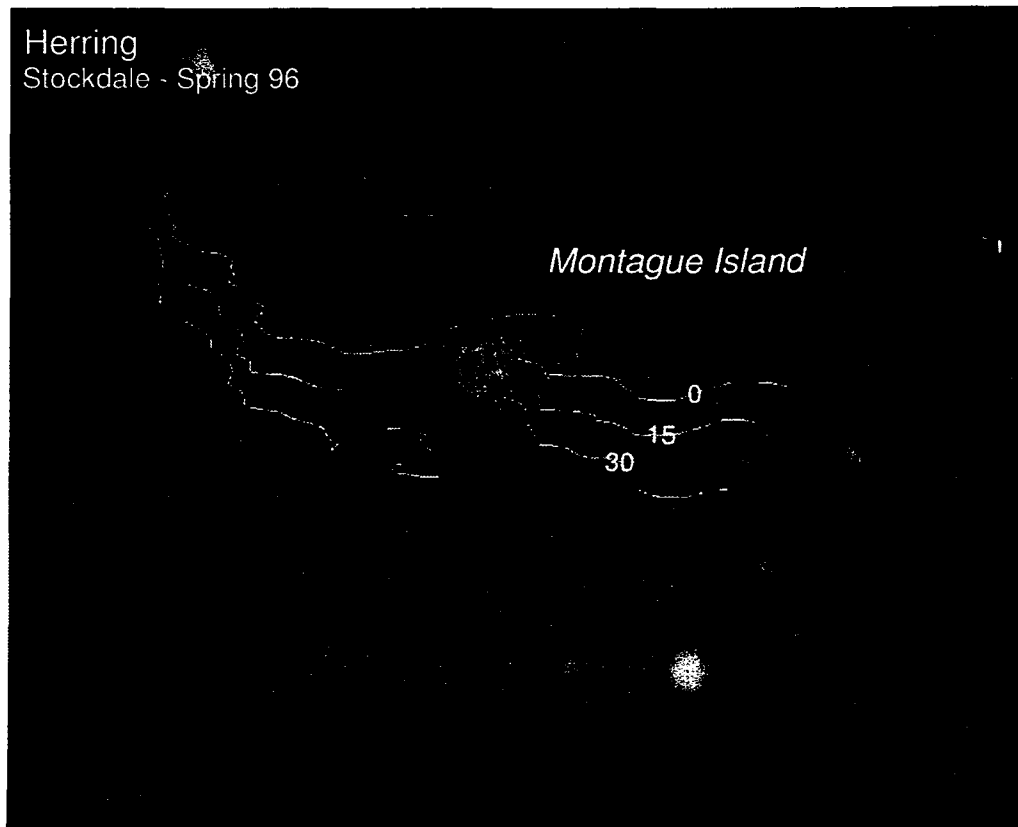
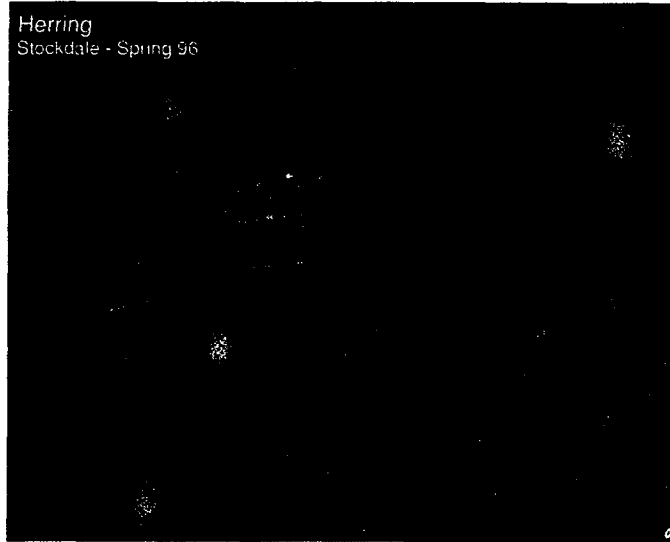
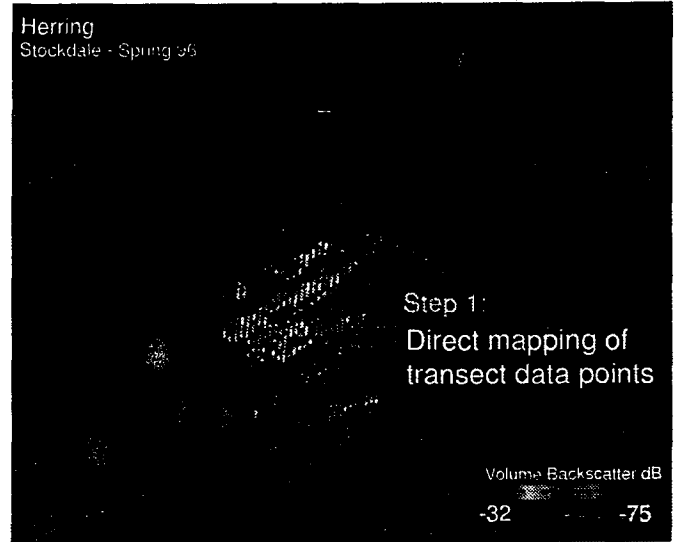


Figure 9

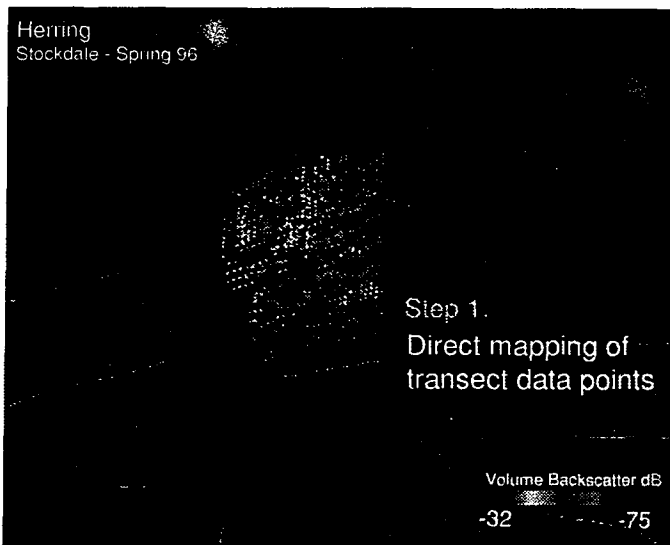
Color versions available for viewing at www.pwssc.gen.ak.us/sea/evos97rpt/



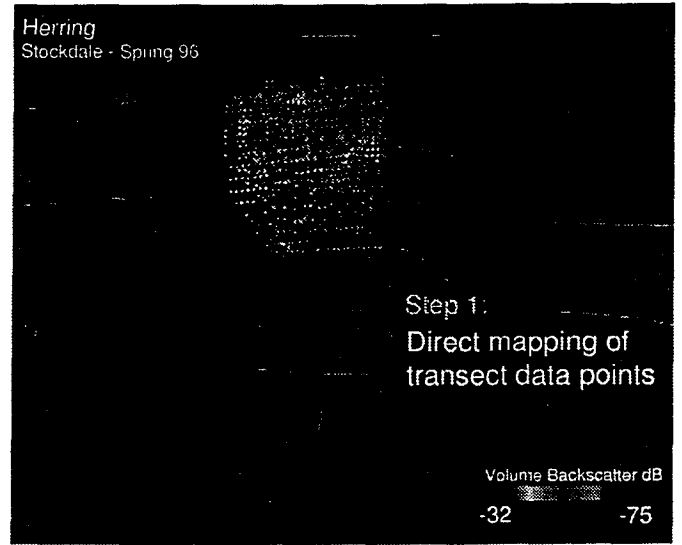
A



B



C



D

Figure 10

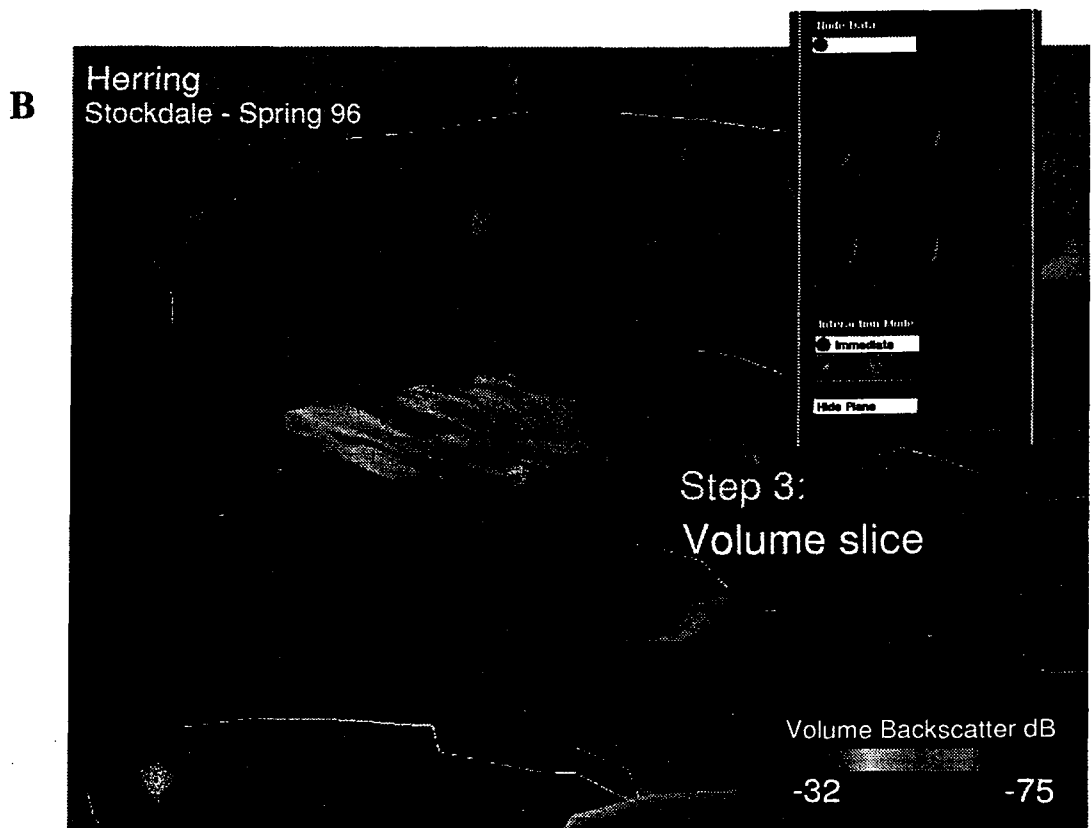
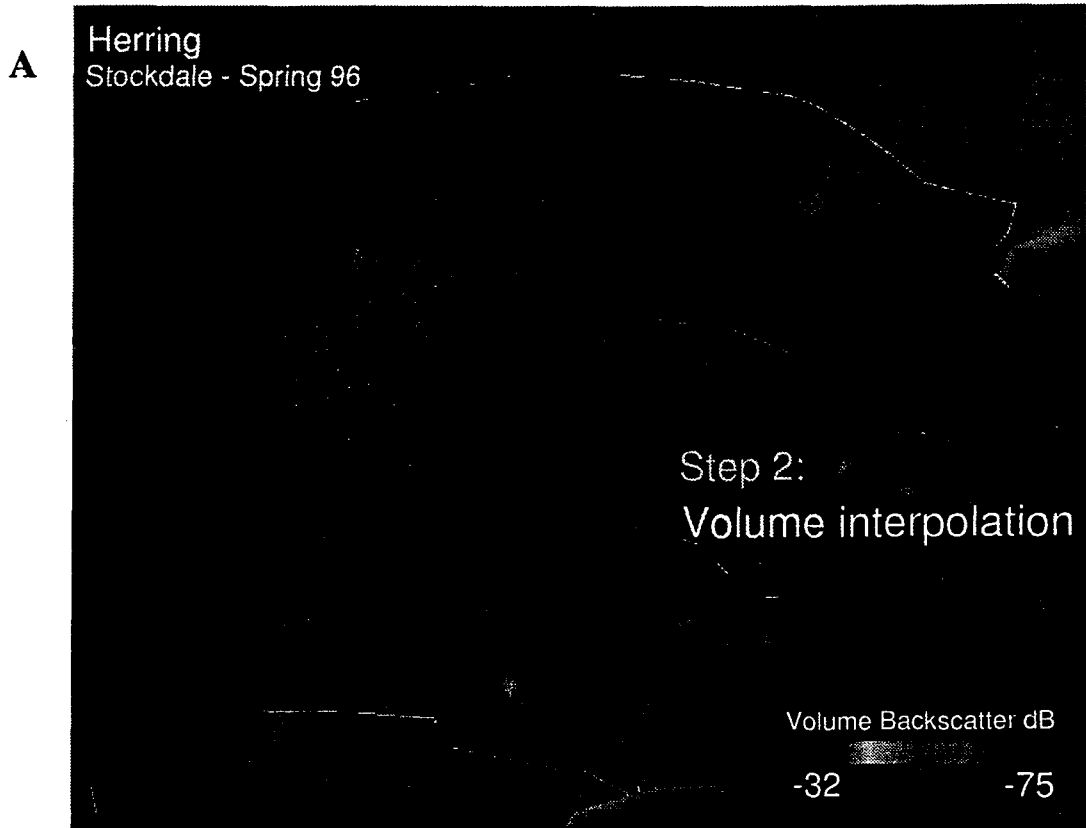
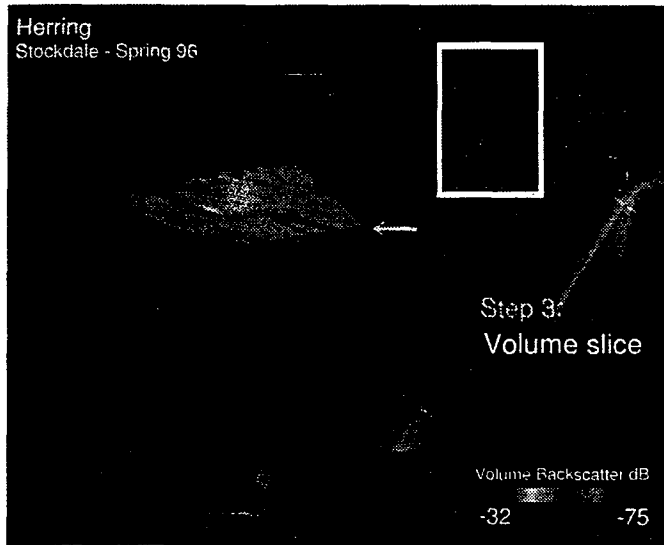
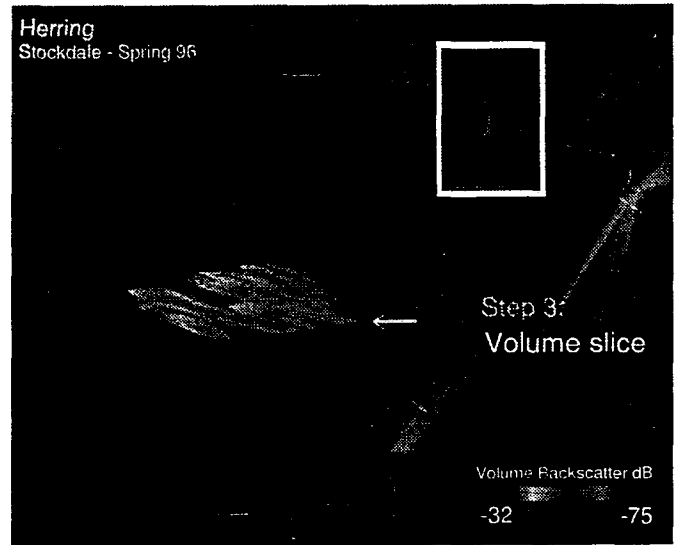


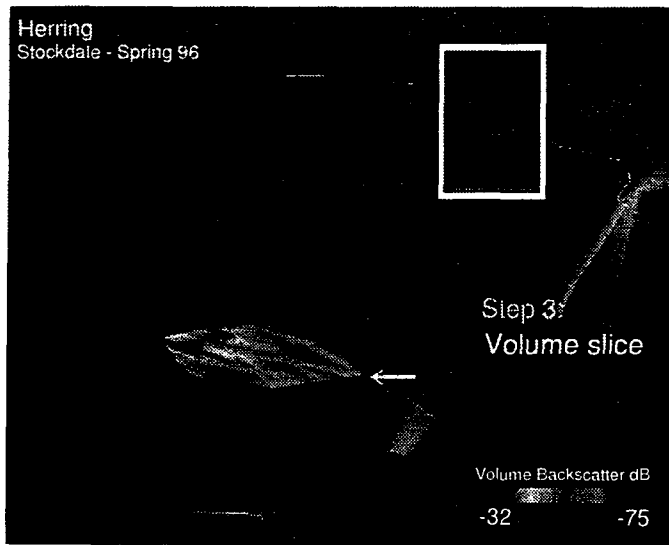
Figure 11



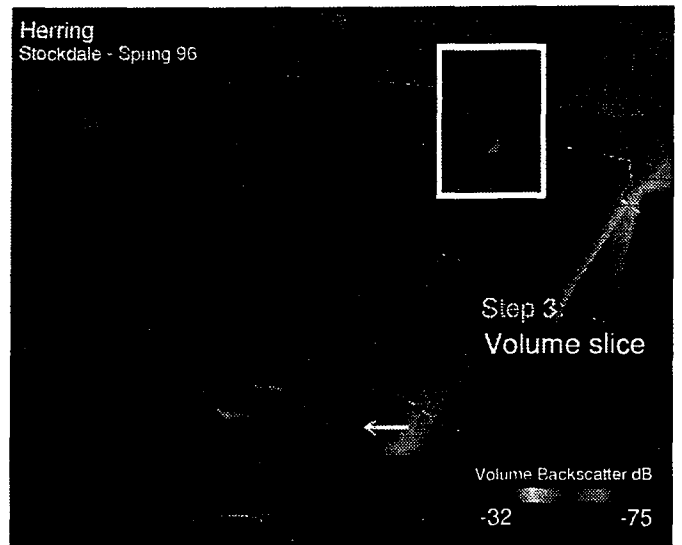
A



B



C



D

Figure 12

Color versions available for viewing at www.pwssc.gen.ak.us/sea/evos97rpt/

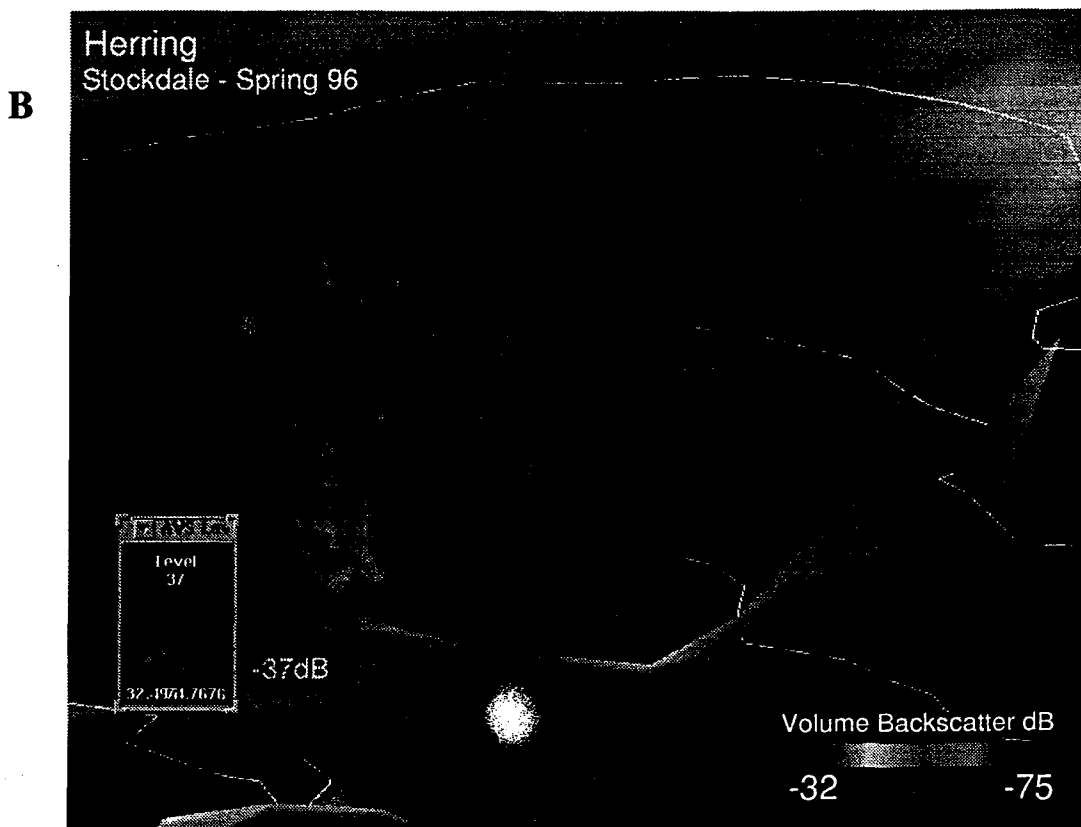
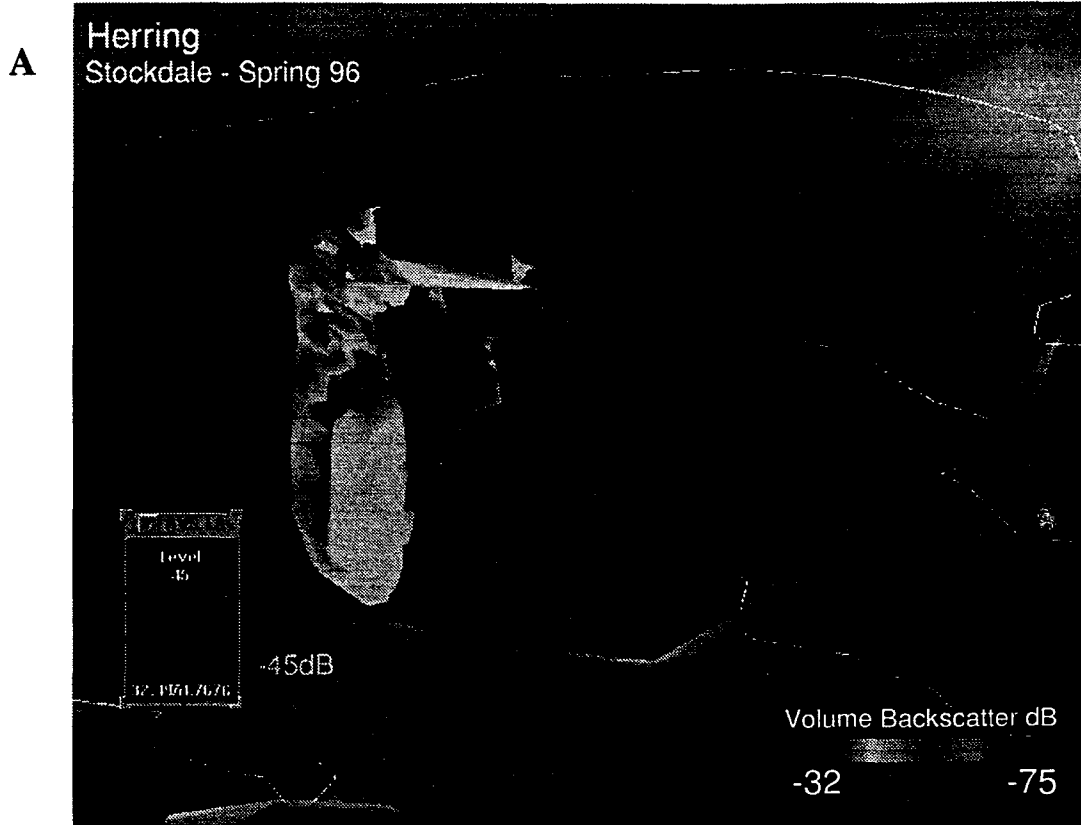


Figure 13

Color versions available for viewing at www.pwssc.gen.ak.us/sea/evos97rpt/

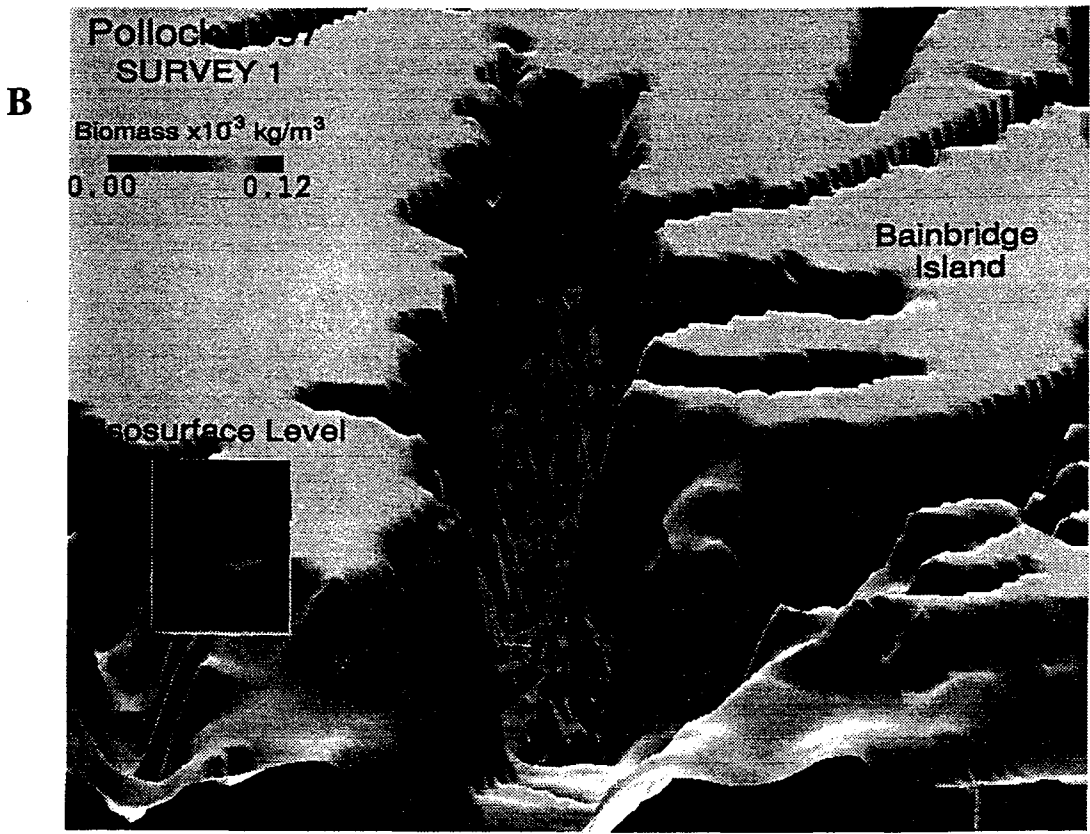
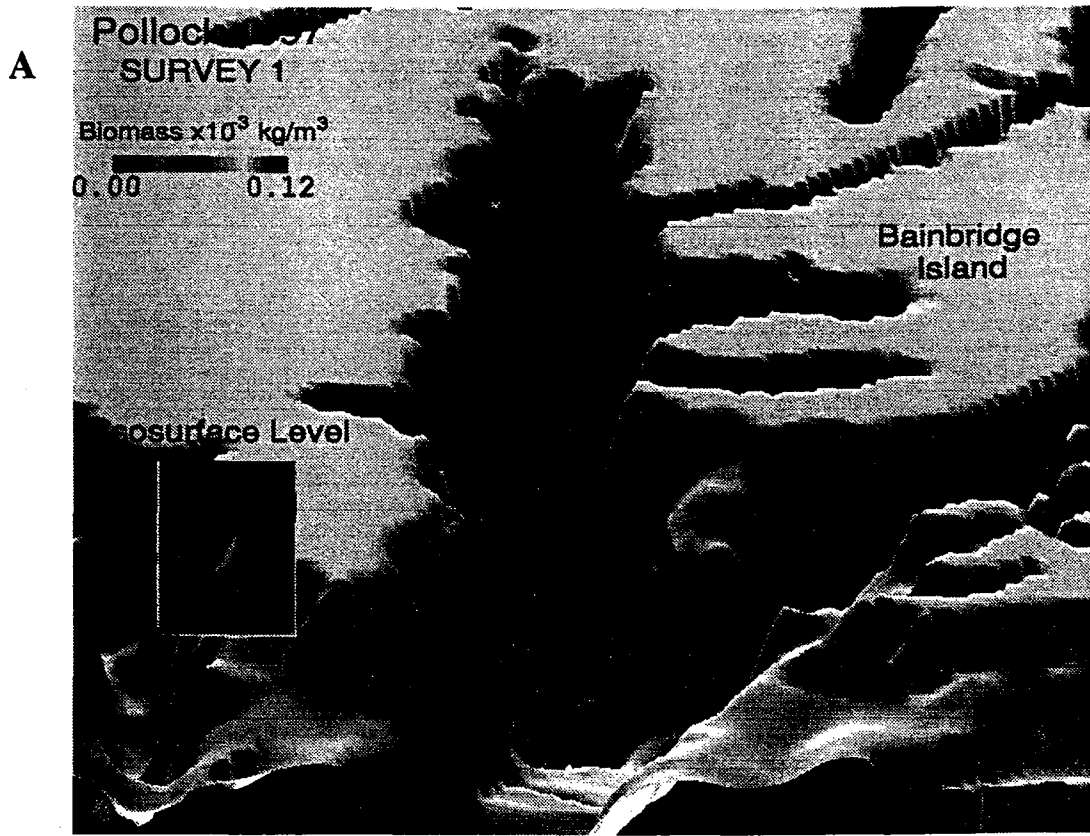


Figure 14

Part IV
Report on 1997 progress
Weather Data Systems
S. Bodnar



Part IV: WEATHER DATA SYSTEMS

Stephen Bodnar
April 15, 1998

The Applegate Weather Station operated through calendar year 1997 with a 95% data coverage, 16673 records out of a possible 17520. The station is recording wind speed, wind direction, air temperature, solar radiation, and barometric pressure at 30 minute intervals, and data is downloaded via radio-modem to the PWS Science Center on a daily basis.

Work is underway to upgrade the station for near-realtime data download. The current custom DOS download software is being tested under a DOS shell on a linux computer, and is being ported to run under linux. When the Applegate station is capable of reliable communications under all atmospheric conditions, it will be reprogrammed for continuous realtime data transmission to the Science Center.

An interface has been developed to post the most recent Applegate data to the Science Center web page, and to plot the last 24 hours of data in an easily accessible format. The data is archived, along with that from a small weather station located at the Science Center. Software is being written and tested to continuously download realtime weather data from all METAR stations in the Prince William Sound and near-coastal region. It will also download NOAA buoy data, and other relevant climatic datasets to a local master archive for use by researchers in Prince William Sound. This will replace the current manually updated archive.

The Heney Ridge repeater was replaced with an updated radio-modem, removing the last NETROM node from the system. The Naked Island repeater had a similar upgrade last year. The new modems will allow faster, more flexible network routing, as well as the ability to connect RS232 capable equipment at the mountaintop repeater sites. It also adds redundancy as all modems in the network are now identical.

The radio network has been operating successfully with a minor atmospheric related reception problem. During periods of heavy weather (heavy snow, heavy rain, high SE winds), the system operates well above design and theoretical parameters. It has been possible to send data 40 miles with a 2 watt radio under these conditions. Six miles is the theoretical maximum; design parameters state that signals in the uhf band (our operating frequency is 464.425 mhz) are often blocked by heavy precipitation. In our network, the exact opposite has proved true. The Applegate weather station is 21 miles from the Naked Island repeater and has maintained reliable communications with a 2 watt radio and newly installed yagi (directional) antenna. Only during periods of high barometric pressure and cloudless skies does the system lose connectivity. Reasons are as yet unclear, but replacing the existing 2 watt radio with a 5 watt transceiver is expected to alleviate the problem.

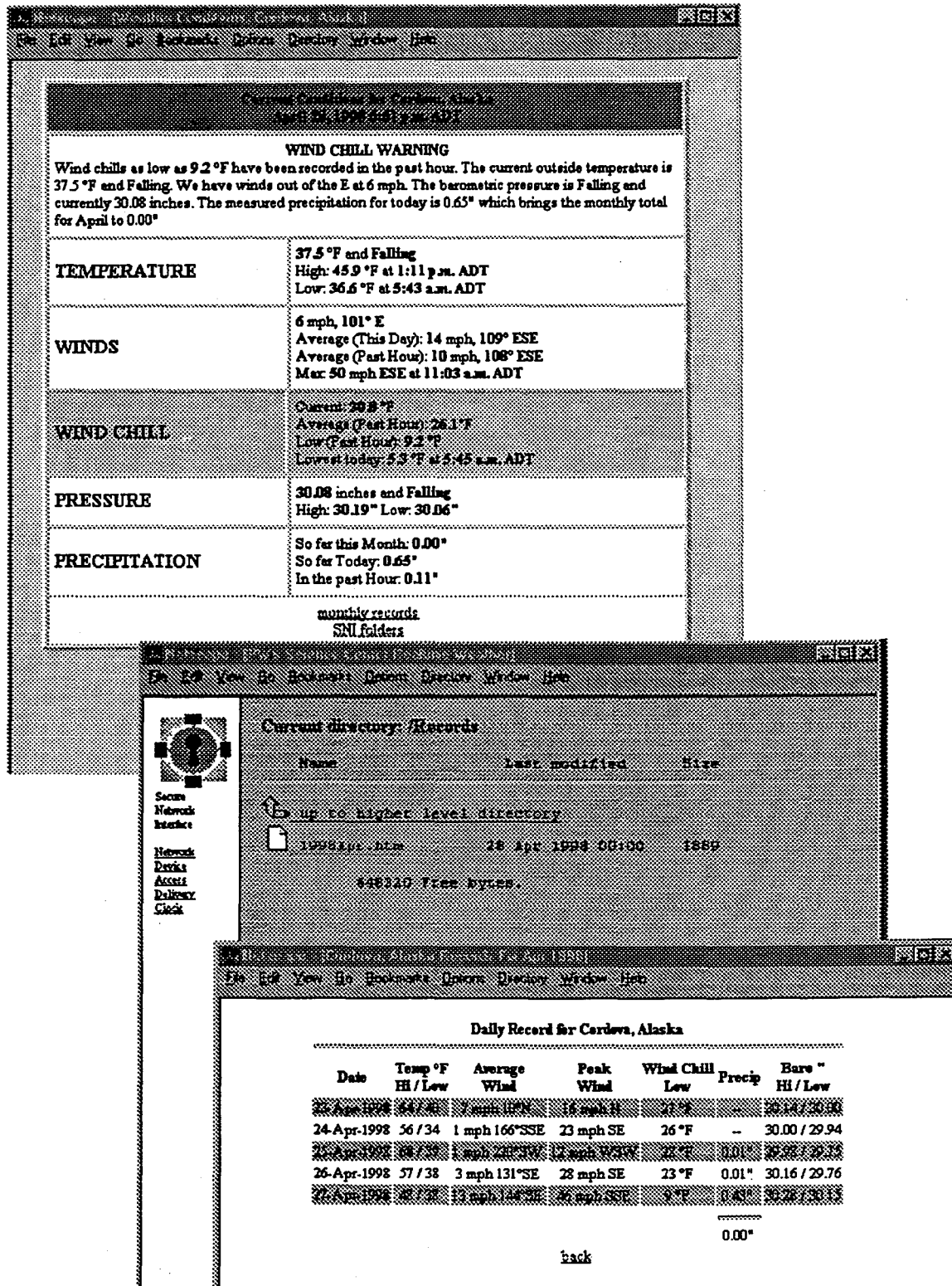


Figure 1. Secure Network Interface configured for realtime delivery of Cordova weather data

APPENDIX 2

A three-dimensional tidal model for Prince William Sound, Alaska
J. Wang, C. N. K. Mooers, V. Patrick
to appear in *Computer Modelling of Seas and Coastal Regions III*

A three-dimensional tidal model for Prince William Sound, Alaska

J. Wang^a, C.N.K. Mooers^a, V. Patrick^b

^a Ocean Prediction Experimental Laboratory and Division of Applied Marine Physics, Rosenstiel School of Marine and Atmospheric Science, University of Miami, Miami, Florida 33149 USA ^b Prince William Sound Science Center, P.O. Box 705, Cordova, Alaska 99574 USA

Email: jia.wang@rsmas.miami.edu

Abstract

A three-dimensional, primitive equation model is used to simulate the ocean tides in Prince William Sound (the Sound), Alaska. Six tidal constituents (M_2 , N_2 , S_2 , K_1 , O_1 , and P_1) are specified on the open boundaries with a partially clamped condition. The model is used to simulate the tidal heights, tidal currents, and residual current. The tide is mixed, mainly semidiurnal. The tidal current vector fields compare reasonably with towed ADCP (Acoustic Doppler Current Profiler) measurements conducted during 1994. The tidal residual current pattern is significant relative to the mean throughflow circulation.

1 Introduction

Prince William Sound (the Sound) is a combination of multiple basins, fjords, channels, islands, inlets, and estuaries along the coast of Alaska. Its area, including estuaries and arms, is approximately 120×120 km² (about 70% covered by water) with an average depth of about 190m. It has several deep basins (with a maximum depth of about 750m in the northwestern Sound) and channels.

Ocean tides entering the Sound from the Gulf of Alaska are a major dynamical feature, although they have not been much studied. Because North America's largest oil spill (by T/V Exxon Valdez on 24 March 1989) seriously impacted the ecosystem of the Sound and the adjacent downstream waters⁶, a large

number of studies have been conducted to address impact, recovery, and restoration. The SEA (Sound Ecosystem Assessment) Program is a restoration project of the Exxon Valdez Oil Spill Trustee Council. The program objective is a quantitative characterization of those components of the ecosystem driving the recovery of the two primary commercial fish species, pink salmon and Pacific herring. The method of approach involves the development of a coupled physical-biological model for critical juvenile stages of the two species. The physical oceanography component consists of a field project and a circulation modeling project. This paper presents numerical simulations of tides and tidal currents in the Sound to assess their influence on the mean circulation. The progress of the SEA Program has been summarized³.

A 3-D ocean circulation model has been developed for Prince William Sound and studies of the circulation patterns due to throughflow and wind-forcing have been described⁴. However, tidal flows were not included. Thus, the purpose of this study is to 1) implement a 3-D numerical model for simulating tides and tidal current and 2) examine the tidal residual currents.

Section 2 briefly describes the 3-D numerical model, plus the model configuration, model parameters, initial and boundary conditions, and forcing. Section 3 presents the simulation results. Finally, section 4 summarizes the results and outlines the future effort.

2 Description and Implementation of the Model

A version of the Princeton Ocean Model (POM²), which has been successfully applied to the circulation of Hudson Bay¹¹, is utilized. It is based on the primitive equations (with hydrostatic and Boussinesq approximations) and has the following features: (1) horizontal curvilinear coordinates (not used here); (2) an Arakawa C grid; (3) sigma (terrain-following) coordinates in the vertical with realistic bottom topography; (4) a free surface; (5) the Mellor-Yamada level 2.5 turbulence closure model for vertical viscosity and diffusivity; (6) the Smagorinsky parameterization for horizontal viscosity and diffusivity; (7) a semi-implicit scheme for the shallow water equations^{1,11}; and (8) a predictor-corrector scheme for the time integration to avoid inertial instability^{9,10}.

The model domain includes the entire Sound with two open boundaries

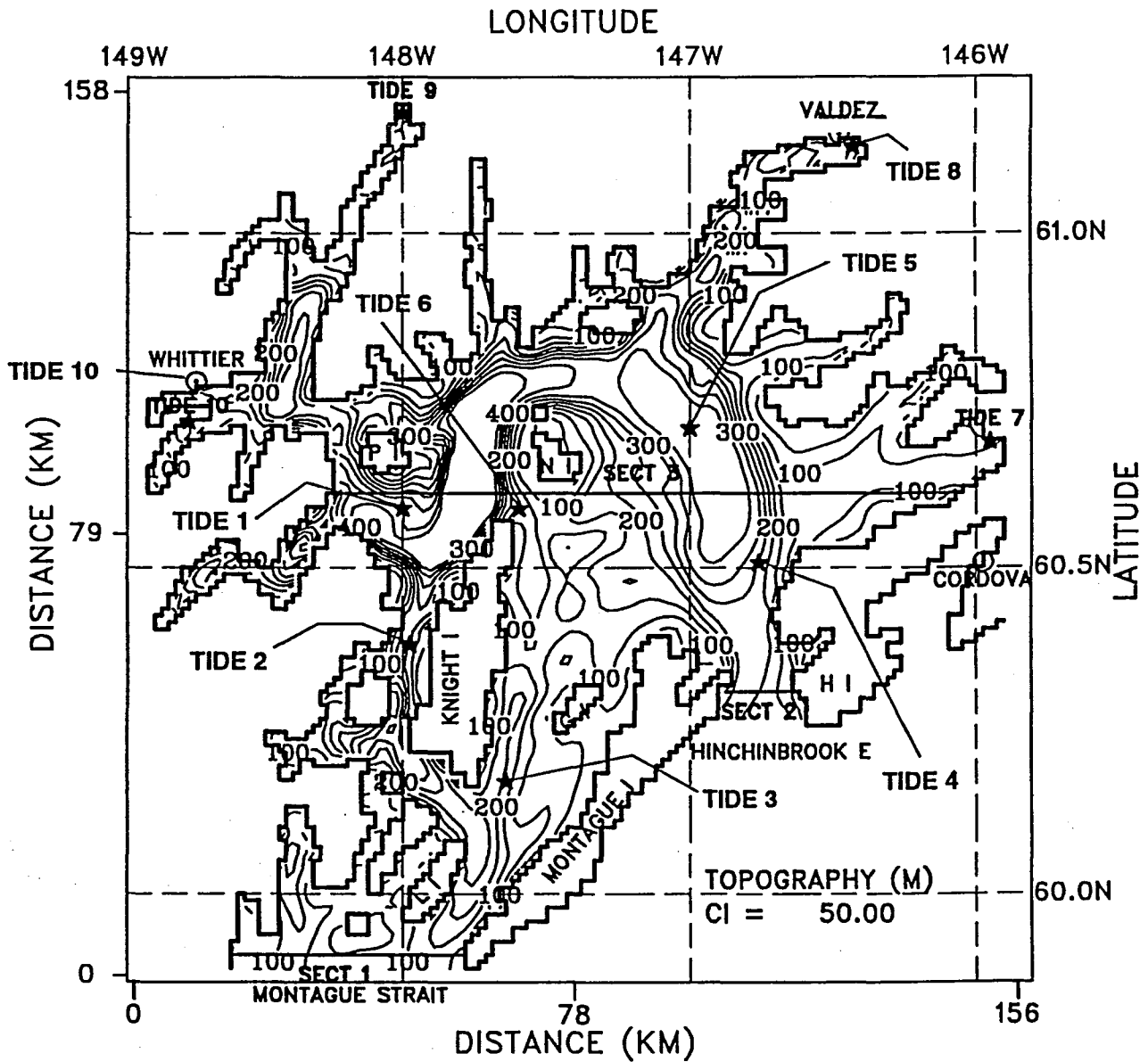


Figure 1, Model domain and topography with depths in meters. Stations, Tide 1 to Tide 10, indicate the stations from which tidal height time series are extracted.

(Hinchinbrook Entrance and Montague Strait, Fig 1), allowing water exchange with the Alaskan coastal waters⁷. The model grid spacing is 1.2 km, which is eddy-resolving because the internal Rossby radius of deformation is about 5km⁵. There are 11 vertical sigma levels. The integration time step is 62.1 seconds, which is about six times the CFL (Courant-Friedrichs-Lewy) constraint because a semi-implicit scheme has been used for the shallow water equations¹¹.

The open lateral boundary conditions are determined by a partially clamped radiation condition in which the sea surface elevation, η , at the boundary is time dependent:

$$\frac{\partial \eta}{\partial t} + C \frac{\partial \eta}{\partial n} - \frac{\eta_k - \eta}{T_f} = 0 \quad (1)$$

where η_k is the tide's elevation, $C=(gH)^{1/2}$ is the surface gravity wave phase speed, and T_f is a time scale for the clamped/radiation boundary condition. The partially clamped condition of this study uses $T_f=10s$ (clamped being the limit for $T_f \rightarrow 0$). [In contrast, a radiation condition would be obtained by using, for example, $T_f=4$ days (pure radiation being the limit for $T_f \rightarrow \infty$ which is not used here)]. For the normal component of throughflow, the 2-D normal velocity (or transport) is defined following Wang et al.¹¹. Furthermore, the 3-D normal velocity (or transport) into/out of the Sound is equal to the 2-D transport and the total transport is conserved when averaged over a tidal cycle.

The initial temperature and salinity fields used are based on typical early summer profiles in the central Sound for late summer 1994, and are specified to be horizontally uniform. The mean throughflow was specified at Hinchinbrook Entrance; two cases were considered: $0.15 \times 10^6 \text{ m}^3 \text{ s}^{-1}$ corresponding to a case treated in Mooers and Wang⁴ and $0.05 \times 10^6 \text{ m}^3 \text{ s}^{-1}$ corresponding to the conditions in the fall of 1994. The model was spun-up for 10 M_2 cycles (about 5 days) to reach a dynamically steady state. The vertical viscosity is determined from the Mellor-Yamada level 2.5 turbulence closure model with a background viscosity of $10^{-5} \text{ m}^2 \text{ s}^{-1}$ (i.e., the value used if the calculated viscosity is smaller than this minimum value). The horizontal viscosity is determined from the Smagorinsky horizontal turbulence closure with the mixing coefficient $C=0.2$.

3 Simulation Results

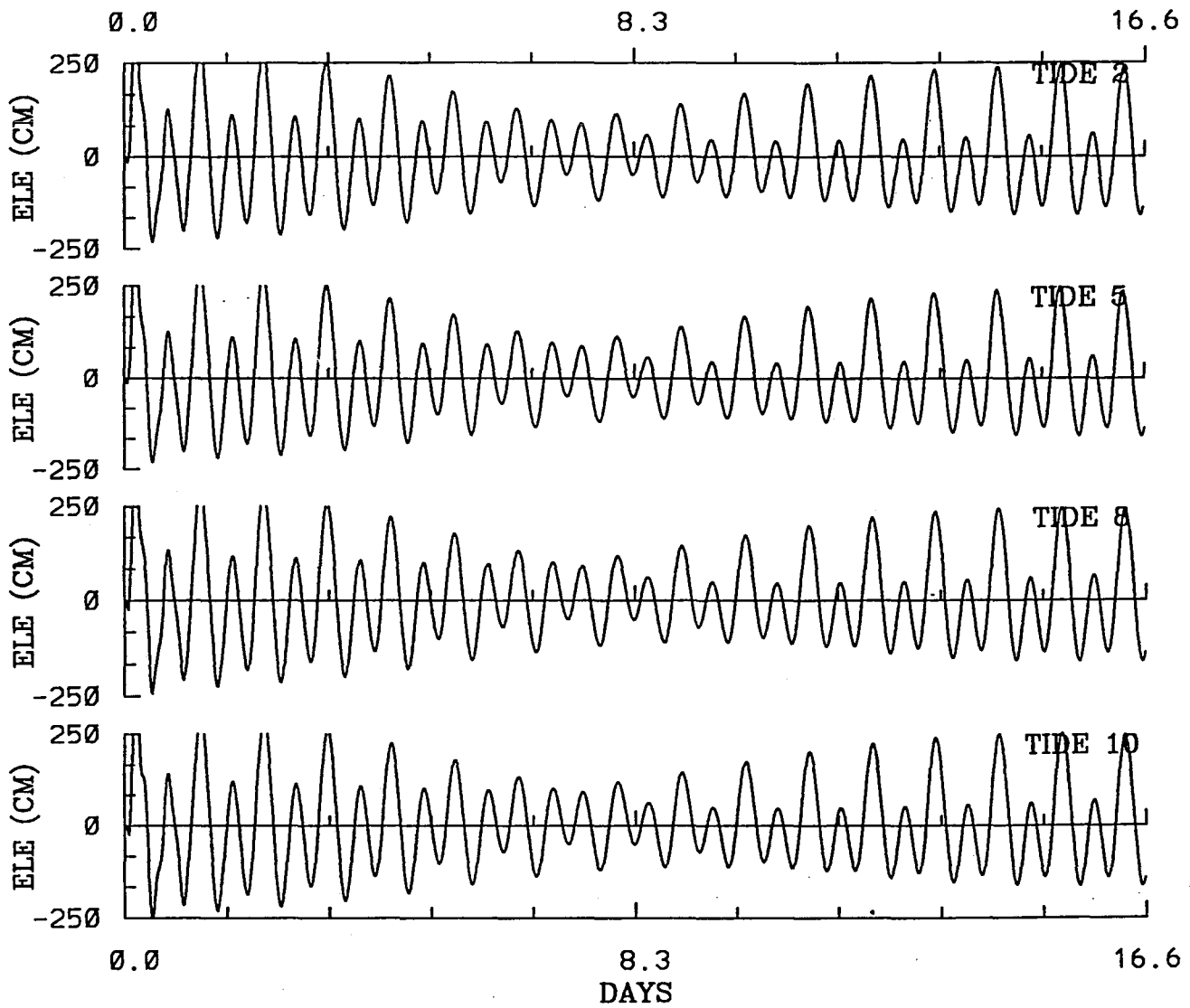


Figure 2. Sixteen-day tidal height time series from stations Tide 2 (Knight Island Passage), Tide 5 (Central Sound), Tide 8 (Valdez), and Tide 10 (Whittier) under forcing of six tidal constituents and throughflow of $0.15 \times 10^6 \text{ m}^3\text{s}^{-1}$.

The harmonic constants of the six tidal constituents [with amplitudes (in meters) and phases (in degrees) for M_2 (1.16m, 286), N_2 (0.24m, 264), S_2 (0.4m, 321), K_1 (0.5m, 274), O_1 (0.28m, 257), and P_1 (0.16m, 273)] were obtained from Schwiderski⁸. The tide type factor, $F=(K_1+O_1)/(M_2+S_2)$, is 0.5, indicating a mixed, mainly semidiurnal tide type.

The simulated tidal heights (Fig. 2) for about 16 days at four stations [Knight Island Passage (Tide 2), Central Sound (Tide 5), Valdez (Tide 8), and Whittier (Tide 10)] demonstrate that the average tidal range (peak-to-peak) is about 5m during spring tide and about 3m during neap tide.

The first experiment was conducted using a throughflow of $0.05 \times 10^6 \text{ m}^3 \text{ s}^{-1}$ corresponding to the conditions in the fall of 1994. The simulated tidal currents on seven different stages (maximum flood, high tide, maximum ebb, low tide, etc.) can be examined and compared with available observations. The towed ADCP tidal current fields (acquired by Prince William Sound Science Center during the fall of 1994 under the SEA Program) were also grouped into the seven tidal stages. For example, the tidal current field at 17m, during early ebb when there is a spring tide (Fig. 3), is compared with the towed ADCP measurements at 17m during the same tidal stage (Fig. 4). The overall pattern (magnitude and direction) is similar, except in the northern Sound (around 60.8N and 147.3W).

For this project it is important to estimate the possible mean circulation pattern induced by the throughflow and tides (residual current) in the Sound, which may modify the dispersal patterns and times of biota (fish eggs and larva and plankton) and pollutants. The second experiment was conducted using a throughflow of $0.15 \times 10^6 \text{ m}^3 \text{ s}^{-1}$ and the six tidal constituents. The tidal residual current averaged over two M_2 tidal cycles (Fig. 5), which can be compared to the mean flow only under the throughflow forcing (Fig. 3 of Mooers and Wang⁴). The overall throughflow pattern is similar; however, the anticyclonic circulation in the Central Sound is very prominent, and there is also an anticyclonic circulation in the northwestern Sound (over the deepest basin). These two mean circulation cells differ in strength and location from those occurring in the absence of the tides, indicating that the tidal residual current is an important factor in the Sound, particularly in the Central Sound and in the northwestern Sound.

4 Concluding Remarks

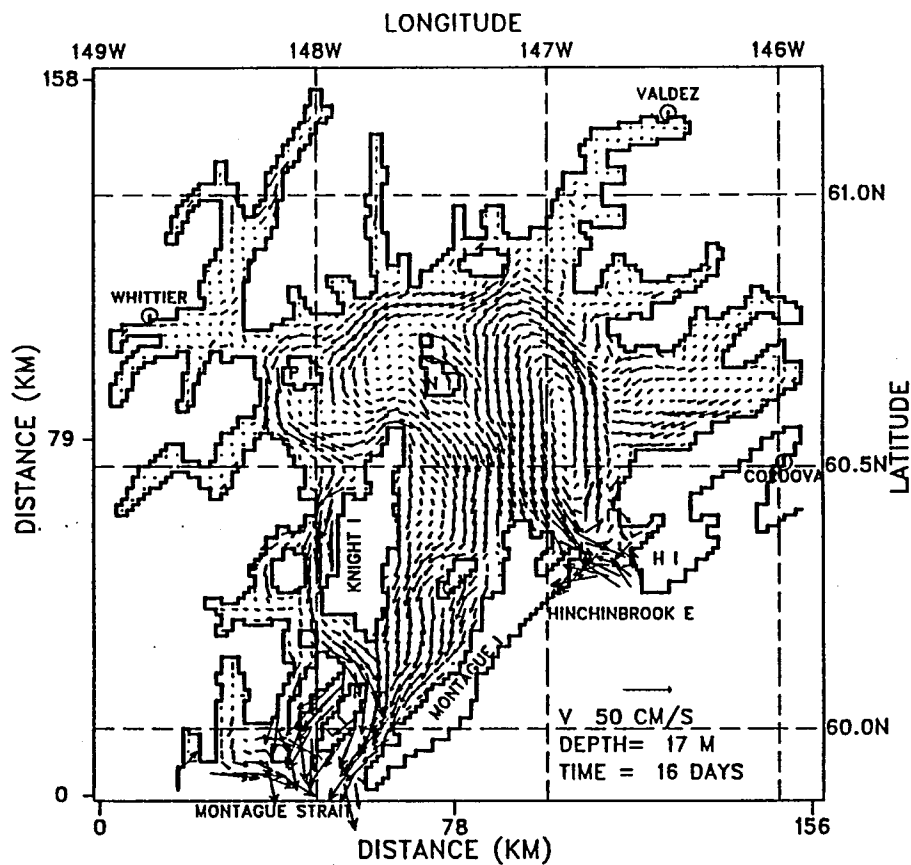


Figure 3. Simulated subsurface (17m) tidal current field at early ebb tide on day 16 (spring tide) with the throughflow of $0.05 \times 10^6 \text{ m}^3 \text{ s}^{-1}$.

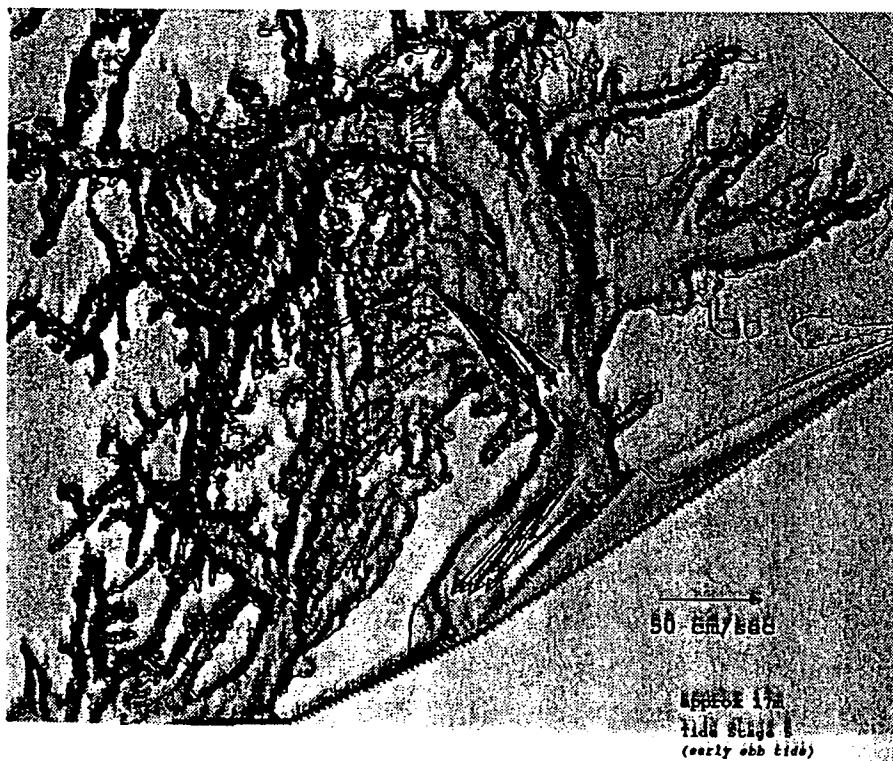


Figure 4. Observed subsurface (17m) tidal current field at early ebb tide using a towed ADCP in the fall of 1994.

The tidal currents play a significant role in the mean and transient circulation of Prince William Sound. The tide is mixed, mainly semi-diurnal. The tidal currents may reach 0.5 ms^{-1} ; hence, they may be influential in the mixing regime. The tidal range is as high as about 5m during spring tide and as low as about 3m during neap tide. The residual currents in the Central Sound and the northwestern Sound are about 3 to 5 cm s^{-1} and will influence the dispersal of suspended, dissolved, and particulate matter. Thus, they may impact the location and residence times of the biological retention zones.

The simulated tidal velocity fields are generally consistent with those from the towed ADCP measurements. The simulated mean circulation pattern under tidal and throughflow forcing differs from the mean circulation pattern induced by a throughflow only. Obviously, the significance of the differences will depend upon the strength of the throughflow. The tidal residual current pattern includes anticyclonic gyres in the Central Sound and an anticyclonic gyre in the northwestern Sound. These two residual current gyres will influence the dispersal properties of the Sound.

Acknowledgements: Financial support from the SEA Program of the Exxon Valdez Oil Spill (EVOS) Trustees Council administered through Prince William Sound Science Center, Alaska, is appreciated. Discussions of the PWS circulation with Drs. T.C. Royer and Z. Kowalik are gratefully acknowledged. We also thank Mr. J. Murphy, Ms. J.R. Allen, and Dr. D.K. Salmon of PWSSC for the analysis of the ADCP data.

References

1. Blumberg, A.F., 1991. A primer for ECOM-si. Technical Report for HydroQual, Inc., Mahwah, NJ, 66 pp.
2. Blumberg, A.F. and G.L. Mellor, 1987. A description of a three-dimensional coastal ocean circulation model. In: Coastal and Estuarine Sciences 4: Three-Dimensional Coastal Ocean Models, N.S. Heaps, ed., American Geophysical Union, Washington D.C.: 1-16. 18: 775-787.

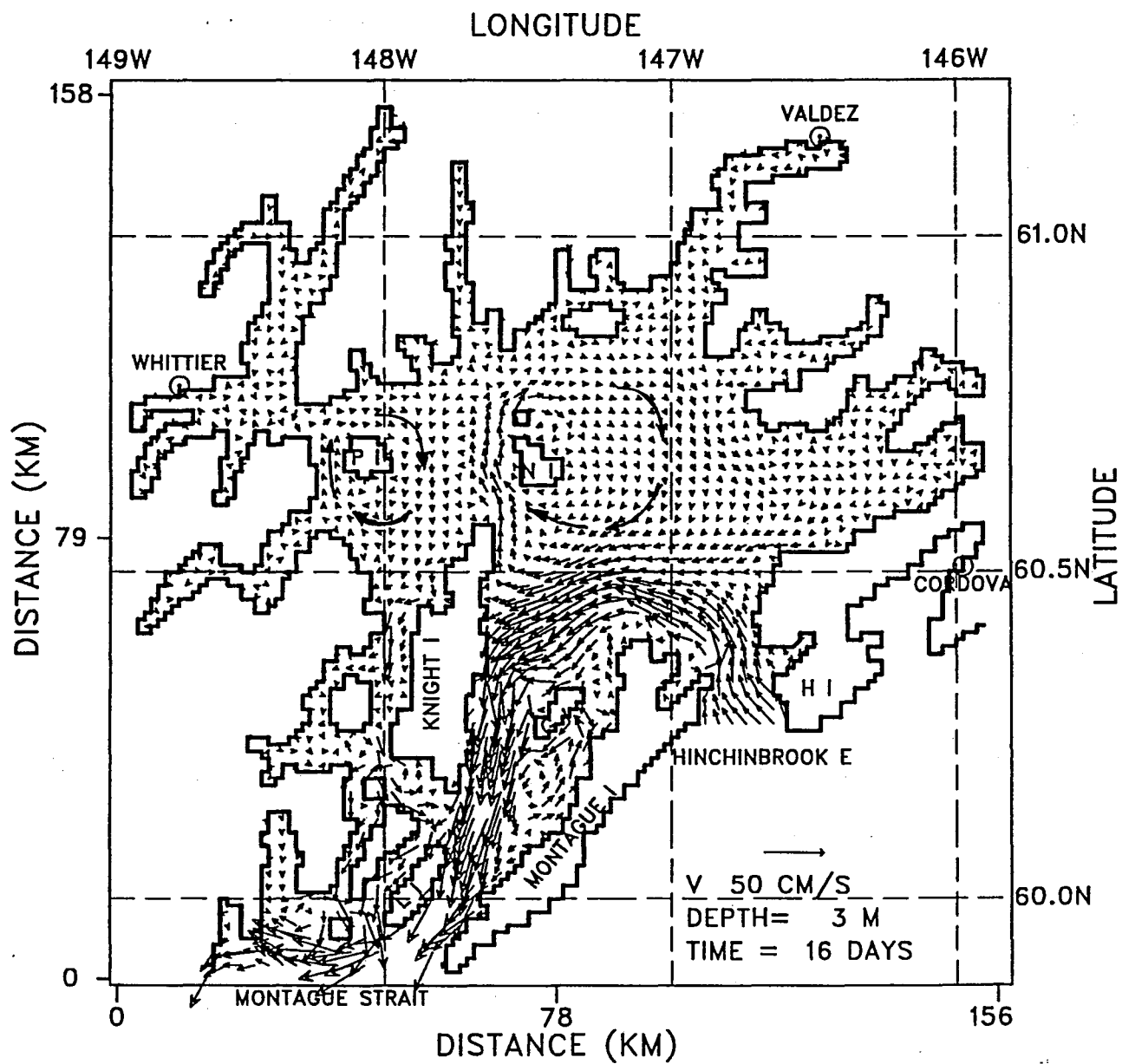


Figure 5. Simulated surface (3m) residual current field averaged over two M_2 tidal cycles under forcing of both the six tidal constituents and throughflow of $0.15 \times 10^6 \text{ m}^3 \text{ s}^{-1}$.

3. Cooney, R.T. 1996. Sound Ecosystem Assessment (SEA): A Science Plan for the Restoration of Injured Species in Prince William Sound, Alaska. Exxon Valdez Oil Spill Restoration Project Annual Report (Restoration Project 95320). Alaska Depart. of Fish and Game, Anchorage, Alaska.
4. Mooers, C.N.K. and J. Wang, 1997. On the development of a 3-D circulation model for Prince William Sound, Alaska, **Cont. Shelf Res.** (in press).
5. Niebauer, H.J., T.C. Royer and T.J. Weingartner, 1994. Circulation of Prince William Sound, Alaska. **J. Geophys. Res.**, 99: 14,113-14,126.
6. Royer, T.C., J.A. Vermersch, T.J. Weingartner, H.J. Niebauer and R.D. Muench, 1990. Ocean circulation influencing the Exxon Valdez oil spill. **Oceanography**, 3-10.
7. Schmidt, G.M., 1977. The exchange of water between Prince William Sound and the Gulf of Alaska, M.S. thesis, Univ. of Alaska, Fairbanks, 116 pp.
8. Schwiderski, E.W. 1980. On charting global ocean tides. **Rev. Geophys. Space Phys.**, 18: 243-268.
9. Wang, J. and M. Ikeda, 1996. A 3-D ocean general circulation model for mesoscale eddies-I: Meander simulation and linear growth rate. **Acta Oceanologica Sinica**, 15: 31-58.
10. Wang, J. and M. Ikeda, 1997. On inertial stability and phase error of time integration schemes in ocean general circulation models. **Mon. Wea. Rev.** (in press).
11. Wang, J., L.A. Mysak and R.G. Ingram, 1994. A 3-D numerical simulation of Hudson Bay summer circulation: topographic gyres, separations and coastal jets. **J. Phys. Oceanogr.**, 24: 2496-2514.

**A two-compartment model for understanding
the simulated three-dimensional circulation
in Prince William Sound, Alaska**

E. Deleersnijder, Université catholique de Louvain, Belgium

J. Wang and C. N. K. Mooers, RSMAS, University of Miami

to appear in *Continental Shelf Research* JONSMOD '96 Special Issue

submitted to *Continental Shelf Research*
JONSMOD '96 Special Issue
July 1997

A two-compartment model for understanding
the simulated three-dimensional circulation
in Prince William Sound, Alaska

by

Eric DELEERSNIJDER

Institut d'Astronomie et de Géophysique G. Lemaître,
Université catholique de Louvain,
2 Chemin du Cyclotron, B-1348 Louvain-la-Neuve, Belgium

Jia WANG and Christopher N.K. MOOERS

Ocean Prediction Experimental Laboratory and Division of Applied Marine Physics,
Rosenstiel School of Marine and Atmospheric Science, University of Miami,
4600 Rickenbacker Causeway, Miami, Florida 33149-1098, USA

(accepted)

corresponding author address:

Eric Deleersnijder Unité ASTR - UCL
--

to be submitted to *Continental Shelf Research*
(JONSMOD '96 Special Issue)
July 1997

2 Chemin du Cyclotron
B-1348 Louvain-la-Neuve, Belgium
Tel: +32-10-472.676 or +32-10-473.297
Fax: +32-10-474.722
E-mail: ericd@astr.ucl.ac.be

ABSTRACT

A two-compartment model of Prince William Sound (PWS), Alaska, is developed. One compartment, corresponding to the southern part of the Sound, represents advective phenomena, while the other is dominated by diffusion. This simple model is shown to reproduce rather well the temporal evolution of the mass of a passive tracer contained in PWS simulated by a complex, three-dimensional model under five types of surface forcing. The three parameters of the box-model have clear physical meanings, which helps to understand the hydrodynamics of PWS. In particular, the fraction of the flow entering the northern PWS is estimated, as well as the turnover time of the two regions considered.

INTRODUCTION

One of the largest oil spills onto the seas occurred in Prince William Sound (PWS), Alaska, on 24 March 1989, as the result of a navigation error of the Exxon Valdez. Since then, considerable efforts have been devoted to the study of the ecosystem of this region. In this framework, Mooers and Wang (1997) — hereafter referred to as MW — used a version of the three-dimensional Princeton Ocean Model (*e.g.* Blumberg and Mellor, 1987) to simulate the water circulation in PWS.

For details about the topography of the domain of interest, refer to MW. Herein, it is sufficient to mention that the lateral computational boundary is impermeable, except for two narrow passages in the southern part of PWS, Hinchinbrook Entrance and Montague Strait. Moreover, it must be underscored that, in general, water originating from the Gulf of Alaska enters PWS through the former and leaves through the latter.

MW conducted a sensitivity analysis of the PWS circulation to the surface stress. In the control run, no wind forcing was applied. Four additional simulations were carried out in which the wind was assumed to be blowing with the same speed toward the east, the north, the west, and the south, respectively. For each type of forcing, a flow in a statistical equilibrium was obtained. The latter was then used to simulate the fate of a passive tracer released at a constant rate for four days by a line source located in Hinchinbrook Entrance.

In each model run, the source released tracer in the upper 40 m at the constant rate Φ from time $t=0$ until it was cut off, at time $t=T$, with $T=4$ days. Thus, the total amount of tracer injected into PWS was $M=\Phi T$. The tracer content of PWS, m_s , was simulated for 33 days by MW (Fig. 1).

The temporal evolution of the tracer mass present in PWS exhibits four distinct phases which are qualitatively similar in every model run (Fig. 2). First, from $t=0$ until $t=T$, m_s grows approximately linearly, since almost no tracer parcel has yet left PWS

through Montague Strait. Then, as long as the outgoing tracer flux is negligible, the tracer mass remains virtually constant. This regime lasts until $t = \tau$, which is the time period that a tracer parcel needs to travel from Hinchinbrook Entrance to Montague Strait following the most direct pathway. Then, the tracer mass diminishes monotonically. During the third phase, the tracer mass decreases approximately linearly as time progresses. The transition from the third to the fourth phase is characterised by an abrupt change in the pace at which the mass diminishes. Finally, during the final phase, the rate of decrease of the mass is much smaller.

The processes which are at work during the first two phases are readily understood. That the mass must decrease during the subsequent phases is obvious too. However, explaining why the rate of decrease of the mass changes is not straightforward. To do so, a simple, compartmental model is established, which will help infer major properties of the PWS circulation, as well as reveal the influence of the wind on them.

A TWO-COMPARTMENT MODEL

An attempt will be made to represent the evolution of PWS tracer content by means of an elementary model. The tracer mass estimated therefrom will be denoted m so as to distinguish it from its counterpart, m_s , simulated by MW using a complex, three-dimensional model.

The tracer mass obeys

$$\frac{d}{dt}m(t) = \phi^{in}(t) - \phi^{out}(t), \quad (1)$$

where ϕ^{in} is the tracer flux entering PWS through Hinchinbrook Entrance while ϕ^{out} represents the rate at which tracer leaves PWS through Montague Strait. The flux ϕ^{in} is due

to the tracer source, while the outgoing flux depends on the tracer content of the Sound and the hydrodynamic processes occurring in it, the major features of which must be understood for a suitable parameterization to be devised.

A tracer parcel behaves like a water parcel, since the tracer considered is passive.

The MW modelled current maps clearly suggest that a tracer parcel may follow two distinct types of path leading from Hinchinbrook Entrance to Montague Strait. The largest current speeds occur between Knight Island and Montague Island, implying that the quickest pathway is associated with advection through this region. The second route is that of parcels going further north into the Sound, where the circulation is much slower and intricate, partly because of numerous topographic features, such as islands, fjords, or headlands. At the scale of the northern PWS, these advective processes may amount to diffusion.

This description provides a basis for dividing PWS into two parts, the southern PWS — also termed “region 1” below — dominated by advection and the northern PWS — also called “region 2” hereafter — where diffusive mechanisms prevail. Therefore, the tracer mass present in PWS at a given time, $m(t)$, may be regarded as the sum of $m_1(t)$ and $m_2(t)$, where $m_i(t)$ ($i = 1, 2$) is the tracer mass contained in region i . If ϕ_i^{in} and ϕ_i^{out} denote the fluxes entering and leaving region i , respectively, m_i obeys

$$\frac{d}{dt}m_i(t) = \phi_i^{in}(t) - \phi_i^{out}(t), \quad i = 1, 2. \quad (2)$$

Since region 1 is assumed to be dominated by advection,

$$\phi_1^{out}(t) = \phi_1^{in}(t - \tau), \quad (3)$$

where the time lag τ , as already mentioned in the preceding section, is the period of time that a tracer parcel, following the quickest path, needs to transit from Hinchinbrook Entrance to Montague Strait.

If the diffusive processes taking place in region 2 are rather strong, then the tracer concentration therein may be assumed to be sufficiently homogeneous for the tracer flux leaving this region to be proportional to the tracer mass present in it, *i.e.*,

$$\phi_2^{out}(t) = \frac{m_2(t)}{\theta}, \quad (4)$$

where the time scale θ is the turnover time of region 2. The latter is defined to be the average over the northern PWS of the residence time — which, at a given point of region 2, is the period of time that a water parcel, initially located at the point considered, needs to leave the northern PWS. Additional explanations and appropriate references on such hydrodynamic time scales, as well as parameterizations similar to (4), may be found in Bolin and Rodhe (1973) and Tartinville *et al.* (1997).

Let α denote the fraction of the tracer flux entering PWS that goes directly into region (2). Hence,

$$\phi_2^{in}(t) = \alpha \phi^{in}(t). \quad (5)$$

The tracer flux leaving region 2 may be assumed to join that exiting the southern PWS. However, it is readily seen that such a flux arrangement would prevent the PWS tracer content from growing linearly during the first phase of the tracer mass evolution. In addition, m could not remain almost constant for a certain period of time after the source is cut off. To circumvent these problems, the tracer pathway involving region 2 must include an appropriate time lag. For the sake of simplicity, it is decided that the flux leaving region 2 enters the southern PWS (Fig. 3), *i.e.*,

$$\phi_1^{in}(t) = (1-\alpha)\phi^{in}(t) + \phi_2^{out}(t). \quad (6)$$

This is a modelling choice which does not require introducing a time lag specific to the northern PWS, since use is made of that associated with region 1.

The two-compartment model meant to represent the major features of the tracer evolution in PWS consists of equations (1) to (6), the solution of which reads

$$m(t) = \int_0^t [\phi^{in}(\mu) - (1 - \alpha e^{-\frac{\mu-t}{\theta}}) \phi^{in}(\mu-\tau)] d\mu, \quad (7)$$

if $m(0)=0$. In the case considered above, $\phi^{in} = \Phi$ if $0 \leq t \leq T$ ($=4$ days), and $\phi^{in} = 0$ otherwise. Therefore, if $T < \tau$,

$$m(t) = \Phi t, \quad 0 \leq t \leq T, \quad (8a)$$

$$m(t) = \Phi T, \quad T \leq t \leq \tau, \quad (8a)$$

$$m(t) = \Phi(T + \tau - t) + \alpha \Phi \theta (1 - e^{-\frac{\tau-t}{\theta}}), \quad \tau \leq t \leq T + \tau, \quad (8a)$$

and

$$m(t) = \alpha \Phi \theta (e^{\frac{T}{\theta}} - 1) e^{-\frac{\tau-t}{\theta}}, \quad T + \tau \leq t. \quad (8a)$$

ASSESSMENT AND DISCUSSION

As expected, the solution above exhibits four different phases. It remains to be seen whether or not the three parameters τ , θ and α may be calibrated in such a way that the evolution of the tracer content predicted by the compartmental model, m , is close to that simulated by MW, m_s .

The dimensionless distance between m and m_s may be defined as

$$\varepsilon = \frac{\left[\int_0^{t_{max}} (m - m_s)^2 dt \right]^{1/2}}{\Phi T (t_{max})^{1/2}}, \quad (9)$$

where $t_{max} = 33$ days is the duration of MW's three-dimensional simulations. Obviously, the values of the parameters τ , θ , and α to be considered are those that minimise ε . They are obtained by means of a simple, iterative algorithm. As may be seen in Table 1, for every type of surface forcing, ε is rather small, indicating that there is an excellent agreement between the evolution of the tracer mass simulated by MW and that derived from the present compartmental model, which is clearly confirmed by the similarity of Fig. 1 and Fig. 4.

The parameters of the simple model are such that $\tau - t \ll \theta$ during the third phase of the tracer mass evolution, *i.e.*, during the time interval $\tau \leq t \leq T + \tau$. As a result, m admits the following asymptotic expansion

$$m(t) \approx \Phi [T - (1 - \alpha)(t - \tau)], \quad \tau \leq t \leq T + \tau, \quad (10)$$

which is the reason why the tracer mass decreases almost linearly during the third phase, as may be seen in Fig. 1 and Fig. 4.

It is clear that the turnover time of the southern PWS, as modelled above, is equal to $\tau/2$. That, in all cases, the turnover time of region 1 is much smaller than that of region 2 enables suggesting the following scenario: during the third phase, the outgoing flux at Montague Strait is essentially due to the tracer parcels that followed the quickest route, *i.e.*, those that did not enter region 2; most of the tracer parcels which penetrated into the northern PWS leave PWS during the final phase.

The fraction of the tracer parcels entering the northern PWS, α , is largest, or smallest, when the wind is northward, or southward, respectively. This is no surprise!

When the wind is northward or westward — which induces a net northward Ekman transport —, it is conceivable that tracer parcels leave the northern PWS less frequently to enter the southern region, so that it is in such circumstances that the turnover time of region 2, θ , is largest (Table 1). Conversely, θ is smallest when the wind is southward or eastward.

For reasons which are still unclear, the advective time lag τ depends weakly on the surface forcing considered (Table 1). However, it may be that τ is dominated by the specified constant throughflow and not much influenced by the Ekman flow which varies from case-to-case, a hypothesis consistent with MW's modelled current fields.

It would be foolhardy to assert that the simple model above is more realistic than the three-dimensional Princeton Ocean Model applied by MW to PWS. That the compartmental model provides at almost no cost an estimate of the tracer transport through PWS is marginally interesting, since most three-dimensional models may now be run routinely in domains like PWS. The most appealing feature of the two-compartment model is that it involves only three parameters, which all have a clear physical meaning, helping to understand the hydrodynamics of PWS — since the passive tracer and water parcels behave similarly. So, it has been possible to estimate, for every type of surface forcing considered, the fraction of the water flux crossing Hinchinbrook Entrance which first goes northward, instead of flowing directly toward Montague Strait. In addition, the turnover times of the southern and the northern regions have been evaluated. Finally, it has been suggested that the hydrodynamic processes taking place in the latter region amount to diffusion, while the former is dominated by mere advective mechanisms.

To design the two-compartment model, it has not been necessary to precisely mark out the limit between the two regions considered. In fact, the only clear-cut difference between

the two boxes is that they are dominated by hydrodynamic processes of a different nature, which does not prevent them from overlapping geographically. In other words, it is hydrodynamics rather than topography that allows distinguishing the two compartments. Therefore, it would be difficult to validate the simple model by direct comparison with fluxes computed, or measured *in situ*, through a given section of PWS. This consideration is why an inverse approach has been — and should continue to be — preferred.

In spite of the excellent agreement between the evolution of the tracer mass simulated by MW's complex three-dimensional model and that predicted by the present simple model, the latter may not be deemed to be fully validated. In fact, it would be necessary to compare the predictions of the compartmental model to those of the three-dimensional model over periods of time larger than the largest turnover time, *i.e.*, at least 100 days. On the other hand, for every type of flow, only one tracer release scenario has been considered so far, which is not sufficient. Therefore, for a given flow in PWS, it should be verified that the same set of parameters enables the two-box model to represent the evolution of the tracer mass in a satisfactory way throughout a series of tracer releases. For instance, a constant source located at Hinchinbrook Entrance of magnitude Φ may be considered, in which case the tracer mass should tend to $(\tau + \alpha\theta)\Phi$. Another interesting example consists of a source releasing an amount M of tracer in an arbitrarily short period of time, which corresponds to the case detailed above in the limit $T \rightarrow 0$. In this case, according to the simple model, the tracer mass should remain equal to M until $t = \tau$, then m should undergo a discontinuity, and finally decrease as $\alpha \exp[(\tau - t) / \theta]$ for $\tau < t$.

ACKNOWLEDGEMENTS

ED is a Research Associate with the National Fund for Scientific Research of Belgium. JW and CNKM appreciate the financial support of the Sound Ecosystem Assessment (SEA) Program of the Exxon Valdez Oil Spill (EVOS) Trustees Council through Prince William Sound Science Center, Alaska. ED is indebted to Benoît Tartinville and Marian Scott for the comments they provided on various aspects of this work.

REFERENCES

- Blumberg A.F. and G.L. Mellor (1987) A description of a three-dimensional coastal ocean circulation model. In: *Three-Dimensional Coastal Ocean Models*, N.S. Heaps, editor, American Geophysical Union, Washington, D.C., pp. 1–16.
- Bolin B. and H. Rodhe (1973) A note on the concepts of age distribution and transit time in natural reservoirs. *Tellus*, **25**, 58–62.
- Mooers C.N.K. and J. Wang (1997) On the development of a three-dimensional circulation model for Prince William Sound, Alaska. *Continental Shelf Research* (in press).
- Tartinville B., E. Deleersnijder and J. Rancher (1997) The water residence time in the Mururoa atoll lagoon: sensitivity analysis of a three-dimensional model. *Coral Reefs* (in press).

TABLE AND FIGURE CAPTIONS

Table 1. The values of the parameters τ , θ and α minimising ε as determined for various surface forcings. The direction toward which the wind blows is indicated. The error bars related to these estimates are $(\Delta\tau, \Delta\theta, \Delta\alpha) = (0.1 \text{ day}, 1 \text{ day}, 0.01)$.

Figure 1. The evolution of the dimensionless tracer mass present in PWS, m_s / M , as simulated by MW using the three-dimensional Princeton Ocean Model with various surface forcings. The direction toward which the wind is blowing is indicated. (These curves are obtained by deleting the slight overshootings of the simulated mass, occurring for unidentified numerical reasons, after the source was cut off.)

Figure 2. Schematic illustration of the four phases, labelled I to IV, of the temporal evolution of the tracer mass present in PWS.

Figure 3. Schematic illustration of the tracer fluxes accounted for in the compartmental model.

Figure 4. The evolution of the dimensionless tracer mass present in PWS, m/M , obtained from the compartmental model with various surface forcings. The direction toward which the wind is blowing is indicated.

Table 1. The values of the parameters τ , θ and α minimising ε as determined for various surface forcings. The direction toward which the wind blows is indicated. The error bars related to these estimates are $(\Delta\tau, \Delta\theta, \Delta\alpha) = (0.1 \text{ day}, 1 \text{ day}, 0.01)$.

	no wind	westward	southward <small>(d)</small>	eastward	northward
τ (days)	7.1	7.8	7.4	7.1	7.5
θ (days)	48	80	32	42	97
α	0.68	0.78	0.62	0.62	0.78
ε	0.065	0.066	0.067	0.066	0.066

Figure 1. The evolution of the dimensionless tracer mass present in PWS, m_s/M , as simulated by MW using the three-dimensional Princeton Ocean Model with various surface forcings. The direction toward which the wind is blowing is indicated. (These curves are obtained by deleting the slight overshootings of the simulated mass, occurring for unidentified numerical reasons, after the source was cut off.)

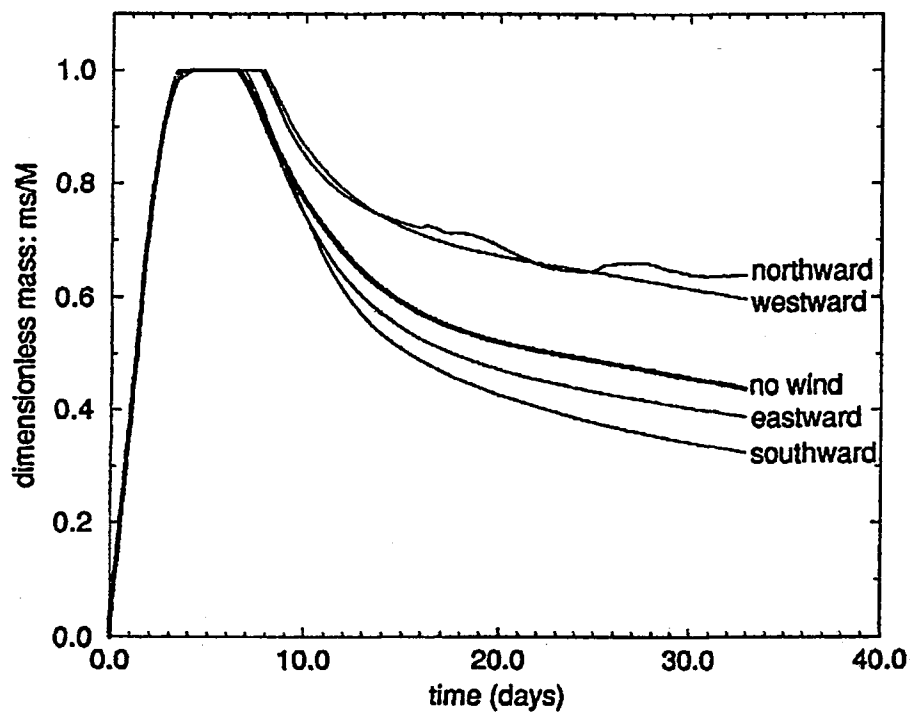


Figure 2. Schematic illustration of the four phases, labelled I to IV, of the temporal evolution of the tracer mass present in PWS.

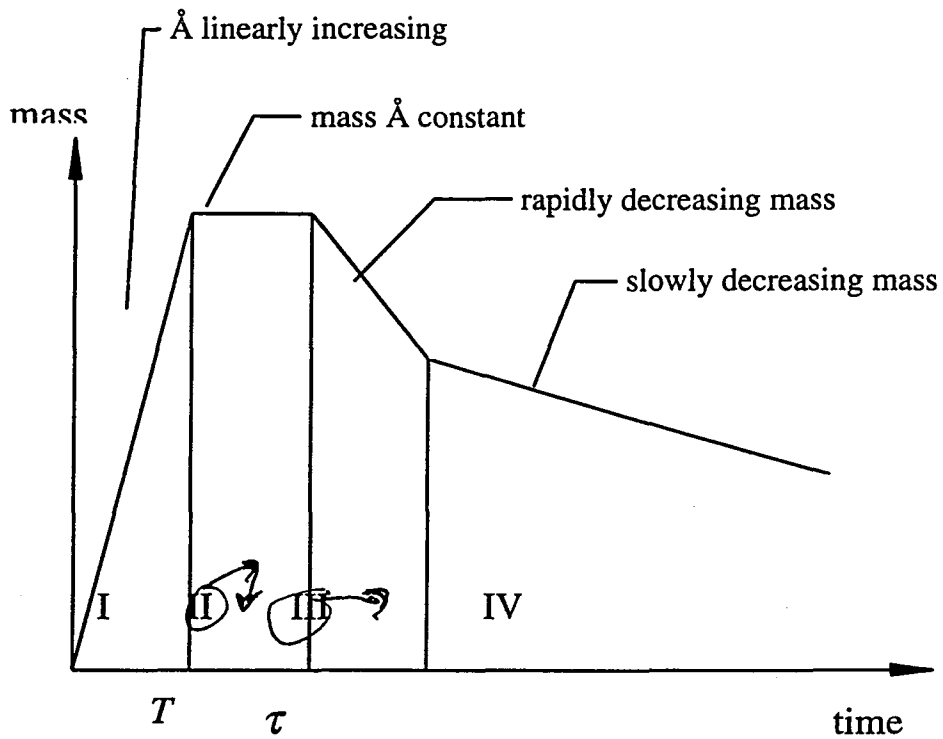


Figure 3. Schematic illustration of the tracer fluxes accounted for in the compartmental model.

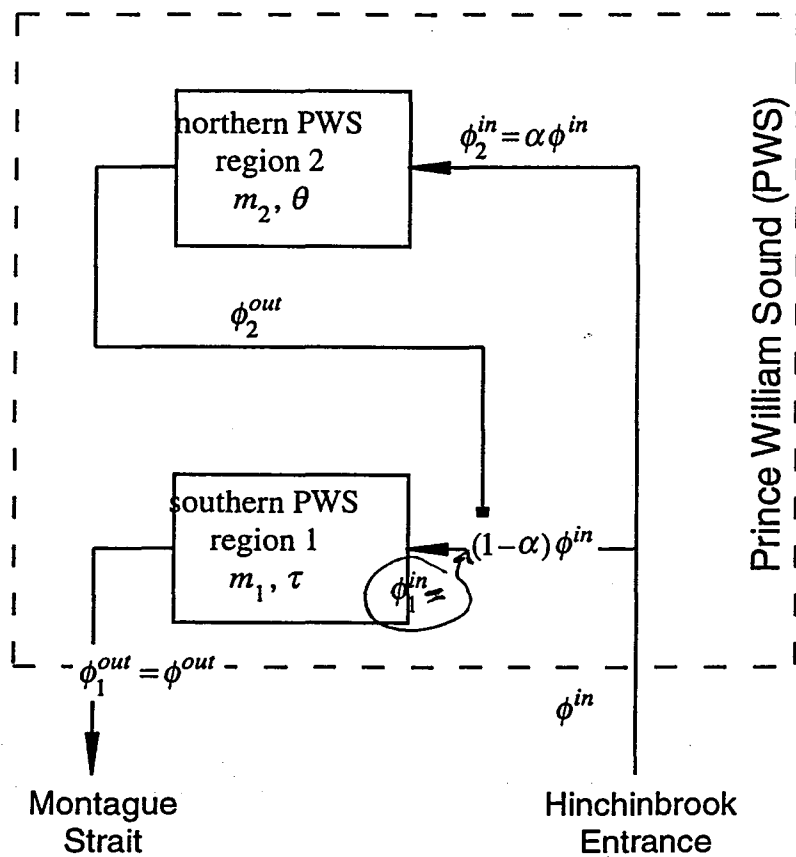
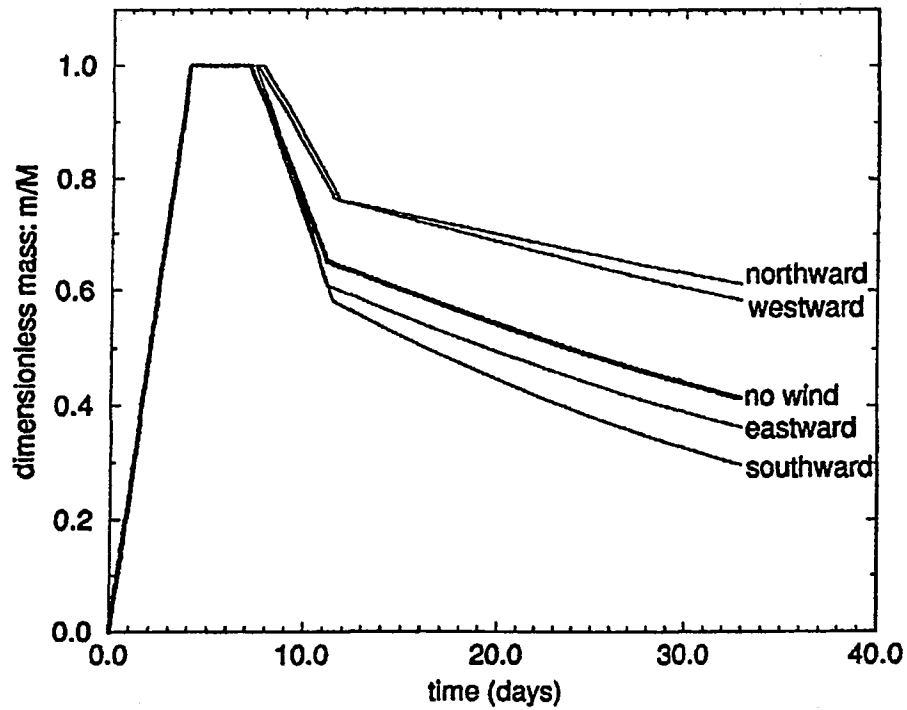


Figure 4. The evolution of the dimensionless tracer mass present in PWS, m/M , obtained from the compartmental model with various surface forcings. The direction toward which the wind is blowing is indicated.



Chapter 8

Observational Physical Oceanography